Lentiviral Gene Therapy from Multi-channel Bridges to Investigate Acute and Chronic Spinal Cord Repair

by

Dominique Smith

A dissertation submitted in partial fulfillment
of the requirements for the degree of
Doctor of Philosophy
(Biomedical Engineering)
in the University of Michigan
2019

Doctoral Committee:

Professor Lonnie Shea, Chair
Associate Professor Tim Bruns
Professor Roman Giger
Associate Professor Parag Patil

Dominique Smith

domsmi@umich.edu

ORCID ID: 0000-0003-4257-8401

Dedication

This dissertation is dedicated to my grandmother with love

Table of Contents

List of Tables

List of Figures

Abstract

Spinal cord injury (SCI) causes paralysis below the level of injury which, at the cellular level, results from neuron and oligodendrocyte cell death, axonal loss, demyelination, and critically, the limited capacity of spinal cord neurons to regenerate[1]. Although central nervous system (CNS) tissue has the innate capacity to repair the local environment that develops after SCI lacks sufficient factors that promote regeneration and has an abundance of factors that inhibit regeneration[2]. Many strategies have been attempted to aid in the regeneration of CNS tissue, yet re-entry into intact spared tissue remains inadequately low. This is due to the complexity of the spinal cord microenvironment post injury and the barriers that must be addressed simultaneously to elicit adequate regeneration. The Shea lab has developed multi-channel poly (lactide-co-glycolide) (PLG) bridges to promote spinal cord regeneration and restore functional losses. These bridges are biodegradable and provide a temporary structure that promotes regeneration[3]. These bridges also serve as a platform for delivery of therapeutics including pharmacological agents, cells, and notably lentivirus.

This dissertation investigated the use of lentiviral gene therapy from multi-channel bridges to barriers to regeneration during acute and chronic phases of SCI. We investigated myelination of regenerating axons by over-expression of platelet-derived growth factor-AA (PDGF) and noggin either alone or in combination in an acute mouse SCI model. The combination of noggin + PDGF enhanced total myelination of regenerating axons and notably oligodendrocyte myelination. Importantly, the increase in oligodendrocyte myelin enhanced functional recovery and was also

associated with a greater density of cells of an oligodendroglial lineage. We investigated synergistic effects of anti-inflammatory and regenerative factors by bi-cistronic delivery of NT-3 and IL-10 using PLG bridges after acute SCI. This work was motivated by the need to delivered multiple factors simultaneously to address the multiple barriers to SCI regeneration. The combination of IL-10+NT-3 enhanced axonal growth and oligodendrocyte myelinated axon density significantly over control, although these factors do not act on oligodendrocyte cells directly. The increased oligodendrocyte myelin resulted in increased locomotor functional recovery compared to IL-10 or NT-3. Furthermore, we observed a strong positive correlation between oligodendrocyte myelinated axon density and functional recovery. These results show oligodendrocyte myelination as a limiting step in attaining enhanced functional recovery. Lastly, we investigated regeneration using the multi-channel bridge implanted into a chronic SCI following surgical resection of necrotic tissue. We noted that scar formation decreased at 4 and 8 weeks post injury (wpi), yet macrophage infiltration increased between 4 and 8 wpi. Subsequently, scar tissue was resected and bridges were implanted at 4 and 8 wpi. We observed robust axon growth into the bridge and remyelination at 6 months post initial injury. Axon densities were increased for 8 week bridge implantation relative to 4 week bridge implantation, whereas greater myelination, particularly by Schwann cells, was observed with 4 week bridge implantation. Taken together, the results of this dissertation show biomaterial bridges as a great tool to manipulate and investigate the spinal cord microenvironment to improve functional outcomes during acute and chronic stages of SCI. This work implies the focus of SCI treatments strategies should be reducing inflammation and enhancing myelination by oligodendrocytes for increased functional recovery. This work also implies resection of necrotic tissue in chronic SCI doesn’t negative impact functional recovery.

Chapter 1. Introduction

Opening

There are more than one million estimated cases of SCI in the United States and repairing an injury to the spinal cord has constituted a difficult clinical challenge. Spinal cord injury is a devastating condition that results in permanent functional loss including paralysis as well as loss of bladder, bowel, and sexual function. The research presented in this dissertation focuses on developing treatments to reduce the morbidity associated with SCI and promoting sufficient regeneration to attain functional recovery using biomaterials, tissue engineering, and gene therapy.

Thesis Overview

Chapter 1 provides a gene introduction to the research topics explored in this dissertation

Chapter 2 describes the prevalence and current state of spinal cord injury treatments. Spinal cord anatomy, pathophysiology of SCI, and barriers to SCI regeneration are also explored.

Chapter 3 explores experimental strategies for spinal cord regeneration including biomaterials, gene therapy, and cell therapy.

Chapter 4 introduces the use of multi-channel poly (lactide-co-glycolide) (PLG) bridges to promote spinal cord regeneration and restore functional losses. These bridges are biodegradable and provide a temporary structure that promotes regeneration post-implantation. The bridges have an interconnected pore structure that allows infiltration of endogenous cell populations and channels that direct axonal growth into and through the lesion. We have demonstrated bridge implantation in the lesion site promotes tissue regeneration and improves functional recovery.

Chapter 5 discusses the use of the PLG bridges as a platform to investigate the role of pro-oligodendrogenic factors in promoting remyelination of regenerating axons. Lentivirus encoding for noggin and platelet derived growth factor α (PDGF) were delivered from the bridge either alone or in combination to determine the extent of remyelination and oligodendrocyte lineage cell differentiation. The combination of noggin + PDGF enhanced total myelination of regenerating axons relative to either factor alone, and importantly, enhanced functional recovery relative to the control condition. The increase in myelination was consistent with an increase in oligodendrocyte-derived myelin, which was also associated with a greater density of cells of an oligodendroglial lineage relative to each factor individually and control conditions. This chapter demonstrates combination of a bridge to support and direct axon growth with a strategy to enhance their myelination represents a potential clinically translatable treatment for SCI.

Chapter 6 builds upon the success of the multiple channel poly(lactide-*co*-glycolide) (PLG) bridges by delivering 2 distinct transgenes alone and in combination to observe synergistic or possibly antagonistic effects on spinal cord regeneration. We employed a bi-cistronic to delivery NT-3 and IL-10. to target multiple barriers to spinal cord simultaneously. Overall our results show that the combination of IL-10+NT-3 enhanced axonal growth and oligodendrocyte myelinated axon density. This resulted in increased locomotor functional recovery compared to IL-10 or NT-3 alone but increased hypersensitivity compared to IL-10 alone. Furthermore, we observed a strong positive correlation between oligodendrocyte myelinated axon density and functional recovery. This suggests oligodendrocyte myelin as an important area of future of research to improve functional recovery. This chapter establishes poly-cistronic vectors as an appropriate vehicle to delivery multiple transgenes to expression multiple proteins simultaneously and further buttresses

multichannel PLG bridges as a growth supportive substrate and a platform to deliver bioactive agents as well as a defined space to investigate the SCI microenvironment and potential treatments.

Chapter 7 investigates tissue regeneration into PLG bridges implanted into a chronic model of SCI. We examined the pathophysiology of the injury including inflammatory cell infiltration, extracellular matrix (ECM) deposition, injury size, and glial scarring. ECM and glial scar formation decreased at 4 and 8 weeks post injury (wpi), yet macrophage infiltration increased between 4 and 8 wpi. Two time points were analyzed for implantation of the bridge (4 weeks post injury (wpi) or 8 wpi), with analysis of axonal growth, myelination, and source of myelination measured 6 months post primary SCI. We observed robust axon growth into the bridge and remyelination at 6 months post initial injury. Axon densities were increased for 8 week bridge implantation relative to 4 week bridge implantation, whereas greater myelination, particularly by Schwann cells, was observed with 4 week bridge implantation. While the bridge alone did not improve functional outcomes for either implantation time point, importantly, the process of bridge implantation did not significantly decrease the post injury function. This chapter demonstrates implantation of PLG bridges without added bioactive agents as a promising building block for axonal regrowth and myelination during chronic implantation.

Chapter 8 concludes the dissertation and summarizes the presented results. Future directions of this research are discussed in detail.

Chapter 2. Barriers to Spinal Cord Regeneration

Significance

There are more than one million estimated cases of SCI in the United States which can amount to $4.6 million lifetime costs per patient depending on the level of the injury[4]. Spinal cord injury is a devastating condition that results in permanent functional loss including paralysis as well as loss of bladder, bowel, and sexual function. More than half of these injuries occur prior to age 30, leaving sufferers with a lifetime of incapacitating injury[5]. A treatment that can restore even 1-2 segmental levels of spinal cord function has the potential to relieve substantial medical costs, in addition to significantly impacting the quality of life and independence of patients[6]. Nationally, the incidence of cervical SCI exceeds thoracic (51% vs. 36%), and the incidence of contusion/compression trauma exceeds penetrating injuries due to violence (e.g. gunshot or stab wounds). However, penetrating SCI accounts for 14% of cases annually in the general population, and astonishingly 28% of cases in the military[7], largely due to the contribution of blast injuries. Penetrating injuries directly sever descending motor and ascending sensory tracts, so they offer many opportunities to study strategies that encourage formation of new axons and myelination. Moreover, while spontaneous recovery within the first days and months post-SCI is a significant component of the final outcome in individuals with contusion/compression injuries[8], the initial deficits resulting from penetrating SCI exhibit essentially no improvement over time[9].

Clinical Strategies for SCI

Surgical intervention

There are currently no consensus clinical treatments for SCI, but the general guidelines are to stabilize the spinal cord and delivery of a pharmacological agent. Stabilization of the spinal cord involves decompression of the lesion site to reduce overall swelling and pooling of cerebral spinal fluid and blood. Spinal decompression has been shown to have a neuroprotective effect in some cases, but no effects or negative effects in other cases[10]. This range of effects can be attributed to timing of the intervention with earlier interventions being associated more frequently with improved functional recovery. However, earlier interventions must occur within 24 hours of the injury which is not necessarily feasible for all cases due to the uncertainty of the extent of the injury[11].

Methylprednisolone

The goal of delivery of a pharmacological agent is to reduce inflammation in the lesion site to preserve and protect the resident cells to ultimately improve neurological function and recovery. Methylprednisolone (MP) is a corticosteroid identified as being able to achieve these goals but is mired in controversy. Initial results from the National Acute Spinal Cord Injury Study II (NASCIS II) showed high dose of MP within 8 hours of injury was associated with a significant improvement in motor and sensory recovery[12]. However, this study was met with resistance due lack of correlation with clinical relevance and real-world functional benefits. This led to NASCIS III which showed MP administration between 3 and 8 hours after injury for a continuous 48 hours led to improvements of motor capabilities at the 6-month checkup. These improvements were not observed at the 1 year checkup[13]. The inconsistency of these results combined with deleterious

side effects including: wound infection, GI hemorrhages, sepsis, pulmonary embolism, severe pneumonia, and death led to significant decrease in clinical use[14].

Locomotor training

Patients with incomplete SCI qualify for rehabilitation training which can restore some sensorimotor functions. Locomotor training capitalizes on neuroplasticity of CNS tissue after injury. Neuroplasticity encompasses the reorganization of spared neuronal circuits by synaptic formation, synaptic strength, axonal sprouting, and changed in intracellular properties of spared neurons. Locomotor training accelerates neuroplasticity by having patients perform daily tasks. under assisted conditions. Patients can be suspended above a moving treadmill which forces their legs to perform basic stepping patterns leading to leg muscle activation and strengthening of spared descending pathway[15]. However, there are questioned related to the timing of the intervention, length of the intervention, and selection of patients for these programs. Selection of suitable patients is the most pressing consideration since the level, severity, and timeline of injury plays a role in recovery. Higher level, more complete injury requires a more robust training program, whereas lower level, partial injury patients can learn to walk without support quickly. Complete spinal cord transections rarely benefit from locomotor training due to complete lack of descending control. Furthermore, the age of patients plays a large role in recovery, older patients experience less recovery. Lastly, some patients experience maladaptive plasticity such as neuropathic pain, autonomic dysreflexia, circulation failure due to undirected synaptic plasticity.

Electrical Stimulation

Complete spinal cord injury deprives neural circuits of signals from the brain which is necessary to trigger activation. These circuits retain the ability of be excited or depressed and can be activated by electrical stimulation to force movement. Electrical stimulation can be achieved

by epidural or intraspinal electrodes. Epidural stimulation involves placement of electrodes outside the spinal cord to initiate or assist locomotor activity[16]. Intraspinal stimulation involves placement of electrode into the spinal cord[17]. Epidural stimulation is seen as less invasive and safer because it does not impact the healthy spared tissue as intraspinal electrode implantation. Both strategies are preferred to functional electrical stimulation in which electrodes are implanted into the muscle to initiate movement[18]. Stimulation of the spinal cord allows for a more natural, coordinated, and control recruitment of muscle groups and cause less muscle fatigue. These strategies are still experimental, but a patient with motor complete spinal cord injury was able to perform controlled leg movements with epidural stimulation and weight assistance[19, 20]. However, these strategies have similar limitations to locomotor training as in it is unclear which patients will respond best to electrical stimulation. Furthermore, locomotor training and electrical stimulation have been combined to enhance recovery, but its unclear what the parameters of stimulation and training should be. Electrical stimulation represents a promising strategy for functional recovery, but more patients must be included, and parameters must be investigated.

Spinal cord anatomy

The main purpose of the spinal cord is to relay signals between the brain and the peripheral nerves to produce movement or sensation. The spinal cord resides in the vertebral column which is comprised of individual vertebrae that physically protect the spinal cord. It has added protection provided by three layers of connective tissue called meninges. From the outside in, the meninges are the dura mater, arachnoid mater, and pia mater. These layers are lubricated and cushioned by cerebrospinal fluid and loose connective tissue. The spinal cord also has biochemical protection from the blood brain barrier (BBB). The BBB is comprised of endothelial cells that form tight

junctions to resist infiltration of most molecules and protects the spinal cord from pathogens and toxins[21].

The spinal cord is comprised of two distinct parts: gray matter and white matter. Gray matter is made up of the neuron cell bodies, neural fibers, and glial cells. Neurons are responsible for production, transmission, and integration of electrical signals. The white matter surrounds the grey matter and is composed of groups of myelinated axons that run longitudinally through the spinal cord. The groups of myelinated axons are separated into tracts which are classified as ascending or descending tracts. Ascending tracts carry information from the periphery to the brain and are called afferent fibers. This information is mainly sensory such as pain, temperature, proprioceptive, or most importantly touch. Descending tracts carry information from the brain to the periphery and are called efferent fibers. This information generally encodes movement of limbs. Lastly, the spinal cord contains many supportive cells called glial cells. The glial cells can be broken into oligodendrocytes, astrocytes and microglia. Oligodendrocytes create myelin sheathes that provide insulation to preserve saltatory conduction for efficient transmission and propagation of action potentials[22]. Astrocytes perform several regulatory functions in the healthy spinal cord: clearance of neurotransmitters[23], ion balance[24], production of extracellular matrix proteins (ECM)[25, 26], and maintenance of the blood brain barrier (BBB)[27]. Lastly, microglia are specialized macrophages that reside in the spinal cord. Microglia perform many actions including maintenance of synapses[28], removal of damaged or unnecessary axon terminals[29], phagocytosis of pathogens and debris associated with infections or injury[30], and initiation of the inflammatory response in the spinal cord[31].

Spinal cord injury

SCI results in the death of neurons and oligodendrocytes, severance and retraction of axons, demyelination of axons, and formation of an inhibitory glial scar (**Figure 2.1**) Although central nervous system (CNS) tissue has the innate capacity to repair, the local environment that develops after SCI lacks sufficient factors that promote regeneration and has an abundance of factors that inhibit regeneration[2]. This complex series of cellular and molecular events can be divided into acute and chronic phases.

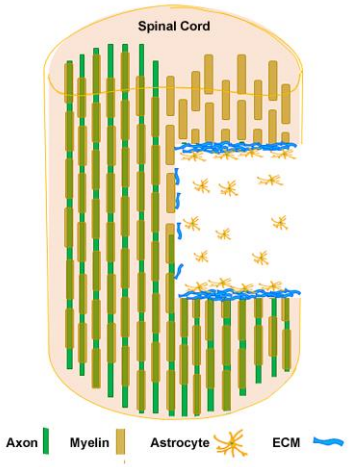

Figure 2.1 Spinal cord injury. SCI results in axonal dieback, demyelination, and ECM deposition.

Acute phase of SCI

The acute phase of SCI occurs over the time course of minutes to weeks and can be further subdivided into the primary and secondary injury. The primary injury is the physical penetrating, contusion, or compression of the spinal cord which leads to direct loss of axon connectivity and myelination[10]. The physical injury leads to a cascade of biological events called the secondary injury. Secondary injury is marked by continuous inflammation that ultimately results in the development of a non-permissive environment for regeneration. Infiltrating immune cells[32, 33] and immune-activated neural and glial cells[34, 35] produce inflammatory cytokines and reactive oxygen species (ROS) in response to the primary injury[33, 36, 37]. These inflammatory cytokines recruit and

activate circulating neutrophils and macrophages[38, 39] and stimulates the microglia[40]. Neuron death results in excessive glutamate causing excitotoxicity and subsequent neuronal death[41]. Oligodendrocyte death results in the destruction of myelin and accumulation of neuroinhibitory myelin debris and, particularly, the potent neurite growth inhibitors, Nogo-A, myelin associated glycoprotein (MAG), and oligodendrocyte myelin glycoprotein (OMgp) [42, 43]. NogoA blocks axon sprouting by collapsing growth cones using the NgR1 receptor[44]. MAG modulated the axonal cytoskeleton and activated the RhoA/ROCK signaling pathway[45]. OMgp is a potent growth inhibitory molecule that associates with the NgR1 and PirB receptors[46]. The resulting microenvironment causes ongoing tissue damage, including more neural and glial death[39, 47] furthering deteriorating spinal function.

Intrinsic regulators of axon growth post-SCI

In addition to external factors affecting axonal growth, there are several intrinsic neuronal mechanisms that limit axonal growth in the CNS. For axonal regeneration, there must be a coordinated regulation of protein expression through the activation of specific signaling networks, yet these networks are deficient in various CNS population including upper motor neurons that form the corticospinal tract responsible for movement. Some pathways have emerged as the most important including mTOR, Rho, and JAK/STAT signaling. pTEN is a negative regulator of the mTOR pathway that controls axon elongation. pTEN inhibition or deletion has been shown to stimulate axon regrowth in some rodent models[48]. The mTOR signaling pathway is also involved in mediating downstream effects of neurotrophic factors such as BDNF to promote synaptic plasticity[49]. Rho signaling negatively regulates the actin cytoskeleton and microtubule polymerization and its inhibition post-SCI has results in enhanced regeneration after injury[50]. The JAK/STAT signaling pathway regulates neuroinflammation, synaptic plasticity, axon

regeneration, neuronal differentiation, and neuron survival[51]. SOCS3 expression is induced by the JAK/STAT signaling pathway and acts as a feedback inhibitor of JAK/STAT signaling. Studies have shown that down regulating SOCS3 in spinal cord neurons with SOCS3-targeting shRNA decreases neuronal death and demyelination as well as enhances dendritic regeneration and axonal growth[52]. Collectively, these signaling pathways show there is a balancing act and crosstalk between growth promoting and growth inhibitory cues after injury.

Chronic phase of SCI

The chronic phase of spinal cord injury occurs over months to years. In response to the ongoing destruction, astrocytes undergo a controversial process called reactive gliosis. The astrocytes become hyperfilamentous and cluster tightly together[53]. Astrocytes start to produce many ECM proteins, most notably, chondroitin sulfate proteoglycans (CSPGs) and the combination of tightly packed astrocytes and ECM form the glial scar[54, 55]. The glial scar acts as the primary barrier at the injury border, both as a physical blockade and as a set of cellular and biochemical signals[56, 57]. The goal of the glial scar is to isolate the initial injury, reinstitute the BBB, and prevent the spreading of cytotoxic molecules to spared tissue[26, 57]. However, CSPGs are the most potent inhibitory cue within the glial scar[58-60]. CSPGS have been observed to directly prevent axon extension in numerous studies, leading to increased numbers of dystrophic axons as well as axons that turn at or are repulsed by a CSPG barrier[61-63]. In addition to the abundance of neuroinhibitory factors, the microenvironment after SCI has a lack of trophic support to promote regeneration. Together these barriers prevent recovery of motor function and complicate the design of regenerative strategies.

Chapter 3. Experimental Strategies for Spinal Cord Regeneration

CNS tissue was thought not to regenerate until seminal work done in the 1970-80s. In these studies, the spinal cord of rats was completely transected and reconnected using peripheral nerve grafts isolated from the sciatic nerve[1]. This strategy suggested that CNS tissue could regenerate if given the proper substrate and factors. Since this work, many strategies have been developed to aid the regeneration of the CNS. These strategies can be simplified into three main components: biomaterials, gene therapy, and cell transplantation. These components combined in different ways establish the field of tissue engineering.

Biomaterials

Biomaterials for spinal cord regeneration have the primary goal of providing structure and support for lesioned axons to traverse injury site. Most biomaterials used for this purpose are polymers. Polymers are large molecules comprised of repeating units. These polymers can be natural or synthetic. There is no consensus on the best material for spinal cord regeneration, but both classes of polymers have strengths and weaknesses. Natural polymers are less toxic, biodegradable, and ubiquitous. Their weaknesses are variability in properties, complexity of structure, difficult to modify, and can be costly to extract. Synthetic polymers can have tuned degradability depending on the use, easily tunable properties, and reasonably modified chemically. However, they can be toxic and expensive to process. Many biomaterials of both types have been used extensively in spinal cord regeneration (**Table 3.1**) Regardless of the source of the

biomaterial, the same considerations of biocompatibility, biodegradability, mechanical properties, and architecture must be addressed to provide the best substrate for tissue regeneration.

Table 3.1 Common biomaterials used for spinal cord regeneration

Natural Polymers			
Material	**Form**	**SCI Model**	**Findings**
Collagen	Porous cylindrical scaffold	Thoracic acute hemisection	Motor recovery [64]
	Porous cylindrical scaffold	Thoracic acute complete transection	Reduced cystic cavity[65]
	Longitudinal filaments	Thoracic acute contusion	Improved motor recovery, axon regeneration, improved SSEPs [66]
Laminin	Aligned nerve conduit	Acute complete transection	Increased axon regeneration [67]
	Bulk injection	Thoracic contusion	Increased axon regeneration [68]
	Multi-channel scaffold	Thoracic lateral acute hemisection	Increased vascularization, axon regeneration [69]
Fibronectin	Bulk injection	Knife cut transection	Increased axon regeneration, reduced neuron survival [70]
	Bulk injection	Cervical dorsal hemisection	Increased forelimb reaching scores, no difference in injury size [71]
Hyaluronan	Bulk injection	Thoracic clip injury	Improved motor recovery [72]
	Longitudinal multi-tubular scaffold with PLGA microparticles	Thoracic dorsal hemisection	Improved vascularization, axon regeneration, motor recovery [73]
Chitosan	Bulk hydrogel	Thoracic bilateral dorsal hemisection	Diminished glial scarring, increased Schwann cell myelination, axon regeneration, motor recovery [74]
	Single tube scaffold	Thoracic complete transection	NSC recruitment and neurogenesis improved sensory and motor recovery, increased axon regeneration and myelination [75]
	Sponge scaffold	Thoracic lateral hemisection	Increased axon regeneration, reduced glial scarring
Synthetic Polymers			

Poly (ethylene glycol) (PEG)	Bulk hydrogel	Thoracic complete transection	Improved cell invasion, vascularization, axon regeneration, myelination [76]
	Aligned microchannel scaffold	Thoracic complete transection	Some axon regeneration, no motor recovery, no MEPs [77]
	Aligned porous tubes	Thoracic lateral hemisection	Increased axon regeneration, myelination, functional recovery [78]
Poly (2-hydroxyethyl methacrylate) PHEMA	Bulk hydrogel with oriented pores	Thoracic transection	Axon regeneration, vascularization [79]
	Sponge scaffold	Thoracic hemisection	Improved functional recovery, some axon regeneration [80]
Poly (lactic-co-glycolic acid) PLGA	Electrospun aligned fibers sheath	Thoracic lateral hemisection	Improved functional recovery [81]
	Parallel channel scaffold	Thoracic complete transection	Increased axon regeneration [82]
	Multichannel scaffold	Thoracic lateral hemisection	Increased axon regeneration, myelination, decreased ECM deposition [83]

Biocompatibility

Biocompatibility refers to the ability of a material to elicit a minimal inflammatory response when implanted into the target site. The severity of the immune response can cause the material to be rejected or slow the healing process. The spinal cord is an immune-privileged site normally, however post injury there is destruction of the BBB and invasion of inflammatory cells [84]. The implanted biomaterial may exacerbate the inflammatory response, so it is necessary to determine the exact immune response to specific material. In addition to a negligible immune response, the materials must not cause any changes in cell function. Cells must be able to adhere, function normally, proliferate in the material, and migrate to and from the material. In this context, natural polymers such as collagen, laminin, and hyaluronan have an obvious advantage. They are cell-

derived and tend to be biocompatible in the spinal cord. Accordingly, they have been used extensively in SCI regeneration to increase axon elongation, synapse formation, and motor recovery[85-91]. However, this advantage is not afforded to all natural polymers. Chitosan, a non-mammalian natural polymer, when injected into the CNS is engulfed by macrophages and sequestered from the surrounding tissue in a fibrotic scar [92].

Biodegradability

Biodegradability refers to the material's ability to be degraded naturally or by host cells over a reasonable timescale. The by-products of the degradation should be biocompatible, non-toxic, and able to exit the body easily without buildup in other organs. Poly(α-hydroxyacids) such as poly(glycolic acid) (PGA), poly(lactic acid) (PLA), and their copolymer poly(lactic-co-glycolic acid) (PLGA) are biodegradable polymers used extensively in SCI regeneration (**Table 3.1**) [93-96]. These polymers have highly tunable control of degradation. They have been shown to support regeneration after complete spinal transections and can be combined with cells or growth factors [97]. However, there are many non-biodegradable biomaterials used in SCI regeneration including Poly(2-hydroxyethyl methacylate) (PHEMA), poly (2-hydroxyethylmethacrylate-co-methylmethacrylate) (PHEMA-MMA), and poly (ethylene glycol) (PEG) [98-103]. PHEMA actively increases axon regeneration but lacks structural integrity [97]. The goal of biomaterial implantation in SCI is to allow the host cells to entirely replace the implanted scaffold, which suggests biodegradable scaffolds are optimal.

Mechanical Properties

The mechanical properties of the scaffold should be matched with the target site properties. The spinal cord is a complex and viscoelastic structure with varying mechanical properties of tissue components and structure [104]. For the spinal cord, scaffolds must have appropriate stiffness,

but also be strong to not collapse and obstruct tissue growth and nerve regeneration. When implanted, the material must be able to withstand repetitive compression from movement and maintain reasonable properties when degrading to not collapse [105]. Scaffold mechanical properties may also alter wound healing and the inflammatory response. For example, PEG hydrogels with lower stiffness led to reduced macrophage activation and foreign body response when implanted in the spinal cord [106]. Additionally, mechanically matched PHEMA has also been shown to reduce the inflammatory response and fibrotic scarring after implantation when compared to stiffer formulations [98].

Architecture

The architecture of the biomaterial scaffold is one of the most important considerations. The scaffold must be permissive to cellular infiltration, molecule diffusion, and vascular infiltration. Furthermore, the scaffold must allow diffusion of waste products, sequestration of bio-active molecules, and deposition of ECM. These requirements can be fulfilled by establishing an interconnected pore structure with high porosity, utilizing grooves, or aligned or random fibers. The size of pores also plays a huge role. The pores need to be large enough to allow cells to migrate into, within, and out of the structure. However, they must also be small enough to meet surface area requirements to allow efficient and effective binding of cells to the scaffold to integrate the scaffold into the host tissue [107, 108]. The porous channel structure prevents the ingrowth of scar tissue, concentrates bio-active molecules and supporting cells, and directs growth of axons in one direction [109]. Typical architectures are bulk hydrogels, microparticles, and nerve conduits. Bulk hydrogels are injectable, fill any space, and highly porous, but offer no guidance cues to regenerating axons. The lack of guidance cues reduces the axonal regeneration found in hydrogels as seen in studies using alginate or Matrigel [103]. Nanoparticles can be embedded in materials to

allow for controlled release of bioactive molecules but also do not offer any guidance cues for axonal regeneration into and through the lesion site [110] . Nerve conduits give physical guidance cues and can be made very porous but are difficult to place in the lesion site and cannot conform to irregular lesion areas. This makes them optimal for encouraging guided neurite extension through the lesion site in the case of aligned fibers or nerve conduits [111-113].

Gene Therapy

Gene therapy is a promising therapeutic approach capably of addressing the multiple barriers to SCI regeneration. CNS tissue has the innate capacity to repair the local environment that develops after SCI but, lacks sufficient factors that promote regeneration and has an abundance of factors that inhibit regeneration[2]. Some studies have reported removal of these barriers by bioactive molecule delivery. Long term delivery of these molecules generally requires osmotic pumps. The efficacy of these pumps is attenuated by clogging, damage to the spinal cord, and effectively distributing the molecule throughout the injury. An alternative is repeated infusions into the spinal cord, but this method is hampered by repeated injury with risk of infection and poor distribution. Furthermore, bioactive molecules deteriorate, have limited penetration in small doses, and can generate negative off target effects. Gene therapy overcomes these pitfalls by inserting a gene in the host's cells allowing for sustained delivery of factors. Gene therapy can be subdivided into two main strategies, viral or non-viral vectors. These strategies have several subdivisions and associated strengths and weaknesses.

Viral Vectors

Viral vectors are the most common form of gene therapy. These vectors are actively transported in the cell by surface proteins, shuttled to the nucleus, transcribed to RNA, and subsequently translated into protein. Viral vectors have undergone extensive modification to

ensure their safety. The genes involved in replication are generally separately and the vector becomes replication deficient as a result[114]. While the viral vector cannot replicate to create more viral particles, the transgene delivered using these vectors can persist in transduced cells for an extended period. The most commonly used viral vectors include adenovirus, adeno-associated virus, herpes simplex virus, and lentivirus (**Table 3.2**).

Adenovirus

Adenoviruses are large double stranded DNA viruses are double stranded DNA viruses that do not integrate into the host genome, rather they remain extra chromosomal in the nucleus where they can still be transcribed and translated into protein. These vectors can transduce dividing and non-dividing cells with high efficacy. Expression of this vector appears relatively quickly, within 24 – 36 hours, but the expression is reduced following cell division and eventual degradation of the DNA due to its extra chromosomal nature[115]. This vector induces a potent immune response depending on the serotype used with the most common serotype, AD5, producing the most severe response. Adenoviruses have been used extensively in CNS regeneration to deliver neurotrophins including NT-3, NGF, and BDNF for axonal regeneration[116-119].

Adeno-associated virus

Adeno-associated viruses (AAVs) are small satellite viruses similar in structure to adenoviruses but have a lower packing capacity. They generally do not integrate in the host genome. These viruses transduce dividing and non-dividing cells with high efficiency but expression of the vector lags for 2 weeks and has relatively low expression leading to overall low efficacy. However, this vector has variable tropism to different cells depending on the serotype. AAV-9 and AAV-6 target motor neurons specifically independently of route of administration which can be useful for motor neuron dysfunction diseases including SMA and ALS [120]. AAV-1

and AAV-5 have been reported to directly infect supraspinal neurons using retrograde transport by axons severed by SCI in the spinal cord and then traveling to brain regions with some specificity[121]. This has the potential to promote functional recovery by expressing factors locally in the brain without delivering virus directly to the brain.

Herpes simplex virus

Herpes simplex viruses (HSV) are extra chromosomal DNA viruses capable of high infection and high expression immediately after administration. However, the expression of HSV turns on and off randomly resulting in transient expression on average. This vector can transduce dividing and non-dividing cells but causes a high immune response. HSV displays several natural adaptations to the CNS that have been exploited to target CNS regeneration. The virus can move in retrograde and anterograde directions using synapses to jump from neuron to neuron. This has made them instrumental in investigating neural circuitry between muscles tissue and sensory or motor neurons[122]. The retrograde transport of HSV makes it an attractive vector for non-invasive transgene expression in the spinal cord from muscle injection[50, 123]. It has been shown that HSV mediated expression of IL-4 can reduce neuropathic pain[124]. HSV encoding IL-10 after a hemisection injury has demonstrated improved axonal sparing, functional recovery, and direct trophic support of neural cells [125, 126]. HSV constructs have also been used to promote axonal regeneration. HSV mediated delivery of bacterial C3 transferase, a Rho kinase (ROCK) inhibitor that reverses myelin debris inhibition of neurons, has promoted extensive axonal regeneration in the spinal cord that is correlated with improved sensory motor coordination [50].

Lentivirus

Lentiviruses are a subclass of retroviruses that integrate in the host genome allowing for immediate and long-term stable gene expression. They can transduce dividing and non-dividing

cells and cause a very low immune response. While lentiviruses do integrate into the host genome, the risk for mutagenesis of oncogenes is relatively low due to its insertional affinity for gene ends rather than promoter regions[114, 127]. However, over longer periods, the gene can be silencing depending on the promoter used in the construct[128]. Lentiviral delivery of NGF [129, 130], BDNF [83, 131], and NT-3 [132, 133] have been reported to increase axonal plasticity and enhance neuron sparing. Lentiviral delivery of IL-10 or IL-4 to the spinal cord post-injury promotes macrophage polarization towards an M2 phenotype which activate encourages tissue regeneration , neuronal survival, and attenuates neuropathic pain [134-136]. Chondroitinase, a bacterial protein which inactivates CSPGs such that they no longer inhibit axon elongation has been delivered by lentivirus to create a permissive environment for axonal growth [63, 137].

In summation, lentiviral vectors and specific serotypes of AAV have the most stable gene expression and an attenuated immune response when compared to other viral vectors. This suggests that lentiviral vectors are most appropriate in situations where stable long-term transgene expression is needed. HSV delivery or AAVs are appropriate when transient expression is desired within spinal tissue or translocation to the brain is necessary. The immune response of adenoviruses makes them an inappropriate choice in most use cases, but they exhibit the highest packaging capacity and transduction efficacy .

Table 3.2 Viral gene therapy strategies

Virus	Package	Efficacy	Integration	Transduced Cells	Immune response	Length
Adeno	>8 Kb	High	No	Dividing/Non-dividing	High	24 hours - Transient
Adeno-Associated	4.5 Kb	Low	No	Dividing/Non-dividing	Very Low	2 weeks - Transient
Herpes Simplex	<8 Kb	High	No	Dividing/Non-dividing	High	24 hours - Transient
Lentivirus	<8 Kb	Moderate	Yes	Dividing/Non-dividing	Very Low	48 hours - Stable

Non-viral vectors

Non-viral vectors are more common clinically due to their assumed safety and avoidance of other pitfalls of viral vectors. These vectors are not transported to the cell nucleus but reside in episomes. This drastically reduces their delivery efficiency and subsequent ability to produce high level of proteins but also reduces immunogenicity and toxicity associated with viral vectors. The most common non-viral vectors are naked DNA and lipofection. Naked DNA refers to direct injection of transgene encoded plasmids in the target site. This may be able to achieve high levels of expression quickly after administration because multiple plasmid copies encoding the transgene can be incorporated into a signal cell but these plasmids are degraded more quickly than in viral constructs[138, 139]. This make viral constructs more desirable for SCI treatment because the regenerative factors must be expressed over long periods of time to ensure repair. Lipofection uses liposomes to surround transgene encoded plasmids to facilitate entry into the cell. This is more successful than naked DNA delivery but has disadvantages including uncontrolled expression, off target effects, and a significant immune response[140].

Cell Transplantation

Cell transplantation strategies for SCI have three main goals. The first goal is to replace the dead oligodendrocytes, neurons, and astrocytes in the lesion site. The second goal is to produce scaffolding for regenerating axons and tissues by laying down ECM materials. The third goal is to function as bioreactors for increased production of growth factor in the lesion site to promote axonal regeneration, reduce inflammation and secondary damage, and potentiate differentiation of endogenous stem cells. Many cells types have been implanted to achieve these goals including fibroblasts[141, 142], Schwann cells[143-145], olfactory ensheathing cells[146-151], neural stem cells[152-154],

and mesenchymal stem cells[155-157]. These strategies have had varying degrees of success but generally suffer from poor cell survival and engraftment and require immunosuppression.

Neural stem cells are among the most commonly used following SCI, as they have the highest potential to repopulate the host cells by differentiating into neurons, oligodendrocytes, and astrocytes that will form the new tissue. Furthermore these cells actively release neurotrophic factors, ECM, other growth factors[158, 159]. Exogeneous neural stem cells and progenitors are reported to enhance myelination and improve motor function [152, 160-164]. Embryonic neural stem cells have shown increased potential for differentiation, growth factor, and subsequent improvements in tissue structure and motor recovery[152].

The largest drawbacks of cell transplantation are immunogenicity and tumorigenicity. Embryonic stem cells (ESCs) and induced pluripotent cells (iPSCs) are less susceptible to immune rejection than adult stem cells due to an absence of major histocompatibility complex (MHC)-II, CD80/CD86, and low MHC-I expression [165, 166]. However, iPSCs are susceptible to tumorigenesis due to uncontrolled growth, angiogenesis, and proliferation [167]. Stem cells also have the ability to modulate the local immune response, such as macrophage polarization and T cell phenotype after SCI, further decreasing their risk for rejection [168-173].

Although cell transplantation strategies have demonstrated regeneration with some functional recovery, they still remain limited by cell survival [174] and distal migration from the implant site leading to ectopic colonies of grafted cells at long distances from the transplant site, including in the central canal of the spinal cord, adhered to the surface of the spinal cord, and in the fourth ventricle of the brainstem [175]. Future work will require controls for the proliferation of these cells and the immune responses they may elicit and improving their survival.

Chapter 4. Multi-channel Bridges for SCI Regeneration

The Shea lab has developed multi-channel poly (lactide-co-glycolide) (PLG) (**Figure 4.1)** to promote spinal cord regeneration and restore functional losses. PLG has been employed for decades as a biodegradable suture, a matrix for the culture of numerous cell types, and as a vehicle for drug delivery, and thus is readily translatable[176]. We have developed a sugar fiber templating procedure to create channels within the bridge and also enabled salt to be mixed into PLG to provide porosity to the structure[177].

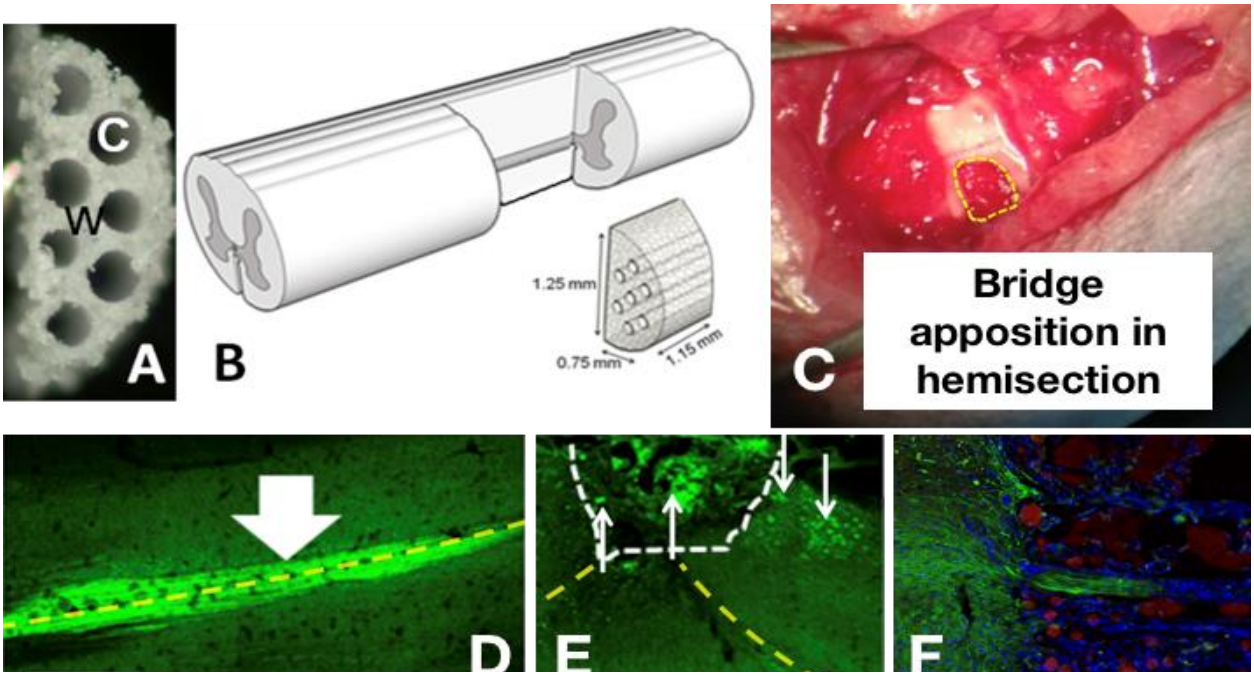

Figure 4.1 PLG bridges for SCI regeneration. PLG bridges (A) implanted into a lateral hemisection injury (B). Bridge has good apposition with intact tissue (C). (D) Crym:GFP reporter expression in spinal cord CST is robust, and clearly identified within and exiting the PLG bridge 12 weeks after acute implantation (E). Axons entering bridge channels are apparent at the rostral bridge margin (F).

These bridges are biodegradable and provide a temporary structure that promotes regeneration for between 2 and 6 months post-implantation[3]. The bridges have an interconnected pore structure,

that allows infiltration of endogenous cell populations, including macrophages, Schwann cells, and oligodendrocytes[83, 178-180]. Additionally, the bridge mechanically stabilizes the injury with tissue ingrowth and reduces secondary injury and axonal dieback[178]. Longitudinal channels encourage axons to regenerate into the bridge with cells aligned along its major axis. Both motor and sensory axons have been identified in bridge channels[3]. Glial scarring is limited to the bridge periphery and resolves by 6 weeks[83]. Importantly, the effects seen with the bridge structure are not replicated when using Gelfoam as a control due to its random orientation and lack of structural integrity[181]. These bridges also serve as a platform for delivery of therapeutics including gene therapy and cell transplantation.

PLG bridge for localized gene therapy

Delivery of lentivirus from these bridges causes stable transgene expression for at least 8 weeks after SCI[182]. Maximum transgene expression is localized to the implantation site and falls sharply outside the adjacent vertebrae [183].

Gene therapy for axon elongation

We have delivered NT-3 and BDNF lentivirus from bridges to promote significant increases in axon growth into our bridge post-SCI. Both viruses significantly increased axon number per channel at 4 weeks by 2-fold compared to bridges with no lentivirus. There were no significant differences between each neurotrophic factor [83]. Though BDNF and NT-3 overexpression did not differ in their ability to promote axonal growth, NT-3 resulted in some myelination of axons although it was very low at 13%. These results suggest a need for a treatment to promote myelination of regenerating axons to improve functional outcomes.

Gene therapy for axon myelination

We investigated SHH and NT-3 lentiviral delivery from bridge to promote axon growth and myelination[183]. Overexpression of these factors increased both regeneration of axons and total myelination at 8 weeks post-SCI. However, myelination can occur from CNS-derived oligodendrocytes or PNS-derived Schwann cells. Schwann cell-derived myelin is expected to be less effective for CNS function[184]. While these studies did increase total myelination, there exists a need for a strategy to increase oligodendrocyte myelination specifically.

Gene therapy to reduce inflammation

While the bridge alone reduces inflammation, immuno-modulation provided by localized expression of anti-inflammatory cytokines, IL-10 and IL-4, substantially enhanced regeneration. cDNA microarray heat maps indicated more than a 2-fold downregulation of pro-inflammatory associated genes with delivery of IL-10 and IL-4 relative to control, while more than a 2-fold upregulation of regeneration associated genes in IL-10 and IL-4 groups compared to control. In addition to these changes in gene expression, an increase in myelinated and unmyelinated axon density was observed at 3 and 12 weeks post injury within the bridge of mice receiving IL-4 or IL-10 overexpression [185]. Moreover, overexpression of these factors resulted in increased locomotor recovery as early as 2 wpi compared to control groups [185]. These data indicate that localized anti-inflammatory overexpression in an acute injury can enhance the potential for recovery, but there is a need to investigate these factors combined with growth promoting factors to support regeneration of spared and new tissue.

PLG bridges for cell therapy

We have delivered exogenous E14-NSCs that enhanced axon elongation, myelination, and ultimately functional recovery. $EGFP^+$ spinal progenitors derived from either adult or embryonic

(E14) mice were cultured on PLG bridges for transplantation into a unilateral hemisection. Bridges transplanted with E14 progenitors supported an earlier increase in axon elongation and remyelination compared to adult progenitor or blank bridges [186]. Increased axon density correlated to an earlier onset of hindlimb stepping than adult stem cells or blank bridges. Interestingly, a significant increase in $NeuN^+$ neuronal cell bodies within bridges loaded with E14-NSCs was seen. Neuronal cell bodies were observed within the bridge in all conditions with few $EGFP^+$ cells present (1-2 cells/mm^2), suggesting there may be an enhancement of an endogenous regeneration response [186].

Remaining Questions

We have made significant strides in the acute regeneration and myelination of CNS axons through a biomaterial bridge resulting in increased motor function [181]. However, there are still many areas for further investigation using the multi-channel PLG bridges.

First, there is a need to investigate further myelination of regenerating axons, specifically oligodendrocyte mediated myelination. Oligodendrocyte myelin is needed to restore proper conduction to regenerating axons and improve functional recovery [187]. Furthermore, oligodendrocytes also perform several roles in maintenance and protection of axons [188]. Second, we have reported the ability of anti-inflammatory cytokines to reduce the initial tissue destruction and ameliorate losses in functional recovery. However, we have not investigated enhancing the functional recovery by combining these effects with neurotrophic factors that will support regeneration of spared and new tissue. Last, our previous work has been completed in acute models of SCI, but most SCI cases have progressed into chronic stages due to lack of treatment options available to patients immediately. Furthermore, chronic SCI is seldom studied due to many pitfalls of chronic SCI models and the complexity of injury microenvironment. There exists a need to

develop a repeatable chronic SCI model and determine the efficacy of our biomaterial approaches in the chronic space. This will allow us to determine the efficacy of our acute treatments in the chronic space and develop future treatments for clinical translation. This thesis aims to answer these questions and elucidate future directions of spinal cord regenerations research.

Chapter 5. Combinatorial Lentiviral Gene Delivery of Pro-Oligodendrogenic Factors to Improve Myelination of Regenerating Axons after Spinal Cord Injury

Authors

Dominique R. Smith, Daniel J. Margul Courtney M. Dumont, Mitchell A. Carlson, Mary K. Munsell, Mitchell Johnson, Brian J. Cummings, Aileen J. Anderson, Lonnie D. Shea

Abstract

Spinal cord injury (SCI) results in paralysis below the injury and strategies are being developed that support axonal regrowth, yet recovery lags, in part, because many axons are not re-myelinated. Herein, we investigated strategies to increase myelination of regenerating axons by over-expression of platelet-derived growth factor-AA (PDGF) and noggin either alone or in combination in a mouse SCI model. Noggin and platelet-derived growth factor aa (PDGF) have been identified as factors that enhance recruitment and differentiation of endogenous progenitors to promote myelination. Lentivirus encoding for these factors were delivered from a multi-channel bridge, which we have previously shown creates a permissive environment and supports robust axonal growth through channels. The combination of noggin + PDGF enhanced total myelination of regenerating axons relative to either factor alone, and importantly, enhanced functional recovery relative to the control condition. The increase in myelination was consistent with an increase in oligodendrocyte-derived myelin, which was also associated with a greater density of cells of an oligodendroglial lineage relative to each factor individually and control conditions. These results

suggest enhanced myelination of regenerating axons by noggin + PDGF that act on oligodendrocyte-lineage cells post-SCI, which ultimately led to improved functional outcomes.

Introduction

Spinal cord injury (SCI) causes paralysis below the level of injury, which, at the cellular level, results from neuron and oligodendrocyte cell death, axonal loss, and demyelination[1, 83, 179]. Though spinal cord neurons have an innate capacity to regenerate, they are limited by a microenvironment that features an insufficient supply of factors that promote regeneration and an abundance of inhibitory factors including the glial scar[39, 58, 189-193]. Post-mitotic oligodendrocytes, the myelinating cells native to the central nervous system (CNS), infrequently myelinate regenerating axons as oligodendrocytes undergo apoptosis due to excitotoxicity and the inflammatory milieu[194-196]. Remyelination by Schwann cell of the peripheral nervous system is observed, though it is expected that Schwann cell-derived myelin is less effective for CNS function[184]. Surviving oligodendrocytes are inefficient at proliferation or extensive migration that is necessary for the cells to myelinate the majority of regenerating axons[196, 197]. Thus, strategies are needed to overcome the inhibitory microenvironment to enhance the number of available oligodendrocytes, such as through the recruitment of endogenous progenitors, and supporting their capacity for myelination[197-200].

Modulating the microenvironment following injury has proven to be difficult, with a multitude of cell, gene, and biomaterial approaches having been evaluated. Transplantation of Schwann cells, stem cells, or cells genetically engineered to secrete inductive factors have been used to shift the microenvironment towards a pro-regenerative phenotype [201-203]. However, the impact of cell transplantation is frequently limited by the extent of survival and engraftment [204, 205], which may not provide factors for times that are necessary to promote regeneration. Alternatively, injection

of proteins into the lesion space or the spinal cord parenchyma has been employed to deliver trophic factors, yet these strategies cannot sustain the presence of these factors due to their clearance or degradation. Gene delivery represents a versatile strategy in which transduced cells function as bioreactors for the localized production of trophic factors to create a permissive environment for regeneration. We have previously reported that poly (lactide-co-glycolide) (PLG) multi-channel bridges are an effective vehicle for localized, sustained lentiviral gene therapy capable of altering the post-injury microenvironment and promoting regeneration[83]. PLG has been widely used as a material for spinal cord repair or peripheral nerve conduits. PLG is also biodegradable, bioresorbable, and its degradation products are cleared by the body [206]. Lentiviral expression is highest at the site of the implant and decreases as a function of distance. The lentivirus transduces cells in the surrounding area including astrocytes, macrophages, fibroblasts, and invading Schwann cells [83]. Additionally, these bridges feature an architecture that encourages axon growth through channels and infiltration of supporting cells into interconnected pores[83, 137]. Regenerating axons have been observed growing through the bridge and into tissue caudal to the injury[181]. However, the bridge alone is limited in its ability to foster remyelination. We have previously reported on the combinatorial delivery of sonic hedgehog (SHH) and neurotrophin 3 (NT3) to improve myelination of regenerating axons. SHH and NT3 are reported to promote neurite extension that is dependent on the concentration and spatial/temporal distribution[207, 208], with SHH also influencing neuronal and oligodendrocyte differentiation during development and following injury[209, 210]. While SHH alone, but not its combination with NT3, was able to enhance the percentage of axons myelinated by oligodendrocytes, the overall percentage of myelinated axons was lower than normally found in the contralateral tissue. This could be attributed to NT3 promoting Schwann cell recruitment and progenitor quiescence[208]. SHH has also been associated

with ventral patterning, but has not been shown to enhance progenitor recruitment necessary to generate myelinating oligodendrocytes[211]. Factors that more effectively recruit the endogenous progenitor pool toward an oligodendrocyte lineage may further enhance myelination.

Noggin and platelet-derived growth factor aa (PDGF) have been identified as factors that enhance recruitment and differentiation of endogenous progenitors to promote myelination *in vitro* and *in vivo*. Noggin is a bone morphogenetic protein (BMP) receptor antagonist[212]. BMPs, which are upregulated after SCI, promote astrocyte differentiation of proliferating progenitor cells. Although noggin inhibits the BMP pathway, it is not sufficient to increase the overall differentiation of progenitor cells to myelinating oligodendrocytes[213]. PDGF specifically, has been noted for its capacity to enhance proliferation and recruitment of progenitor cells both *in vitro* and *in vivo*[214-217]. PDGF is a potent mitogen for progenitor cell proliferation[215, 218] and is a required signaling molecule for differentiation of embryonic and adult neural stem cells into $O4^+$ oligodendrocytes[22, 219, 220]. These reports elucidated how inductive factors can increase progenitor activity after SCI and even encourage spontaneous remyelination of spared axons[221-223]; however, the ability of these endogenous progenitors to potentiate myelination of large numbers of newly regenerating axons has not been determined.

In this report, we investigated noggin and PDGF individually or in combination for their ability to enhance myelination of regenerating axons growing through a biomaterial bridge implanted into an acute spinal cord lesion. A mouse lateral hemisection model was used, with immediate intervention with PLG bridges inserted into the injury to deliver lentiviral vectors for sustained and localized expression noggin and/or PDGF [183, 224]. Immunohistochemistry (IHC) was initially employed to quantify the extent of axon growth and myelination, and functional recovery was quantified using the Basso Mouse Scale (BMS) scale. As myelination can occur from CNS-derived

oligodendrocytes or PNS-derived Schwann cells, we quantified the source of myelinating cells, as well as the density of cells within the oligodendrocyte lineage. Collectively, these studies demonstrate the potential for synergy between biomaterials to guide tissue growth and the localized expression of factors to modulate the local environment and enhance the recruitment of endogenous progenitors that can restore function.

Materials and Methods

Virus production and validation

HEK-293FT cells (80-90% confluent, American Type Culture Collection (ATCC), Manassas, VA, USA) were transfected with third generation lentiviral packaging vectors [114] and pLenti-CMV-Luciferase, pLenti-CMV-noggin, or pLenti-CMV-PDGF. Correct insertion was validated via DNA sequencing. Plasmids were incubated in OptiMEM (Life Technologies, Carlsbad, CA, USA) with Lipofectamine 2000 (Life Technologies) for 20 minutes prior to being added to cells. After 48 hours of incubation, supernatant was collected, centrifuged to remove cellular debris, and then incubated with PEG-It (System Biosciences, Palo Alto, CA, USA) for 16-24 hours at 4°C. Virus was centrifuged at 1500g at 4°C for 30 min, supernatant was removed, and the pellet was re-suspended in sterile phosphate buffered saline (PBS; Life Technologies). Viral solution was aliquoted and frozen at -80°C until use. Viral titers used throughout the study were 3E9 IU/mL as determined by the Lentivirus qPCR Titer Kit (Applied Biological Materials, Richmond, BC, Canada).

Fabrication of multi-channel bridges

Bridges were fabricated using a sacrificial template variation[225] of the gas foaming/particulate leaching technique, as previously described[83, 177]. Briefly, PLG (75:25 lactide:glycolide; i.v. 0.76

dL/g; Lakeshore Biomaterials, Birmingham, AL, USA) was dissolved in dichloromethane (6% w/w) and emulsified in 1% poly (ethylene-alt-maleic anhydride) using a homogenizer (PolyTron 3100; Kinematica AG, Littau, Switzerland) to create microspheres (z-average diameter ~1μm). D-sucrose (Sigma Aldrich), D-glucose (Sigma Aldrich), and dextran MW 100,000 (Sigma Aldrich) were mixed at a ratio of 5.3:2.5:1 respectively by mass. The mixture was caramelized, cooled, and drawn from solution with a Pasteur pipette to make sugar fibers. Fibers were drawn to 150 – 250 μm, coated with a 1:1 mixture of PLG microspheres and salt (63-106 μm) and pressed into a salt-lined aluminum mold. The sugar strands were used to create 7 channels and the salt create a porous structure. The materials were then equilibrated with CO_2 gas (800 psi) for 16 h and then gas foamed in a custom-made pressure vessel. Bridges were subsequently cut into 2.25 mm sections and leached for 2 h to remove porogen. The bridges are dried overnight and stored in a desiccator.

Virus loading into bridges

Viruses were adsorbed onto bridges, with multiple steps to increase lentiviral loading. Prior to virus addition, bridges were disinfected in 70% ethanol and washed with sterile water. Bridges were then dried by touching sterile filter paper to the bridge. Bridges were then saturated with 2 μL of virus. After 2 minutes of incubation, sterile filter paper was touched to the surface of the bridge to remove excess moisture. This process was then repeated until a total of 8 μL of virus was added. After the final addition, the bridges were not dried with filter paper and were stored on ice until use. Bridges were used within 3 hours of coating with lentivirus. Lentivirus loading conditions included FLuc, PDGF, noggin, and noggin + PDGF. Lentiviral loading was done to ensure the same number of lentiviral particles per bridge.

Mouse spinal cord hemisection

All animal procedures were approved and in accordance with the Institutional Animal Care and Use Committee at the University of Michigan. A hemisection model of SCI was performed as previously described[177] on female C57BL/6 mice (6-8 weeks old; Jackson Laboratories). After administration of bupivacaine (.8 ml/kg), a laminectomy was performed at T9-T10 to allow for a 2.25 mm lateral hemisection for immediate bridge implantation. The injury site was covered using Gelfoam (Pfizer, New York, NY, USA) followed by suturing together of the muscle and stapling of skin. Postoperative care consisted of administration of enrofloxacin (2.5 mg/kg; daily for 2 weeks), buprenorphine (0.1 mg/kg; twice daily for 3 days), and Lactated Ringer's solution (5 mL/100 g; daily for 5 days). Bladders were expressed twice daily until function recovered.

Immunohistochemistry and quantitative analysis of nerve regeneration, myelination, and NPC differentiation

Spinal cords were extracted 8 weeks after SCI and flash frozen in isopentane. For immunofluorescence, spinal cord segments were embedded in Tissue Tek O.C.T. Compound (Sakura Finetek, Torrance, CA, USA) with 30% sucrose. Cords were cryo-sectioned transversely in 18-μm-thick sections. Antibodies against the following antigens were used for immunofluorescence: neurofilament 200 (NF-200, Sigma Aldrich), myelin basic protein (MBP, Santa Cruz Biotech, Dallas, TX, USA), Protein-zero myelin protein (P0, Aves Labs, Tigard, OR, USA), Sox2 (Abcam), Olig2 (Millipore), NG2 (Millipore), and O4 (Millipore). Tissues were imaged on an Axio Observer Z1 (Zeiss, Oberkochen, Germany) using a 10x/0.45 M27 apochromatic objective and an ORCA-Flash 4.0 V2 Digital CMOS camera (C11440-22CU, Hamamatsu Photonics, Hamamatsu City, Shizuoka, Japan) or Nikon A1+ (Nikon Inc., Garden City, NY) using a 60x/1.4 apochromatic objective.

To assess the numbers of regenerated and myelinated axons within the PLG bridge area, NF-200 was used to identify axons, NF-200$^+$/MBP$^+$ to determine the number of myelinated axons, and NF-200$^+$/MBP$^+$/P0$^+$ to determine the amount of myelin derived from infiltrating Schwann cells[183]. Twenty-one tissues distributed between conditions were counted by 2 blinded counters to calibrate software for automated counting developed by McCreedy et al[226]. In short, images were imported into MATLAB and the area of the section corresponding to PLG bridge was outlined. A Hessian matrix was created by convolution filtering using second derivative of the Gaussian function in the x, y, and xy directions. Eigenvalues were determined by extracted from the Hessian matrix and used to reconstruct the original image. Following filtering, positive NF-200 events were identified by intensity threshold, single pixel events were removed, and the number of connected objects were identified. This ensures highly branching axons are counted as one object and long axons are also counted as one object. For calibration, the software will output a matrix of potential axon counts based on this method. These values are directly compared to manual counts for the initial 22 tissues used for calibrating the software. The appropriate filter size and threshold sensitivity are selected based on the correlation between the manual and automated counts to properly calibrate the software for use in quantifying the remaining tissues that had not been manually counted. To obtain axon densities, total NF-200 counts were divided by the area of the PLG bridge. MBP and P0 events were identified similarly. NF-200 objects containing pixel locations overlapping with positive MBP or P0 staining were counted and compared to total NF-200 counts. To ensure proper calibration, Pearson's coefficients were compared between counters and between the software and the counter averages.

Nine tissues were selected randomly from the rostral, middle, and caudal section of the bridge implant from each animal (n=6) of each condition to be counted for progenitors and differentiated

cells. Immunopositive cells within the PLG bridges were counted manually by four researchers independently. Due to PLG material generally exhibiting high background, cells were counted as Olig2 or Sox2 positive only when appearance of these markers spatially overlapped Hoechst 33342 counterstaining. Co-staining for multiple markers was always assessed by evaluating overlap of pixels above a set threshold in images acquired over identical sample areas. Co-localization of Sox2 and Olig2, was evaluated to determine the numbers of NPCs and OPCs. To quantify densities, total immunopositive cells were divided by the area of PLG outlined.

Behavioral analysis

The Basso mouse scale (BMS) open-field locomotor test was used to evaluate functional recovery over period of 8 weeks after SCI as previously described[227] for FLuc (n=12) and noggin + PDGF (n=12) conditions. A baseline was determined prior to SCI, and the mice were tested at 1, 2, 4, 6, and 8 weeks. Observations and BMS scoring were performed by two blinded observers for 4 minutes per animal.

Statistical analysis

For multiple comparisons, statistical significance between groups was determined by one-way or two-way ANOVA with Bonferroni's post-hoc. For single comparisons, the statistical significance between pairs was determined by unpaired t-test. All statistics test significance using a α value of 0.05. Error bars represent standard error in all figures. Prism 7 (GraphPad Software, La Jolla, CA, USA) software was used for all data analysis.

Data Availability

The datasets generated during and/or analyzed during the current study are available from the corresponding author on reasonable request.

Results

Lentiviral construct validation

Initial studies validated the lentiviral constructs encoding noggin and PDGF. HEK-293FT cells were transduced with a multiplicity of infection (MOI) of 10 viral particles per cell with noggin-encoding lentivirus. After 3 days, expression of noggin was assessed with anti-noggin antibody with Hoechst 33342 counterstaining (**Figure 5.1**). There was substantial staining with anti-noggin antibodies throughout cells transduced with lentivirus. There is also substantial staining of noggin in the cytosol. PDGF overexpression was validated by transducing HEK-293FT cells with MOI 10 of PDGF lentivirus and quantifying protein level with an ELISA kit. PDGF protein expression increased 4-fold over cell transduced with FLuc lentivirus.

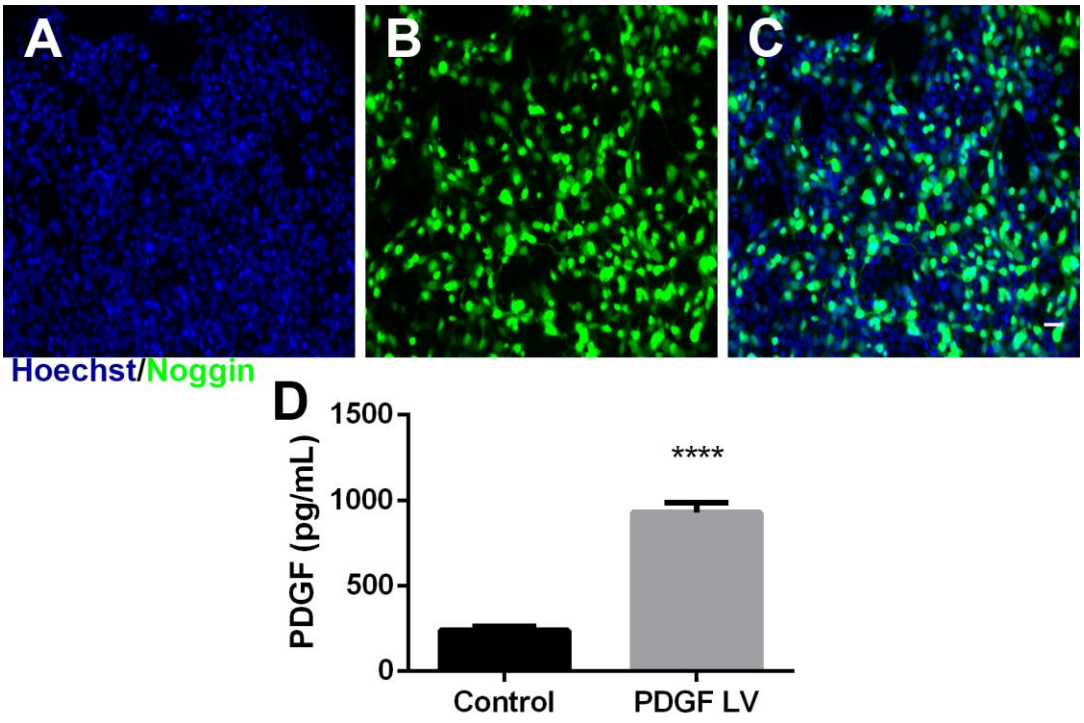

Figure 5.1 Noggin and PDGF expression. (A) Hoechst (blue), (B) Noggin (green), and (C) overlaid images of lentiviral expression of noggin. (D) Quantification of PDGF secretion protein from cells transfected with no virus (Control) or PDGF lentivirus using ELISA. Data presented as mean +/- SEM. Scale: 50 µm **** denotes $p<0.0001$ v. control.

Increased axon numbers and myelination post injury

We quantified axonal density as a function of FLuc, noggin, PDGF, or co-delivery of both factors from the bridge. Axons (NF-200^{+}) were present throughout the bridges (**Figure 5.1**) 8 weeks after SCI in all experimental conditions. NF-200^{+} axons were typically observed in small groups or bundles as previously reported for multi-channel PLG bridges[83, 226]. FLuc bridges had a mean of approximately 800 axons/mm^2, single lentiviral conditions had approximately 1100 axons/mm^2, and noggin + PDGF had approximately 1200 axons/mm^2 (**Figure 5.2**) However, these differences were not statistically significant.

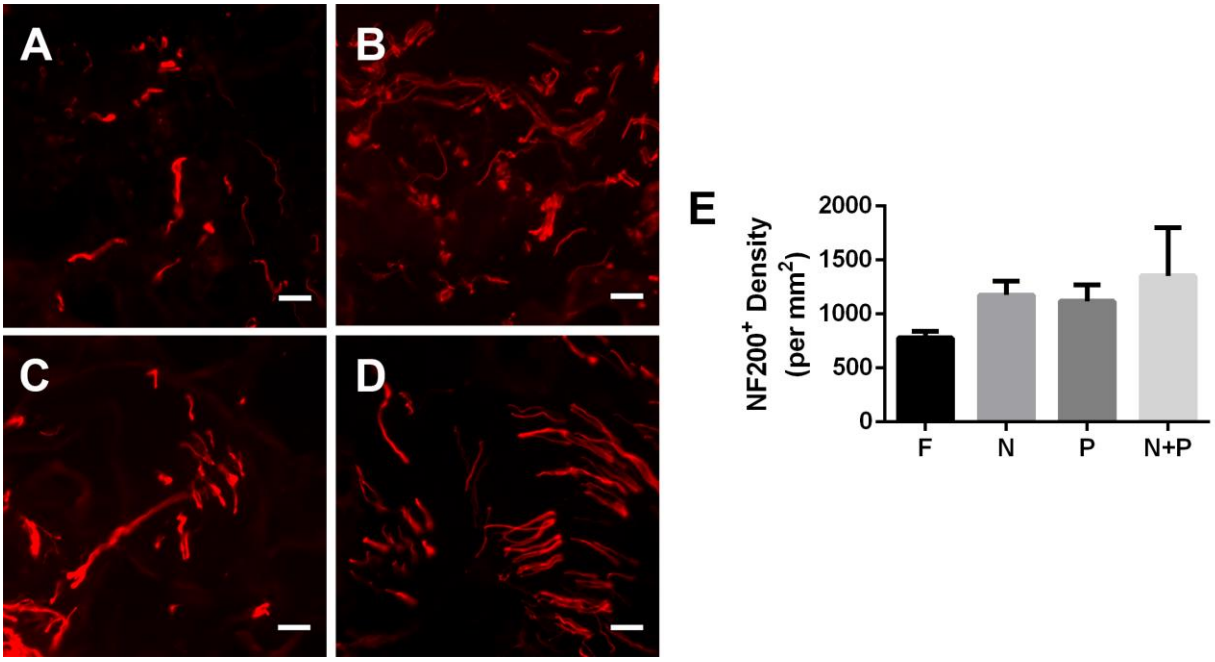

Figure 5.2 Axonal growth at 8 weeks post injury. NF-200+ (red) immunofluorescence from bridge implants delivering (A) FLuc, (B) Noggin, (C) PDGF, or (D) Noggin + PDGF. Brightness and contrast were adjusted for clarity. (E) Quantification of axon density in FLuc, Noggin, PDGF, and Noggin + PDGF conditions. Data presented as mean +/- SEM. Scale: 20 μm. N = 6 per condition.

Myelinated axons (NF-200^{+}/MBP^{+}) (**Figure 5.3**) were present throughout bridge implants and typically appeared in bundles of multiple axons as previously reported. Myelinated axon density in the bridge implants was significantly enhanced, approximately 3-fold by co-delivery of noggin + PDGF relative to FLuc controls (**Figure 5.3E**). While single lentiviral vector delivery increased

the density of myelinated axons compared to the FLuc control, it was not significant. The percentage of axons myelinated, which was determined from the ratio of NF-200^{+}/MBP^{+} axons divided by total number of NF-200^{+} axons, was approximately 30% with no differences between groups for the control and individual factor expression (**Figure 5.3F**); however, combined noggin + PDGF delivery resulted in a significantly higher percentage of myelinated axons at 44%.

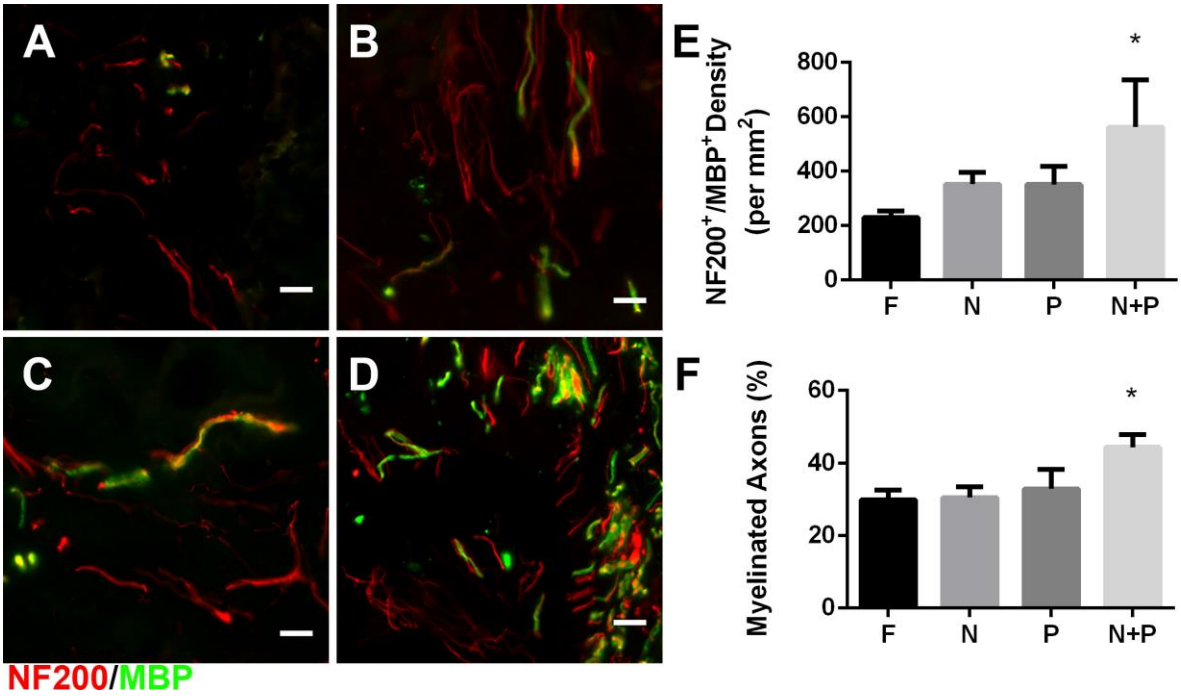

Figure 5.3 Myelinated axons 8 weeks post injury. NF-200+ (red) /MBP+ (green) immunofluorescence from bridge implants delivering (A) FLuc, (B) Noggin, (C) PDGF, or (D) Noggin + PDGF. Brightness and contrast were adjusted for clarity. Quantification of (E) myelinated axon density and (F) percentage of myelinated axons in FLuc, Noggin, PDGF, and Noggin + PDGF conditions. Data presented as mean +/- SEM. Scale: 20 µm. * denotes $p<0.05$ v. FLuc. N = 6 per condition.

Enhanced motor function recovery with combinatorial delivery

We subsequently investigated the capacity for the combination of PDGF + noggin, which enhanced myelinated, to improve functional recovery. Bridges loaded with noggin + PDGF were implanted into the lateral hemisection, with a control cohort receiving FLuc, and motor function was evaluated for 8 weeks post-SCI using the BMS (**Figure 5.4**)

. Prior to surgery, all mice were fully functional with perfect scores (BMS = 9). At 1-week post-SCI, all mice had no movement in the ipsilateral hindlimb. From week 4 onward, mice

receiving noggin + PDGF co-delivery had significantly improved function in comparison to mice that received bridges with FLuc lentivirus. Mice receiving noggin + PDGF lentivirus earned an average BMS score of approximately 4.2, with a score of 4 indicating occasional stepping. By comparison, mice from the control condition mice scored at an average of approximately 1.5,

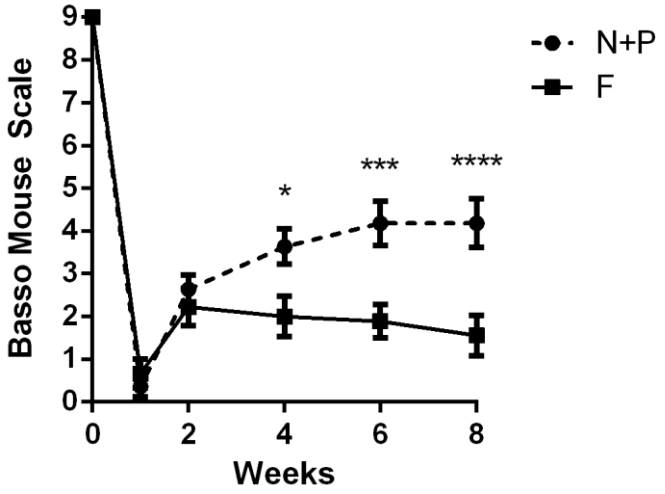

Figure 5.4 Functional recovery induced by Noggin + PDGF co-delivery. The Basso Mouse Scale was used to determine differences in motor recovery in the ipsilateral hindlimb. Data presented as mean +/- SEM. ** denotes $p<0.05$ v. FLuc, *** denotes $p<0.001$ v. FLuc, **** denotes $p<0.0001$ v. FLuc. N = 12 per condition.

.

which indicates ankle movement, yet an inability to achieve paw placement or perform stepping.

Source of myelination post injury

The source of myelination in the bridge was subsequently characterized to further investigate the correlation between increased myelination and motor function recovery. Histological sections were immunostained to identify Schwann cell ($NF\text{-}200^+/MBP^+/P0^+$) or oligodendrocyte-derived myelin ($NF\text{-}200^+/MBP^+/P0^-$) (**Figure 5.5**). No significant difference in density of Schwann cell myelinated axons between conditions was observed. In control, noggin, and PDGF conditions, the density of oligodendrocyte-derived myelin was approximately 100 neurites/mm^2. Overexpression of noggin + PDGF resulted in approximately 250 neurites/mm^2, a significant 2.5-fold increase

(**Figure 5.5E**). The percentage of oligodendrocyte-derived myelin was determined as the ratio of number of NF-200^{+}/MBP^{+}/P0^{-} axons divided by the total number of NF-200^{+} axons. Overexpression of noggin or PDGF alone resulted in similar percentages of oligodendrocyte-derived myelin as control animals at 11-13%. Combined overexpression of noggin + PDGF significantly increased the level of total axons myelinated by oligodendrocytes to 22% relative to all experimental conditions (**Figure 5.5F**).

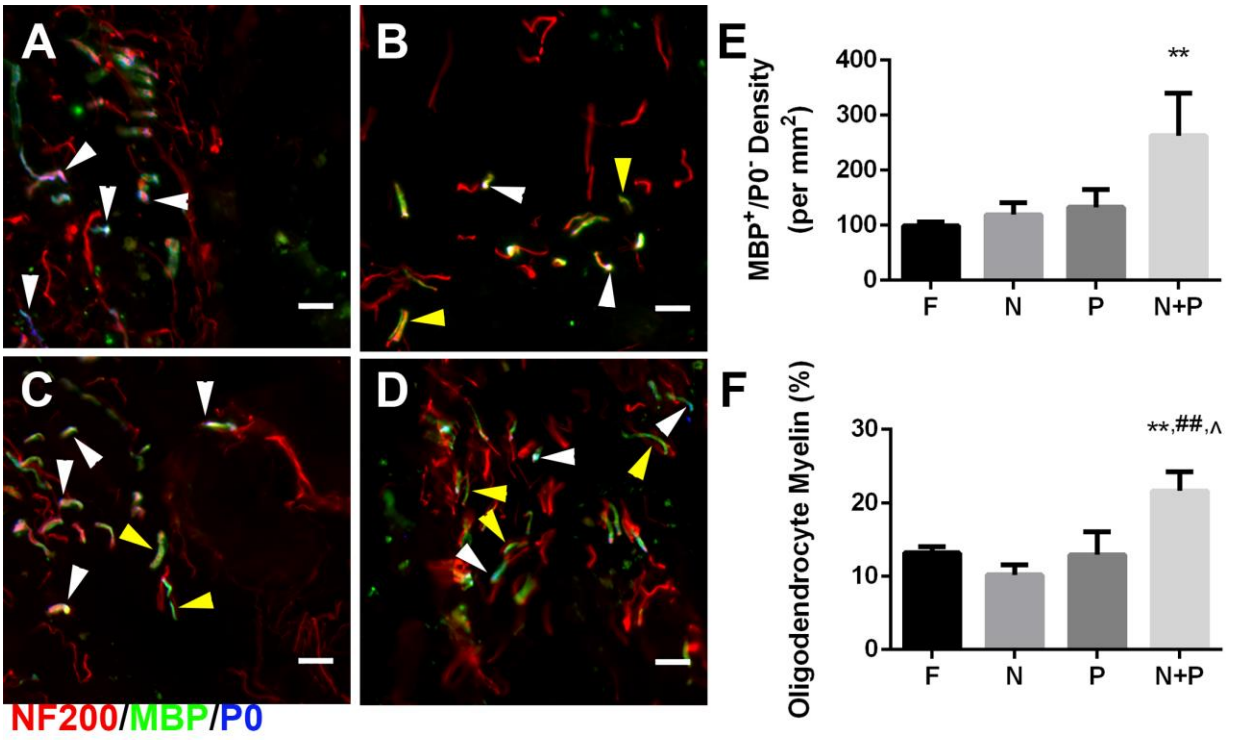

Figure 5.5 Source of myelination 8 weeks post injury. Immunofluorescence from bridges of Schwann cell (NF-200+/MBP+/P0+: red/green/blue, respectively) and oligodendrocyte (NF-200+/MBP+/P0-) derived myelin fibers from bridge implants delivering lentivirus encoding (A) FLuc, (B) Noggin, (C) PDGF, or (D) Noggin + PDGF. White arrows show fibers wrapped by Schwann cell myelin. Yellow arrows show fibers wrapped by Oligodendrocyte myelin. Brightness and contrast were adjusted for clarity. Quantification of (E) oligodendrocyte myelin density and (F) percentage of oligodendrocyte-derived myelinated axons in FLuc, Noggin, PDGF, and Noggin + PDGF conditions. Data presented as mean +/- SEM. Scale: 20 µm. ** denotes p<0.01 v. FLuc, ## denotes p<0.01 v. Noggin, ^ denotes p<0.05 v. PDGF. N = 6 per condition.

Recruitment and differentiation of endogenous progenitors

The increase in CNS-derived oligodendrocyte myelination of regenerating axons at 8 weeks post-injury within the bridge was subsequently interrogated by quantifying the density of cells within the oligodendroglial lineage. The presence of oligodendrocytes was evaluated by staining for O4 (**Figure 5.6**). Few O4^{+} pre-oligodendrocytes were observed in controls (**Figure 5.6J**). A

significant increase in $O4^+$ cells for noggin + PDGF overexpression was observed compared to all other experimental conditions (**Figure 5.6J**).

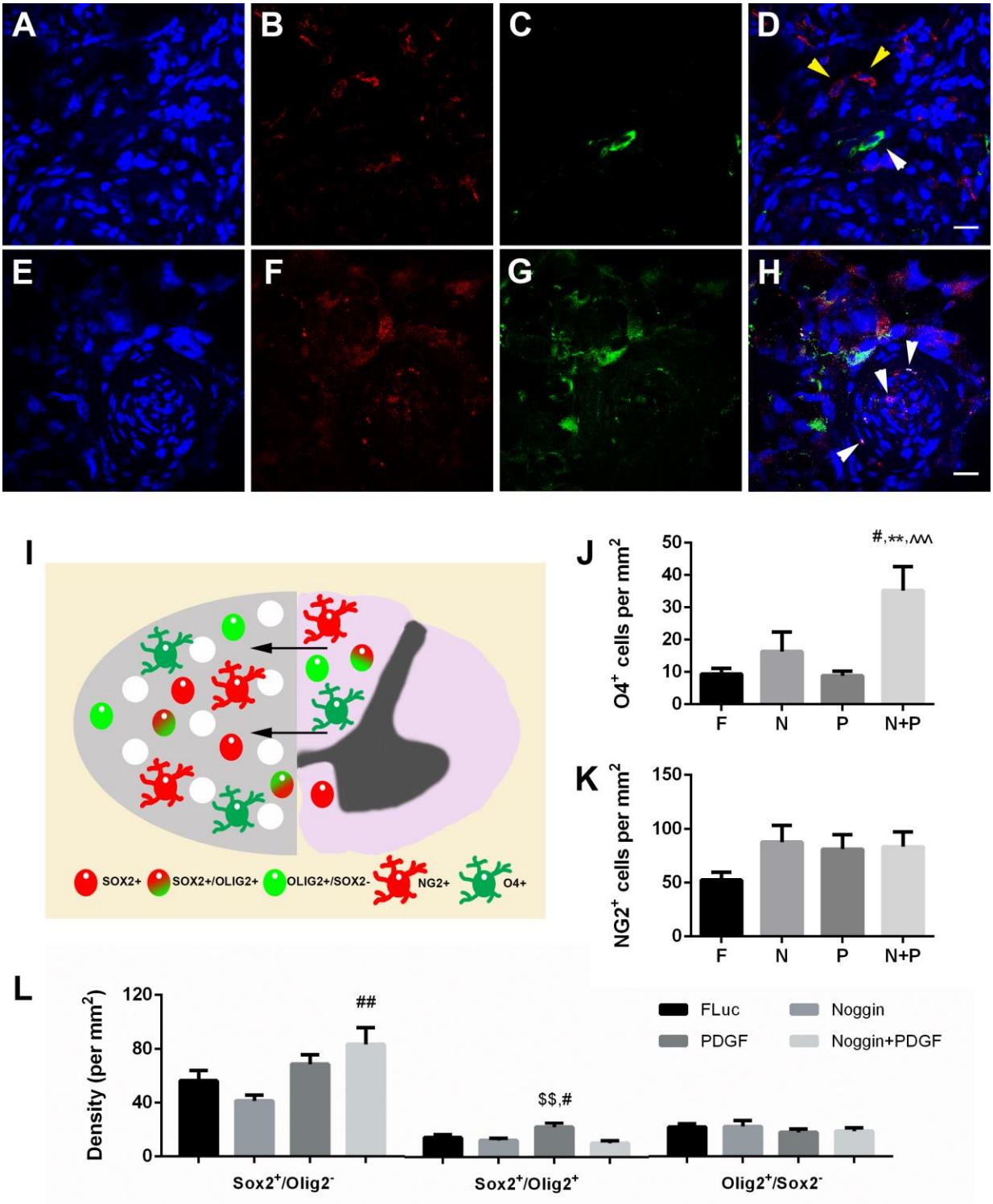

Figure 5.6 Oligodendrocyte-lineage cells in bridge implants at 8 weeks post injury. Images are representative of positive cell counts. (A-D) Oligodendrocyte-lineage cells at 8 weeks post injury. (A) Hoechst, (B) NG2+, and (C) O4+ expression in bridge implants. (D) Merged image. Yellow arrows denote NG2+ cells. White arrows denote O4+ cells. Scale: 20 μm. (E-H) Neural progenitor cells at 8 weeks post injury. (E) Hoechst, (F) Sox2+, and (G) Olig2+ expression in bridge implants. (H) Merged image shows single expression and co-expression of Sox2 and Olig2. White arrows indicate positive nuclei for co-expression. Brightness and contrast were adjusted for clarity. Scale: 20 μm. (I) Schematic of infiltration of cells into bridge implants from uninjured contralateral tissue following injury. Cells nearest the midline migrate into the bridge to support regenerating axons. (J) Quantification of O4+ cells. (K) Quantification of NG2+ cells. (F) Quantification of neural progenitor cell phenotype densities. Data presented as mean +/- SEM. ** denotes $p<0.01$ v. FLuc, # denotes $p<0.05$ v. Noggin, ## denotes $p<0.01$ v. Noggin, $$ denotes $p<0.01$ v. Noggin + PDGF, ^^^ denotes $p<0.001$ v. PDGF. N = 6 per condition.

Cells in the oligodendrocyte lineage (O4+) can arise from either neural progenitor cells (NPCs) that are Sox2+, or from glial-restricted progenitors ($Olig2^+/Sox2^-$ or NG2+), which were subsequently analyzed. This analysis was performed at the 8-week time point, which would provide enough time for the progenitors to develop along the multiple lineages. For glial-restricted OPCs (Fig 6B), no significant differences in the density of $Olig2^+/Sox2^-$ cells or $NG2^+$ cells across experimental conditions were observed (**Figure 5.6L**). However, the density trended toward an increase in $NG2^+$ stained cells for all conditions compared to control (**Figure 5.6K**). Similar levels of $NG2^+$ cells levels were present for noggin, PDGF, and combination of noggin + PDGF overexpression.

For NPCs ($Sox2^+$), noggin over-expression resulted in no significant difference in number of $Sox2^+$ cells relative to FLuc delivery (**Figure 5.6L**). In contrast, PDGF over-expression trended towards elevated numbers of $Sox2^+$ cells relative to noggin over-expression. Interestingly, the combination of noggin + PDGF had an additive effect, producing significantly more $Sox2^+$ cells relative to noggin over-expression alone. We subsequently assessed the co-localization of Sox2 and Olig2 markers, which represents $Sox2^+$ NPCs in the process of differentiating along oligodendrocyte lineages that leads to nuclear expression of Olig2[200, 228, 229]. A significant increase in density of $Sox2^+/Olig2^+$ cells was observed with PDGF overexpression compared to noggin and noggin + PDGF overexpression (**Figure 5.6L**), indicating a greater number of NPCs differentiating into OPCs. Collectively, these studies suggest that the combination of PDGF +

noggin enhances the recruitment of both glial-restricted progenitors and NPCs toward an oligodendrocyte lineage.

Discussion

We investigated remyelination of regenerating axons by endogenous cells responding to lentiviral induced trophic factor production by cells recruited into PLG multi-channel bridges implanted into a T9-10 mouse lateral hemisection SCI. We have previously reported axonal growth post-SCI through an aligned linear multichannel bridge which also provides a porous structure for cellular infiltration[83, 137, 178]. These bridges are a valuable tool to study the spinal cord microenvironment post-injury and investigate treatments in a controlled and defined manner. The bridges are acellular, indicating that any cells, extracellular matrix, or proteins present in the bridge at the time of extraction must have originated from the host tissue. Similarly, any axons entering the implant must be attributed to either regeneration of injured axons or sprouting of new axons from spared or contralateral tissue. This bridge provides a defined space for histological analysis, analysis of cell populations at and near the lesion site, and treatment outcomes. The bridge alone has supported robust axon ingrowth, myelination, and recovery of some motor function[181]. These bridges also provide a vehicle for lentiviral delivery resulting in long-term, localized transgene expression with delivery of multiple factors which is difficult to achieve and generally requires the use of osmotic pumps[83, 183]. Osmotic pumps can clog, require surgery for removal, and can cause further tissue damage. Other reports have used direct injection of vectors, which may not localize delivery to the injury. Unlike other viral vectors, lentivirus does not influence the phenotype of progenitors[230] or cause significant inflammation[128]. The physical properties of lentiviral vectors are independent of the encoding gene, which allows for the exchange of vectors or the potential to deliver multiple vectors encoding various inductive factors without modification to the base

biomaterial creating a high-throughput system. In these studies, we delivered two distinct transgenes from PLG bridges alone and in combination. We have previously demonstrated sustained expression for a minimum of 12 weeks, with peak expression localized within the bridge and decreased expression both rostral and caudal to the bridge[182]. This expression pattern ensures the delivered factors can have prolonged, targeted effects on cells within the intact tissue and infiltrating cells within the bridge.

Co-delivery of noggin + PDGF significantly increased the density of myelinated axons and achieved the largest percentage of myelinated axons (44%) and oligodendrocyte-derived myelin (22%) that we have observed. While, co-delivery of noggin + PDGF did not significantly increase axon density versus control, the combination did enhance myelination relative to individual factors or control. For comparison to the extent of myelination, delivery of SHH and NT3 in our previous studies only resulted in ~30% of myelinated axons and ~13% of oligodendrocyte-derived myelin when compared to total axon counts[183]. Current estimates of myelinated axons in healthy spinal cord of rodent models range from 40 – 60%[231-233]. Therefore, this represents a significant result in the enhancement of axon myelination. Reports from other systems have demonstrated varying degrees of remyelination via delivery of single factors[234, 235] or cell transplantation[154, 201, 236, 237], with these reports not achieving the myelination levels reported herein. Lack of myelination has been demonstrated to be a significant hindrance to recovery of function to regenerating axons[187, 238], and we employed the BMS and identified a significant increase in motor function improvement after SCI compared to control. This result suggests the difference in myelination density and percentage may contribute in part to the improved functional outcomes. This result is consistent with other research suggesting remyelination contributes to normal function recovery[187]. Another interesting outcome is that no difference in Schwann cell myelin between groups was observed,

yet only the noggin/PDGF combination resulted in improved functional outcome, potentially due to the differences in oligodendrocyte-derived myelination. Oligodendrocyte-derived myelin has been reported to be thicker and more supportive of axonal growth. This suggests that oligodendrocyte-derived myelin is necessary for return of function and Schwann cell myelin is inefficient.

The increased myelination and functional recovery were associated with a greater recruitment of progenitor cells into the oligodendrocyte lineage. Post injury, oligodendrocyte-lineage cells have been reported to migrate from the spared tissue to repopulate lost cell populations[239]. These progenitor cells proliferate extensively between 24 hours to 2 weeks post injury but these populations are reduced at later timepoints [199, 240]. Therefore, many progenitor cell populations would not be expected to be present in the bridges at 8 weeks post-injury without trophic factor expression. Our results with the control bridge (i.e., FLuc expression) are consistent with the relatively low density of progenitor cells populations. However, the delivery of lentivirus encoding for noggin, PDGF, or noggin/PDGF combination for sustained transgene expression altered the recruitment and differentiation of progenitor cells. At 8 weeks post-injury, endogenous progenitor pools were present within the bridge with trophic factor delivery. NPCs ($Sox2^+$) can differentiate into OPCs ($Olig2^+$, $NG2^+$) by exposure to various factors, and OPCs can differentiate into multiple other cell types including oligodendrocytes, astrocytes, Schwann cells, and neurons[241]. At the $O4^+$ stage, the cells are lineage locked into becoming mature, myelinating oligodendrocytes. Noggin expression at the bridge would be expected to block the receptors for BMP 2/4/7, which would normally act to inhibit NPC differentiation and migration [212, 242, 243]. The decreased presence of NPCs relative to control with noggin expression is consistent with inhibiting the action of BMPs, which would allow differentiation of NPCs toward an oligodendrocyte lineage. Although noggin

alone increased the presence of $O4^+$ oligodendrocytes, noggin alone was insufficient to induce myelination of large numbers of regenerating axons.

Delivery of PDGF-encoding lentiviral vectors from the bridge significantly increased the presence of OPCs ($Sox2^+/Olig2^+$). PDGF in the spinal cord elicits multiple effects on OPCs, such as increasing the proliferation[215, 217, 244] and differentiation[22, 219, 245] of OPCs at lesions. In contrast, *in vitro* culture studies with oligodendrocytes indicated an inhibition of myelinating properties[246], and has been reported to delay oligodendrocyte differentiation and axonal myelination *in vivo* during development[247]. However, the distinct effects of PDGF may depend on its temporal availability during proliferation, differentiation, and myelination[248], as withdrawal of this growth factor triggers cell-cycle exit and differentiation[249]. Herein, lentivirus was used for the sustained expression of PDGF for the 8-week study resulting in increased OPC density. However, these increases in OPC density did not contribute to increased density of $O4^+$ pre-oligodendrocytes, which is consistent with the lack of increased myelination and oligodendrocyte-derived myelin relative to control. Conditional expression systems such as the tetracycline system have been used for temporal control of lentiviral expression [250]. This type of viral delivery system could allow for PDGF to be expressed transiently to encourage further maturation of OPCs.

Interestingly, combined delivery of noggin + PDGF encoding lentivirus significantly increased the presence of $O4^+$ pre-oligodendrocytes. The noggin + PDGF overexpression significantly increased Sox2+/$Olig2^-$ cell density compared to noggin alone and had similar density compared to PDGF. This result suggests the decrease in $Sox2^+/Olig2^-$ caused by noggin delivery may have been offset by PDGF co-delivery. Co-delivery also resulted in significantly lower densities of $Olig2^+$ cells compared to other conditions. However, the density of $O4^+$ pre-oligodendrocytes was increased 4-fold relative to control and PDGF conditions and 2-fold relative to noggin alone.

Noggin alone increased the density of immature oligodendrocytes, yet when paired with PDGF, the increase was further enhanced. Although these cells were $O4^+$, many cells did not exhibit a typical oligodendrocyte morphology. The O4 marker for differentiation is expressed at many stages of oligodendrocyte lineage so positive cells may not resemble the classical mature oligodendrocyte morphology. Furthermore, biomaterials and SCI have varying effects on the morphology of cells dependent on stiffness, modulus, and severity of injury [251-254], thus cells may not exhibit classical morphology due to biomaterial interactions and injury. However, we note that $O4^+$ cells are lineage locked to becoming myelinating oligodendrocytes [255]. These findings suggest that combinatorial delivery of inductive factors can considerably enhance the recruitment and differentiation of endogenous OPCs that persist at long time points.

Conclusion

Collectively, we report the ability of noggin + PDGF to promote remyelination by endogenous progenitor cells post-SCI. Co-delivery of noggin + PDGF encoding lentivirus significantly increased total myelinated axon density and percentage. Co-delivery also promoted greater myelination by oligodendrocytes compared to all other conditions (22% vs 11%). This result was consistent with the increased density of $O4^+$ pre-oligodendrocytes via co-delivery. Overall, we have demonstrated that lentivirus-based expression of multiple factors, such as noggin and PDGF, from multichannel PLG bridges provides a strategy for identifying synergistic actions with the potential to target multiple barriers to regeneration.

Bridges are increasingly being considered for both penetrating wounds as well as for chronic injuries in which the scar is surgically resected that creates a defect [256]. While the bridge provides a path and support for axon regeneration, it is insufficient alone to promote regeneration. As we have shown, PDGF and noggin may be used to recruit and differentiate endogenous progenitors

after spinal cord injury to encourage remyelination. Lentivirus represents an effective strategy to increase and sustain levels of these target proteins at the injury. Lentiviral vectors are currently in clinical trials [257] and, at a minimum, represent a tool to identify factors or combinations of factors that enhance myelination. An alternative to lentivirus delivery would be the direct delivery of these proteins, which is being attempted by various delivery strategies [115]. This combination of a bridge to support and direct axon growth with a strategy to enhance their myelination represents a potential clinically translatable treatment for SCI.

Chapter 6. Polycistronic Delivery of IL-10 and NT-3 Promotes Oligodendrocyte Myelination and Functional Recovery

Authors

Dominique R. Smith, Courtney M. Dumont, Jonghyuck Park, Andrew J. Ciciriello, Amina Guo, Ravindra Tatineni, Brian J. Cummings, Aileen J. Anderson, Lonnie D. Shea

Abstract

There are more than one million estimated cases of spinal cord injury (SCI) in the United States and repairing an injury has constituted a difficult clinical challenge. Many strategies have been unsuccessful due to the complex, dynamic, inhibitory microenvironment post injury. This inhibitory environment is characterized by pro-inflammatory signaling from invading leukocytes and lack of sufficient factors that promote axonal survival and elongation. We have developed multi-channel PLG bridges for spinal cord regeneration. The bridges provide a vehicle for lentiviral delivery for continuous and localized transgene expression. However, there are limitations to viral delivery and expression based on bridge surface area and cell density in the spinal cord. Therefore, we have investigated an alternative strategy using polycistronic vectors. Polycistronic vectors encode multiple transgenes for co-expression of multiple factors. In the present study, we investigated polycistronic delivery of IL-10+NT-3 using PLG bridges after acute SCI. We observed a significant increase in the density of regenerative macrophages for IL-10+NT-3 condition. Combined delivery of IL-10+NT-3 produced a significant increase of axonal density and notably corticospinal tract axons compared to all other conditions. Furthermore, we observed

a significant functional recovery for IL-10+NT-3 delivery at 12 wpi that was significantly positively correlated to oligodendrocyte myelinated axon density. This suggests oligodendrocyte myelin as an important area of future of research to improve functional recovery. These results further buttress multichannel PLG bridges as a growth supportive substrate and platform to deliver bioactive agents as well as a defined space to investigate the SCI microenvironment and potential treatments.

Introduction

There are approximately 12, 000 estimated new cases of SCI in the United States each year and repairing an injury to the spinal cord has constituted one of the most difficult clinical challenges[258]. Many strategies have been developed to aid the regeneration of the central nervous system (CNS) but have largely been unsuccessful due to the complex, dynamic, inhibitory microenvironment after the injury. This inhibitory environment is created by a combination of barriers to nerve regeneration, most notably pro-inflammatory signaling from invading immune cells and lack of sufficient factors that promote axonal survival and elongation[2]. This environment has led to the discovery of the cytokine/neurotrophin axis in axon growth. Cytokines (IL-10, IL-4, IL-6) released by invading macrophages can influence the expression of neurotrophins (NT-3, NT-4, NGF) and their receptors[259]. Macrophages invade the lesion site and contribute to both injury and repair [260]. Macrophages exist on a spectrum of activation states ranging from pro-inflammatory to pro-regenerative [261, 262]. Pro-regenerative macrophages present enhanced phagocytosis capabilities [263, 264] and can promote tissue regeneration [260]. The pro-inflammatory/pro-regenerative ratio can expedite or drastically reduce axonal growth into the lesion site[265]. Combinations of different interleukins and neurotrophins have been shown to promote or inhibit neurite extension but these relationships have not been evaluated in vivo [259, 266].

Traditional strategies for localized delivery of factors involve osmotic pumps which can clog and require surgery for removal or direct injection of factors which can be carried away and lead to off target effects in the body [83, 183, 267]. We have developed multi-channel PLG bridges with an architecture for cellular infiltration and axon elongation while also capable of long-term, localized transgene expression of lentivirus. Previously, we have delivered single viral vectors with positive results, but there is a need for delivery of multiple factors to address the multiple barriers to regeneration. The limiting factors of multiple gene expression are the concentration of the virus and its stability. Higher concentrations of delivered lentivirus may increase negative effects associated with immunogenicity and potentiate its clearing. These limitations suggest we need an effective way to delivery multiple factors without increased concentrations of lentivirus.

We have investigated an alternative strategy based on polycistronic viral vectors. Polycistronic vectors negate the limitations of single lentiviral vectors by encoding co-expression of multiple genes by adding "self cleaving" 2A peptide sites between genes. 2A peptides can lead to high levels of downstream protein expression compared to other strategies for multi gene co-expression and are small enough to not negatively interfere with the function of the co-expressed genes[268]. We have previously shown IL-10 can alter the phenotype of invading macrophages towards a pro-regenerative phenotype and lead to improved spinal cord regeneration [135, 224]. We have also previously shown that our bridges are capable of promoting neuron survival and axonal elongation through neurotrophic support with NT-3 [83]. However, we have not investigated if a combination of these factors achieves synergistic or antagonistic effects.

In the present study, we investigated polycistronic delivery of NT-3 and IL-10 using PLG bridges after acute SCI. We investigated the effects of combined delivery on macrophage phenotypes, axonal elongation and myelination, and source of the myelination at 12 weeks post

injury. Subsequently, we assessed the functional benefits of co-delivery of these factors and how it relates to the tissue regeneration we observed. This research builds upon the success of the multiple channel poly(lactide-*co*-glycolide) (PLG) bridges by delivering multiple gene factors that target separate barriers to regeneration to elucidate synergistic relationships.

Methods

Virus Production and validation

HEK-293FT cells (80-90% confluent, American Type Culture Collection (ATCC), Manassas, VA, USA) were transfected with third generation lentiviral packaging vectors and pLenti-CMV-Luciferase, pLenti-CMV-hNT3, pLenti-CMV-hIL10, or pLenti-CMV-hIL10/NT3. Correct insertion was validated via DNA sequencing. Plasmids were incubated in OptiMEM (Life Technologies, Carlsbad, CA, USA) with Lipofectamine 2000 (Life Technologies) for 20 minutes prior to being added to cells. After 48 hours of incubation, supernatant was collected, centrifuged to remove cellular debris, and then incubated with PEG-It (System Biosciences, Palo Alto, CA, USA) for 16-24 hours at 4°C. Virus was centrifuged at 1500g at 4°C for 30 min, supernatant was removed, and the pellet was re-suspended in sterile phosphate buffered saline (PBS; Life Technologies). Viral solution was aliquoted and frozen at -80°C until use. Viral titers used throughout the study were 2E9 IU/mL as determined by the Lentivirus qPCR Titer Kit (Applied Biological Materials, Richmond, BC, Canada).

Fabrication of multi-channel bridges

Bridges were fabricated using a sacrificial template variation[225] of the gas foaming/particulate leaching technique, as previously described[83, 177]. Briefly, PLG (75:25 lactide:glycolide; i.v. 0.70 - .90 dL/g; Lactel, Birmingham, AL, USA) was dissolved in dichloromethane (6% w/w) and

emulsified in 1% poly (vinyl-alcohol) using a homogenizer (PolyTron 3100; Kinematica AG, Littau, Switzerland) to create microspheres (z-average diameter ~1μm). D-sucrose (Sigma Aldrich), D-glucose (Sigma Aldrich), and dextran MW 100,000 (Sigma Aldrich) were mixed at a ratio of 5.3:2.5:1 respectively by mass. The mixture was caramelized, cooled, and drawn from solution with a Pasteur pipette to make sugar fibers. Fibers were drawn to 150 – 250 μm, coated with a 1:1 mixture of PLG microspheres and salt (63-106 μm) and pressed into a salt-lined aluminum mold. The sugar strands were used to create 9 channels and the salt created a porous structure. The materials were then equilibrated with CO_2 gas at 800 psi for 16 h to foam in a custom-made pressure vessel. Bridges were subsequently cut into 1.15 mm sections and leached for 2 h to remove salt porogen. The bridges were dried overnight and stored in a desiccator until use.

Virus loading into bridges

Prior to virus addition, bridges were disinfected in 70% ethanol and washed with sterile water. Bridges were then dried by touching sterile filter paper to the bridge. Bridges were then saturated with 2 μL of virus. After 2 minutes of incubation, sterile filter paper was touched to the surface of the bridge to remove excess moisture. This process was repeated with another 2 μL of virus added. The bridges were not dried with filter paper and were stored on ice until use. Bridges were used within 3 hours of coating with lentivirus to preserve viral activity. Lentivirus loading conditions included NT-3, IL-10, and IL-10+NT-3. Lentiviral loading was done to ensure the same number of lentiviral particles per bridge at 2E9 IU/mL.

Mouse spinal cord hemisection

All animal procedures were approved and in accordance with the Institutional Animal Care and Use Committee at the University of Michigan. A hemisection model of SCI was performed as

previously described[181] on female C57BL/6 mice (6-8 weeks old; Jackson Laboratories, Bar Harbor, ME, USA, N=48) or female Crym:RFP C57BL/6 mice (6-8 weeks old; N=16). B6.Cg-*Gt(ROSA)26Sor*$^{tm9(CAG\text{-}tdTomato)Hze}$/J (Jackson Laboratories, 007909) were bred with Tg(Crym-Ncre,Crym-Ccre)RL89Gsat/Mmucd (MMRRC, 036627) and genotyped (Transnetyx, Cordova, TN, USA) to produce Crym:RFP C57BL/6 mice. After administration of bupivacaine (.8 ml/kg), a laminectomy was performed at C5 to allow for a 1.15 mm lateral hemisection on the left side of the spinal cord for bridge implantation. This ensures the functional deficits are confined to the left limbs of the animal. The injury site was covered using Gelfoam (Pfizer, New York, NY, USA) followed by suturing together of the muscle and stapling of skin. Postoperative care consisted of administration of enrofloxacin (2.5 mg/kg; daily for 2 weeks), buprenorphine (0.1 mg/kg; twice daily for 3 days), and Lactated Ringer's solution (5 mL/100 g; daily for 5 days). Bladders were expressed twice daily until function recovered. No mice were loss using this injury model.

Western blot

Spinal cord tissues were collected at 2 wpi and lysed with RIPA buffer (Thermo Fisher, Waltham, MA, USA) supplemented with Halt Protease Inhibitor Cocktail (Thermo Fisher) in a glass homogenizer on ice. The lysate was then sonicated and centrifuged for 20 minutes at 10000g. The supernatant was added with 2x Lammeli Buffer (Biorad, Hercules, CA, USA) and boiled for 5 minutes at 95°C. Samples were ran on a 4-15% gradient SDS-PAGE gel (Biorad) and proteins were transferred to .45 um nitrocellulose membranes. After blocking with BLOK Casein (G-Biosciences, St. Louis, MO, USA), proteins were probed with primary antibodies against rabbit anti-IL10 (Abcam, Cambridge, UK), rabbit anti-NT3 (Abcam, Cambridge, UK), and rabbit anti-β actin (CST, Danvers, MA). The proteins were detected by chemiluminescence (Clarity Substrate, Thermo Fisher, Waltham, MA). Single proteins were developed, and the membranes were stripped

(Restore PLUS Western Blot Stripping Buffer, Thermo Fisher, Waltham, MA) and reprobed with additional antibodies. Quantification was performed with Image J (NIH, Bethesda, MD)

Immunohistochemistry and quantitative analysis nerve regeneration and myelination

Spinal cords were extracted 12 weeks after SCI and flash frozen in isopentane. For immunofluorescence, spinal cord segments were embedded in Tissue Tek O.C.T. Compound (Sakura Finetek, Torrance, CA, USA) with 30% sucrose. Cords were cryo-sectioned transversely into 12-μm-thick sections. Antibodies against the following antigens were used for immunofluorescence: F4/80 (Abcam, Cambridge, UK), Arginase 1 (Arg1, Santa Cruz Biotech, Dallas, TX, USA), neurofilament 200 (NF-200, Sigma Aldrich), myelin basic protein (MBP, Santa Cruz Biotech, Dallas, TX, USA), and Protein-zero myelin protein (P0, Aves Labs, Tigard, OR, USA). Red fluorescent protein (RFP) was imaged at 488 nm without added antibodies. Tissues were imaged on an Axio Observer Z1 (Zeiss, Oberkochen, Germany) using a 10x/0.45 or 20x/0.75 M27 apochromatic objective and an ORCA-Flash 4.0 V2 Digital CMOS camera (C11440-22CU, Hamamatsu Photonics, Hamamatsu City, Shizuoka, Japan).

For quantification of macrophage phenotypes, nine 12 μm thick transverse tissues were randomly selected from each animal (N=24, 6 per condition). All immunopositive cell events were counterstained with Hoechst 33342 to indicate cell nuclei. $F4/80^+$ cells and $F4/80^+$/$arginase1^+$ ($Arg1^+$) were quantified to determine inflammatory macrophages and non-inflammatory macrophages respectively. Immunopositive cells were counted within the bridge area by 2 blinded researchers independently. Co-staining for multiple markers was assessed by evaluating overlap of different channels in Image J (NIH, Bethesda, MD, USA).

To assess the numbers of regenerated and myelinated axons within the PLG bridge area, NF-200 was used to identify axons, NF-200+/MBP+ to determine the number of myelinated axons,

and NF-200+/MBP+/P0+ to determine the amount of myelin derived from infiltrating Schwann cells[183] Twenty-four tissues distributed between conditions were counted by 2 blinded counters to calibrate software for automated counting as previously described[135, 224, 226, 269]. Briefly, images were imported into MATLAB (Mathworks, Natick, MA, USA) and the area of the tissue section corresponding to PLG bridge was outlined. A Hessian matrix was created by convolution filtering using second derivative of the Gaussian function in the x, y, and xy directions. Following filtering, positive NF-200 events were identified by intensity thresholding, single pixel events were removed, and the number of continuous objects were identified to ensure high branching axons are counted as a single object. For calibration, the software will output a matrix of predicted axon counts based on filtering parameters inputted by the user. These values are directly compared to manual counts for the twenty-four tissues used for calibrating the software. The appropriate filter size and threshold sensitivity are selected based on the lowest mean percentage error between the manual and automated counts. For these studies, the mean percentage error was 3%. Once calibration was complete, nine 12 μm thick transverse tissues per animal (N=24, 6 per condition) were quantified to obtain presented results. To obtain axon densities, total NF-200 counts were divided by the area of the PLG bridge. MBP and P0 events were identified similarly as described above. NF200 objects containing pixel locations overlapping with positive MBP or P0 staining were counted and compared to total NF200 counts to determine percentages of axons populations.

Corticospinal tract regeneration was assessed using total area of pixels illuminated with 488 nm light in the bridge area. Images were analyzed in Image J. The bridge area was outlined and threshold to include the brightest 10% of pixels to eliminate background fluorescence and maintain consistency across images. After thresholding the image, total area of pixels was quantified.

Behavioral analysis

The ladder beam walking task was used to evaluate locomotor recovery over a period of 12 weeks post-SCI as previously described for all conditions (N=48, 12 per condition) [270]. Briefly, animals were trained to walk across a ladder beam of 50 rungs into an enclosure over the course of 2 weeks before injury. Baseline scores were determined to separate animals in equal groups prior to SCI. The mice were tested at 2, 4, 8, and 12 weeks. Observations and ladder beam scoring were performed by two blinded observers for 3 trials per animal. Animals were scored by average left forepaw full placements on the ladder beam during the task.

Thermal hyperalgesia

Cold sensitivity was assessed by acetone evaporative cooling over a period of 12 weeks post-SCI as previously described [271]. Through a mesh floor, 5 applications of acetone were applied to the bottom of the left and right forepaw. Each application was separated by at least 5 minutes. Individual responses were scored based on lifting, licking, or shaking of the forepaw that continued past the initial application. Scores were averaged over the ten applications between left and right forepaws to yield a percentage of positive responses.

Statistical analysis

For multiple comparisons, statistical significance between groups was determined by two-way ANOVA with Tukey's post-hoc. For single comparisons, the statistical significance between pairs was determined by unpaired t-test. All statistics test significance using an α value of 0.05. For all graphs: a, b, c denotes $p<0.05$ compared to Blank control, d and e denotes $p<0.05$ compared NT-3 condition, and f denotes $p<0.05$ compared to IL-10 condition. Error bars represent standard error in all figures. Prism 7 (GraphPad Software, La Jolla, CA, USA) software was used for all data analysis.

Data Availability

The datasets generated during and/or analyzed during the current study are available from the corresponding author on reasonable request.

Results

Bi-cistronic vectors conserve IL-10 and NT-3 production in vivo

We initially assessed protein levels following expression from the lentivirus with a single construct and also the bi-cistronic construct (**Figure 6.1**). Bridges were implanted into mice and explanted at 2 weeks post injury (wpi). This time point was selected based on previous studies using bioluminescence imaging that demonstrates robust transgene expression [83]. The proteins used in these studies are human which enabled differentiation of the IL-10 and NT-3 produced by our constructs from the mouse proteins. No significant difference in protein expression was observed between single constructs or the bi-cistronic construct. Furthermore, for the bi-cistronic construct, no significant difference in protein expression was observed between the first gene, IL-10, and the second gene, NT-3.

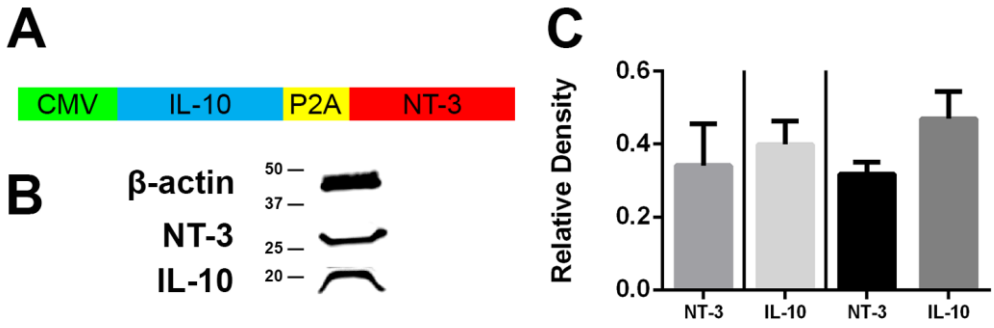

Figure 6.1 Bi-cistronic vectors conserve IL-10 and NT-3 production in vivo. (A) Bi-cistronic lentiviral vector for delivery of IL-10+NT-3. (B) Western blotting was used to show protein levels of NT-3 (27kDa) and IL-10 (21 kDa). (C) Relative densities of single lentiviral constructs and bi-cistronic construct of IL-10 and NT-3 relative to B-actin show no significant difference in protein expression for all comparisons. Left of line are relative densities of single constructs and right of line is the bi-cistronic construct.

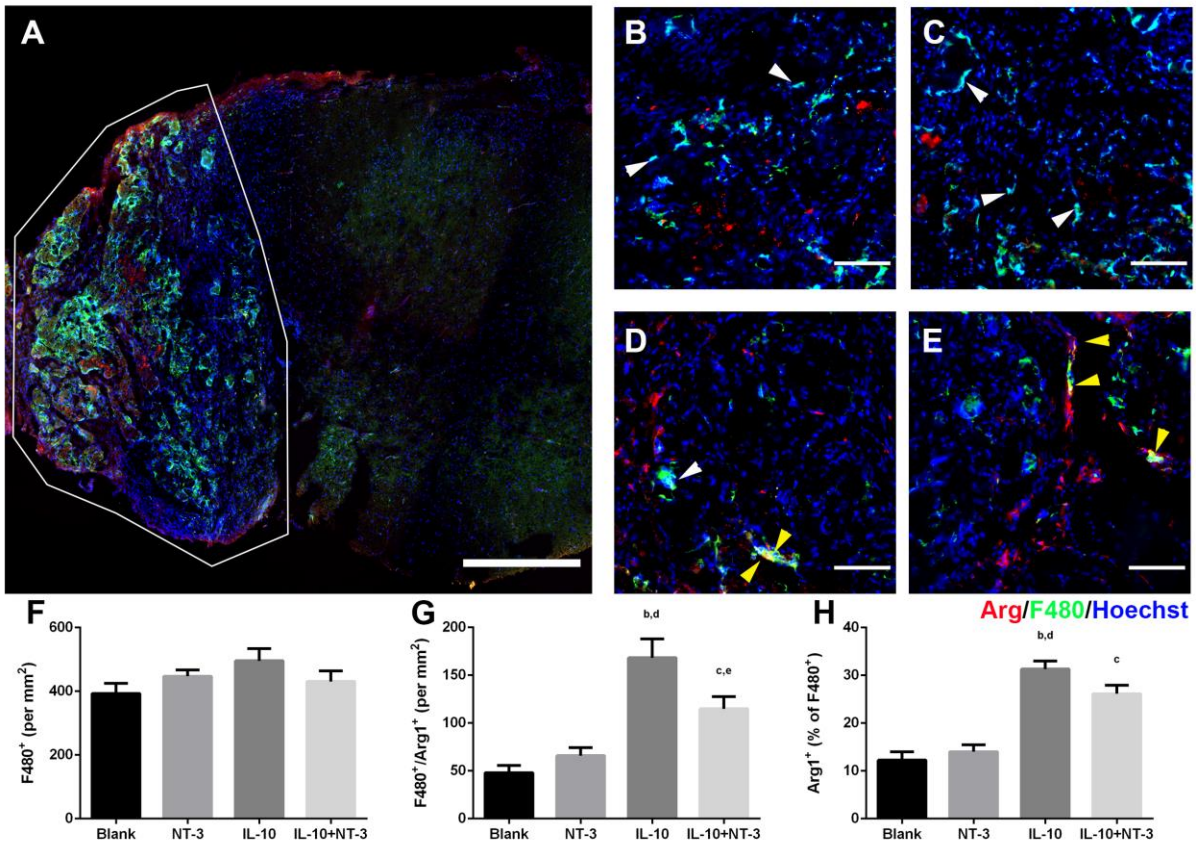

Figure 6.2 IL-10 promotes anti-inflammatory macrophages. (A) Representative image of bridge implantation into spinal cord at 12 weeks post injury. White border denotes bridge area. Scale: 500 um. Macrophage density of (B) Blank (ctrl), (C) NT-3, (D) IL-10, and (E) IL-10+NT-3 from bridge implants. White arrows denote $F480^+$ macrophages. Yellow arrows denote $F480^+/Arg^+$ macrophages. Scale: 100 um. (F) Macrophage density in bridge implants. Density (G) and percentage (H) of anti-inflammatory macrophages in bridge implants. a, b, c denotes $p<0.05$ compared to Blank (ctrl), d and e denotes $p<0.05$ compared NT-3 condition, and f denotes $p<0.05$ compared to IL-10 condition. Data presented as mean +/- SEM. N=8 per group.

IL-10 delivery increases anti-inflammatory macrophages

We next investigated the macrophages populations in the bridge at 12 wpi (**Figure 6.2**), as this population could be influenced by the cytokine and neurotrophin expression. This analysis was performed at 12 wpi to determine the chronic infiltration and phenotype of macrophages. We observed most of the macrophages at the injury were localized to the bridge and not the surrounding tissue (**Figure 6.2A**). The macrophages in the bridge were evenly distributed and were observed in all conditions at similar densities (**Figure 6.2F**). For these studies, pro-regenerative macrophages were assessed by co-localization of F4/80 and arginase (Arg) (**Figure 6.2G**). A significant 3-fold increase in the density of regenerative macrophages was observed for conditions

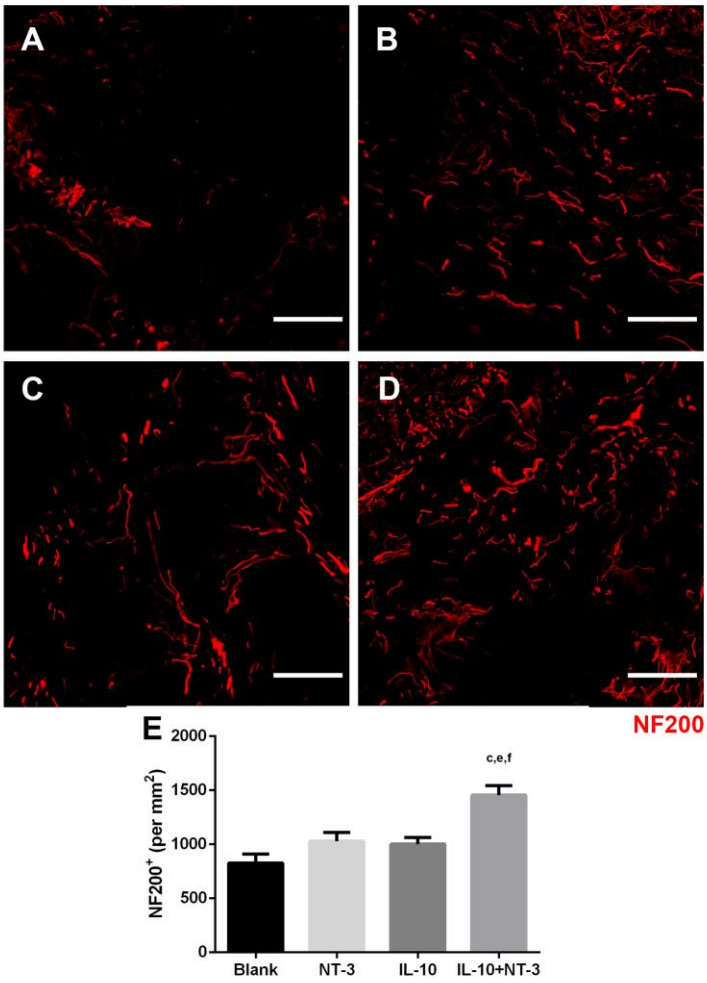

Figure 6.3 IL-10+NT-3 delivery promotes axonal growth at 12 wpi. Axonal growth into bridge implants delivering (A) Blank (ctrl), (B) NT-3, (C) IL-10 or (D) IL-10+NT-3. Scale: 100 um. (E) Axon density in bridge implants. a, b, c denotes $p<0.05$ compared to Blank (ctrl), d and e denotes $p<0.05$ compared NT-3 condition, and f denotes $p<0.05$ compared to IL-10 condition. Data presented as mean +/- SEM. N=8 per group.

with expression of IL-10 compared to the Blank and NT-3 conditions. Differences among these conditions were also significant for the percentage of pro-regenerative macrophages. Notably 31% and 26% of $F4/80^{+}$ macrophages were regenerative for IL-10 and IL-10+NT-3 conditions respectively, a 2-fold increase over Blank and NT-3 conditions (12% and 14%) (**Figure 6.2H**).

Delivery of IL-10+NT3 enhances axonal growth into bridges

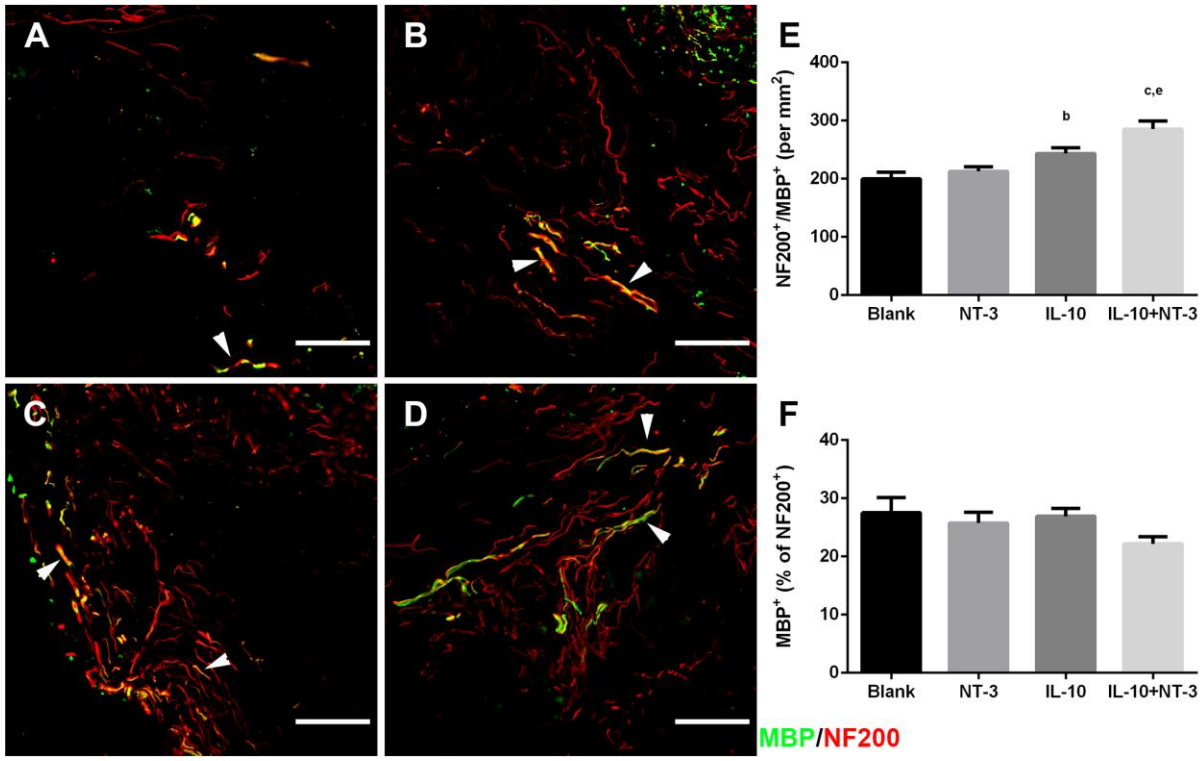

Figure 6.4 IL-10+NT-3 delivery promotes myelination of regenerating axons at 12 wpi. Axon myelination from bridge implants delivering (A) Blank (ctrl), (B) NT-3, (C) IL-10 or (D) IL-10+NT-3. White arrows denote myelinated axons. Scale: 100 µm. Density (E) and (F) percentages of myelinated axons in bridge implants. a, b, c denotes $p<0.05$ compared to Blank (ctrl), d and e denotes $p<0.05$ compared NT-3 condition, and f denotes $p<0.05$ compared to IL-10 condition. Data presented as mean +/- SEM. N=8 per group.

The extent of axonal elongation into the bridge was subsequently analyzed, which reflects the impact of expressing the factors on the capacity of the environment to promote regeneration (**Figure 6.3**). Axons were observed throughout the bridge in all conditions. Axons in treatment groups appeared longer and more diffuse while axons in the control condition appeared bundled and shorter in length (**Figure 6.3A-D**). NT-3 and IL-10 delivery did not significantly increase axonal density compared to control. However, combined delivery of IL-10+NT-3 produced a significant increase of axonal density compared to all other conditions (**Figure 6.3E**).

IL-10+NT-3 delivery promotes myelination of regenerating axons

Myelination of axons is necessary for signal propagation in the spinal cord. Myelinated axons ($NF200^+/MBP^+$) were observed throughout the bridges for all conditions (**Figure 6.4**). Significantly more myelinated axons were observed in the IL-10 condition compared to the Blank bridge. IL-10+NT-3 delivery resulted in significantly more myelinated axons compared to Blank and NT-3 conditions (**Figure 6.4E**). There was no significant difference in percentage of myelinated axons across the conditions at ~27% (**Figure 6.4F**).

Myelinated axons were sub-divided into oligodendrocyte-derived myelin ($NF200^+/MBP^+/P0^-$) and Schwann cell-derived myelin ($NF200^+/MBP^+/P0^+$) (**Figure 6.5**) to determine their relative contribution to total myelination. A significant 2-fold increase in oligodendrocyte-derived myelin

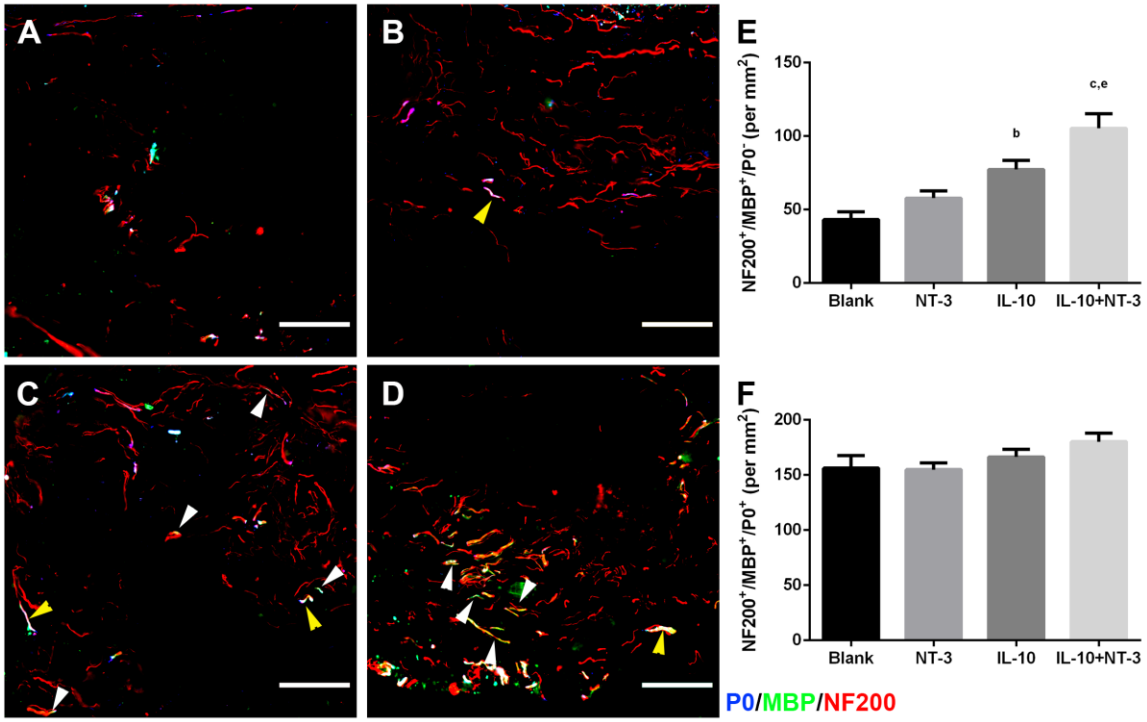

Figure 6.5 IL-10+NT-3 delivery promotes oligodendrocyte myelination of regenerating axons at 12 wpi. Source of myelination from bridge implants delivering (A) Blank (ctrl), (B) NT-3, (C) IL-10 or (D) IL-10+NT-3. White arrows denote oligodendrocyte myelinated axons. Yellow arrows denote Schwann cell myelinated axons. Scale: 100 µm. (E) Density of oligodendrocyte myelinated axons. (F) Density of Schwann cell myelinated axons. a, b, c denotes $p<0.05$ compared to Blank (ctrl), d and e denotes $p<0.05$ compared NT-3 condition, and f denotes $p<0.05$ compared to IL-10 condition. Data presented as mean +/- SEM. N=8 per group.

density was observed for IL-10+NT-3 compared to Blank and NT-3 conditions (**Figure 6.5E**). IL-10 delivery resulted in a significant increase of oligodendrocyte myelin compared to control. However, no significant difference in density of Schwann cell-derived myelin was observed across all conditions (**Figure 6.5F**).

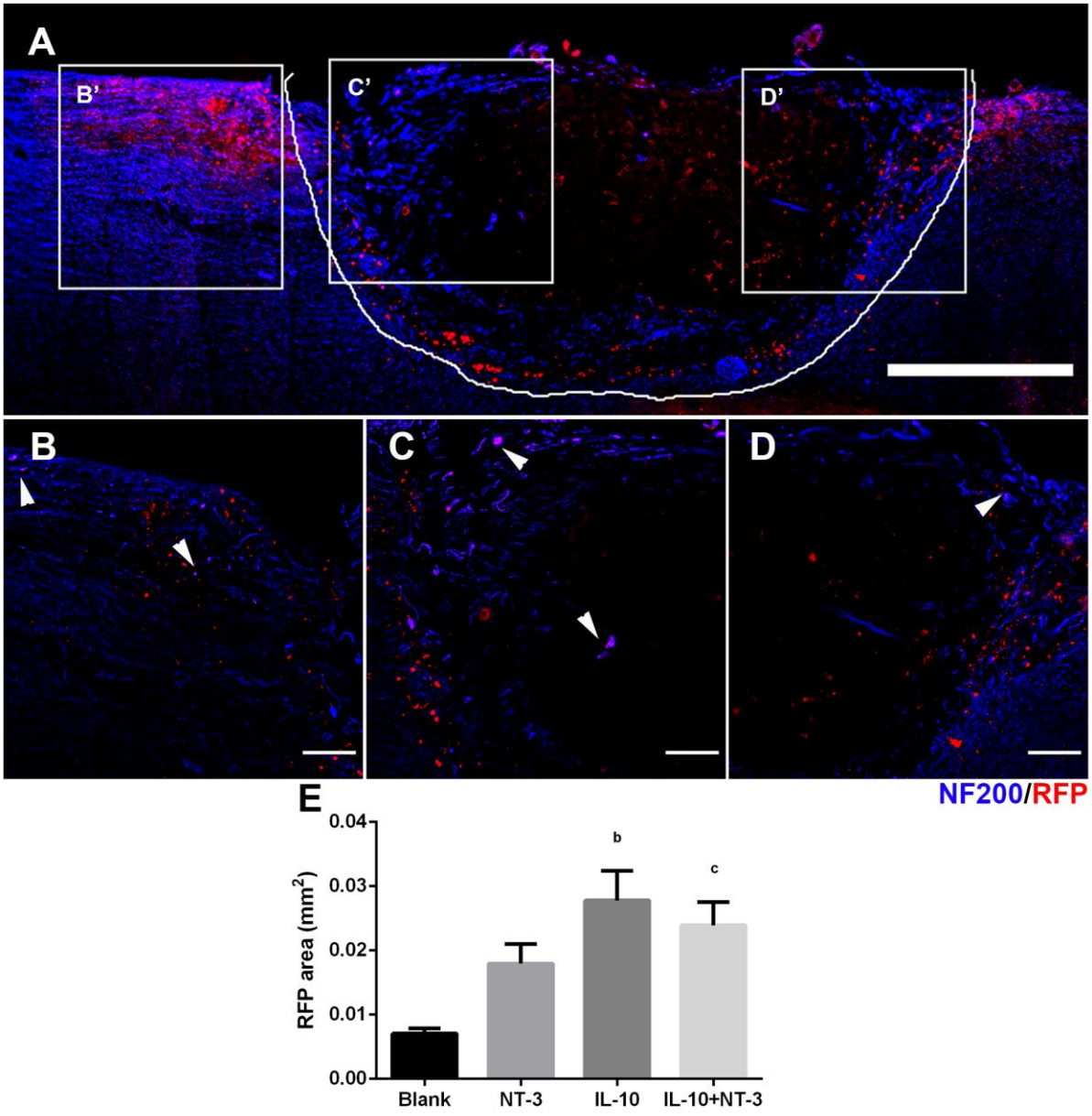

Figure 6.6 Crym-RFP CST fibers penetrate and transverse bridge implant. (A) Horizontal image of Crym-RFP CST fibers in bridge area. Bridge area outlined in white. Area to the right of the bridge is rostral and area to the left is caudal. Lettered boxes indicate regions shown in higher magnification. Scale 500 µm (B) RFP CST fibers are present caudal to bridge implant. (C) RFP CST fibers are present at the caudal tissue bridge interface. (D) RFP CST fibers are present at the rostral bridge tissue interface. White arrows denote RFP fibers co-localizing with NF200 regenerating axons. Scale 100 µm (E) Quantification of RFP CST fiber area in the bridge area. a, b, c denotes $p<0.05$ compared to Blank (ctrl), d and e denotes $p<0.05$ compared NT-3 condition, and f denotes $p<0.05$ compared to IL-10 condition. Data presented as mean +/- SEM. N=4 per group.

Crym-RFP CST fibers penetrate and traverse bridge implant

We investigated the regeneration of corticospinal tract (CST) axons into the bridge at 12 wpi, as this tract is the major descending motor tract in humans. These studies used the transgenic Crym-RFP mouse, which have RFP labeling of the corticospinal tract (**Figure 6.6)** CST fibers were observed rostral (**Figure 6.6D**), caudal (**Figure 6.6B**), and in the bridge (**Figure 6.6C**). CST fibers were observed 500 µm caudal to the bridge implant. We also assessed co-localization of RFP and NF200 fibers to determine its specificity. Only a subset of RFP fibers was co-labeled with NF200. We quantified the area of the CST fibers in the bridge (**Figure 6.6E**). A significant increase of CST fibers was observed for IL-10 and IL-10+NT-3 conditions compared to control. Note that the punctate nature of the RFP label in this image is because we are visualizing axonal transport of the reporter fluorochrome packaged as a protein, not movement of a molecular tracer; the appearance and rate of GFP/RFP axonal transport is dependent on expression paradigm [272].

IL-10+NT-3 improves forelimb locomotor recovery

The ladder beam task was used to evaluate functional motor recovery of the left forelimb to determine if the observed regeneration correlated with an increase in function (**Figure 6.7A**). A

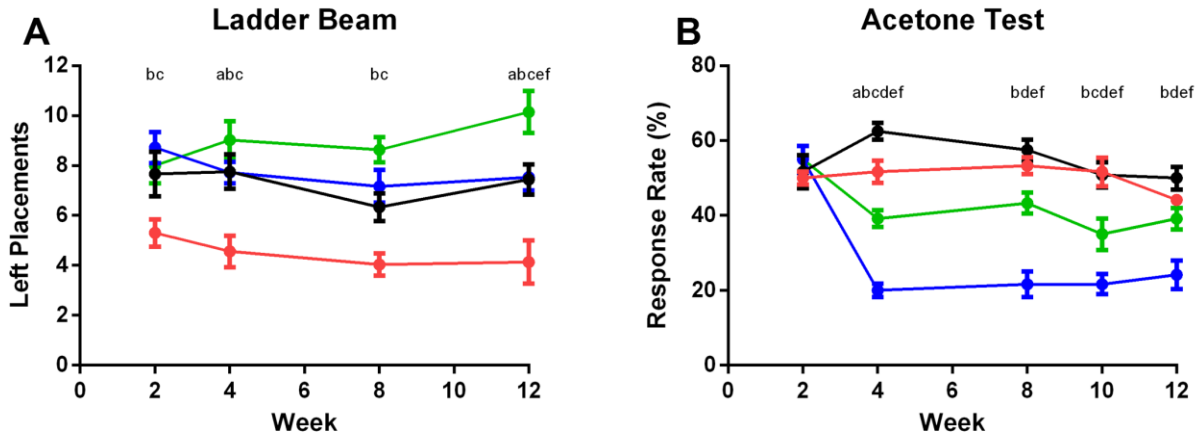

Figure 6.7 IL-10+NT-3 enhances functional recovery and causes some cold hypersensitivity. (A) Ladder beam task was evaluated over 12 weeks post bridge implantation. (B) Acetone cold hypersensitivity test was evaluated over 12 weeks post bridge implantation. a, b, c denotes $p<0.05$ compared to Blank (ctrl) for NT-3, IL-10, and IL-10+NT-3 respectively, d and e denotes $p<0.05$ compared NT-3 for IL-10 and IL-10+NT-3 respectively, and f denotes $p<0.05$ compared to IL-10 for IL-10+NT-3. Data presented as mean +/- SEM. N=12 per group.

significant functional improvement was observed for all conditions compared to Blank. Furthermore, a significant increase in functional recovery was obtained with IL-10+NT-3 delivery compared to all other conditions at 12 wpi. Interestingly, a greater prolonged improvement over time was observed for IL-10+NT-3 condition compared to other conditions. IL-10 and NT-3 delivery were similar in functional recovery, however co-delivery produced a significant additive effect in locomotor recovery.

We also assessed cold hypersensitivity using the acetone test to identify any potential negative effects that may be associated with combined delivery (**Figure 6.7B**). IL-10 delivery alone reduced cold hypersensitivity compared to all other conditions. NT-3 delivery alone exacerbated hypersensitivity compared to all conditions. The combined expression of IL-10+NT-3 led to

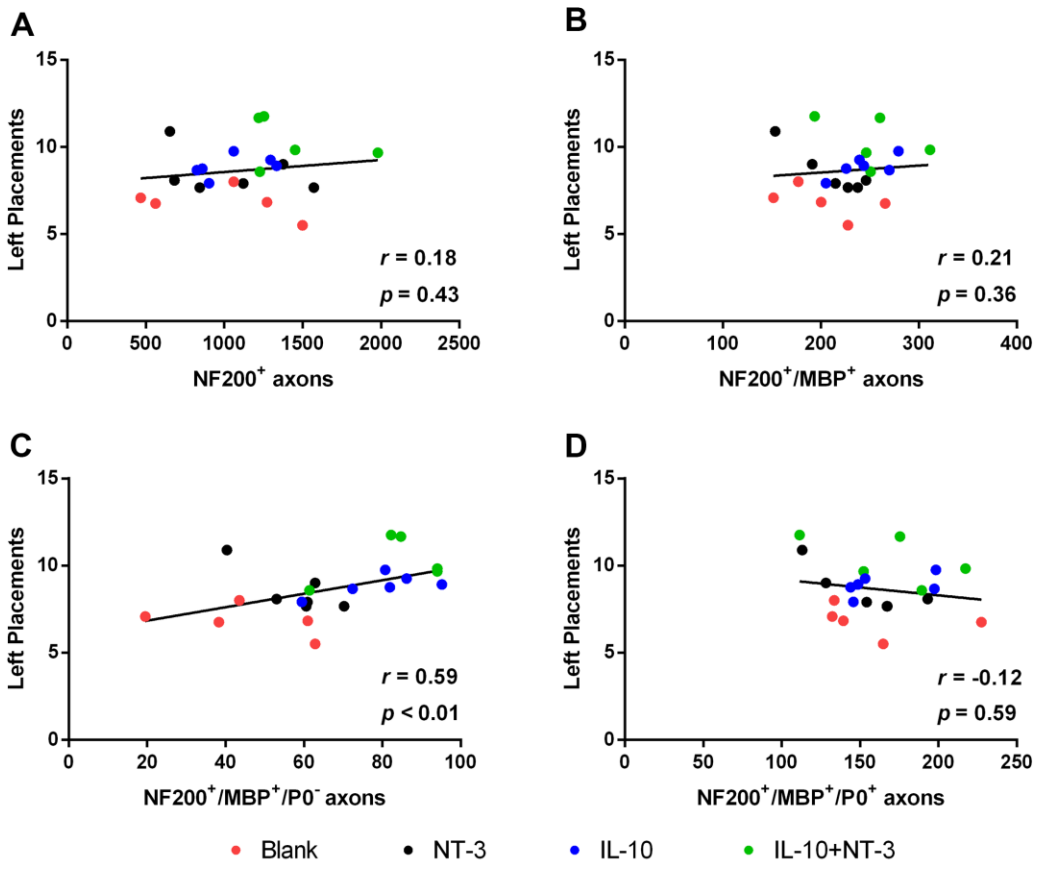

Figure 6.8 Functional recovery is correlated to oligodendrocyte myelinated axon density. Ladder beam left forelimb placements correlated with (A) Axon density, (B) Myelinated axon density, (C) Oligodendrocyte myelinated axon density, and (D) Schwann cell myelinated axon density. p values denote significance from zero slope. N=12 per group.

increased hypersensitivity compared to IL-10 alone, yet decreased hypersensitivity relative to Blank and NT-3 conditions.

As a final analysis, we investigated the association of tissue recovery characteristics with forelimb locomotor function recovery (**Figure 6.8**). The values for axon density (**Figure 6.8A**), myelinated axon density (**Figure 6.8B**), oligodendrocyte-derived myelinated axon density (**Figure 6.8C**), and Schwann cell-derived myelinated axon density (**Figure 6.8D**) were plotted against the ladder beam score for each animal. The oligodendrocyte myelinated axon density was positively correlated with functional recovery (r=0.59, p<0.01). This relationship also segments animals by condition along the interpolated linear fit line. This relationship was the only significant connection between tissue characteristics and functional recovery.

Discussion

The central nervous system has the innate capacity to repair itself post-SCI, yet the spinal cord environment lacks sufficient factors that promote regeneration and has an abundance of factors that inhibit regeneration[2]. We have developed multichannel PLG bridges that can promote nerve regeneration by both acting as a physical guide and serve as a platform for gene therapy vector delivery. The bridges are acellular at time of implantation, indicating that any cells, extracellular matrix, or proteins present in the bridge at the time of extraction must have originated from the host tissue. Similarly, any axons observed inside the implant must be attributed to either regeneration of injured axons or sprouting of new axons from spared or contralateral tissue. This bridge provides a defined space for histological analysis, analysis of cell populations at and near the lesion site, and treatment outcomes. The bridge has an architecture that supports regeneration by combining micro-porosity for cellular infiltration with channels that direct axonal elongation along the major axis of the cord. These bridges can also be seeded with recombinant lentiviral

particles containing genes of interest for subsequent cellular transduction. Unlike other viral vectors, lentivirus does not influence the phenotype of progenitors[230] or cause significant inflammation[128]. Lentiviral vectors physical properties are also independent of the gene of interest making them the ideal system to deliver multiple vectors encoding various inductive factors without modification to the base biomaterial. Poly-cistronic lentiviral vectors can deliver multiple genes by the inclusion of self-cleaving 2A peptide sites between genes. This technology is useful and beneficial to target multiple barriers to spinal cord regeneration by delivering multiple proteins simultaneously. The genes being used in this study were chosen because each addresses a different aspect of the inhibitory microenvironment around the injury site. NT-3 enhances axon elongation and neuroprotection of regenerating and spared axons[83, 273, 274]. IL-10 is largely responsible for dampening and resolving the immune response toward restoring homeostasis [262, 275, 276]. This research builds upon the success of the multiple channel poly(lactide-*co*-glycolide) (PLG) bridges by delivering 2 distinct transgenes alone and in combination. The goal of this investigation was to activate growth promoting cues while attenuating growth inhibitory cues to observe synergistic effects on spinal cord regeneration.

Similar macrophage infiltration into bridges was observed across experimental conditions delivering, yet the gene expression could alter the phenotype. Lentiviral constructs are minimally immunogenic, yet the transgene can influence the microenvironment[128, 257, 277, 278]. Macrophage phenotypes exist on a spectrum of inflammatory to regenerative and we have previously shown that $Arg1^+$ macrophages have a regenerative phenotype in SCI [135, 260]. For the purposes of this paper, regenerative macrophages were assessed by co-localization of $F4/80^+$ and $Arg1^+$. The early phase of the regenerative response following SCI relies on pro-inflammatory macrophages, which participate in recruitment of immune cells and clearance of cell debris. Subsequently, these

macrophages shift to a pro-regenerative phenotype to coordinate cell differentiation and tissue reconstruction. Dysregulation of this transition from pro-inflammatory to pro-regenerative hampers regenerative success and tissue recovery. In the CNS, microglia and macrophages express several neurotrophins and their receptors, allowing them to act both as sources and targets creating a feedback loop that can modulate proliferation and morphology of axons [279]. Neurotrophins impact immune cell function in varying ways. BDNF stimulates microglial proliferation while NT-3 can stimulate phagocytic activity of microglial cells in vitro and upregulation of nitric oxide production [280-282]. NGF can also act directly on microglial cells by promoting chemotactic migratory activity, potentially contributing to recruitment of additional immune cells at injury sites[283]. Neurotrophins, including NT-3, have been suggested as modulating monocyte chemotaxis without altering their production of inflammatory cytokines [284]. NGF can act directly on microglia and shift them toward a neuroprotective phenotype [283]. In these studies, we did not observe an anti-inflammatory effect of NT-3 on macrophage activity. IL-10 delivery alone produced ~31% of regenerative macrophages, but when combined with NT-3, this percentage decreased to 26%. This difference was not significant. IL-10 has been extensively revered as an anti-inflammatory cytokine capable of shifting the phenotype of macrophages[224, 285-289] and these studies support the previous findings.

A trend of increased axons for NT-3 and IL-10 compared to blank, yet the combination of IL-10+NT-3 produced an additive effect for axonal outgrowth. Axonal outgrowth can be impacted by delivery of NT-3 and IL-10 individually [83, 135, 224], however in our studies, these individual factors did not substantially impact axon density relative to control, which likely results from the relative types of neurons in the C5 lateral hemisection model compared with the previous reports. A larger number of propriospinal neurons are present in the cervical spinal cord than the thoracic spinal

cord, with intrinsic differences also reported for growth factors, cell surface receptors, apoptosis, axonal regeneration, neuroprotection, and cell survival [290-293]. Our results indicate that the combined expression of IL-10 and NT-3 does significantly enhance axon density at the cervical hemisection. This synergy is likely related to the sparing of axons by IL-10 and the neurotrophic effects of NT-3. Effectively, the greater survival of neurons by IL-10 leads to an increase number of axons that can regenerate into the injury.

An increase in myelinated axons for IL-10+NT-3 delivery, notably with oligodendrocyte myelinated axons was observed. Oligodendrocyte myelin is necessary to support saltatory conduction and prevent axon degeneration [294]. Oligodendrocyte proliferation is not altered by NT-3, NT-3 exposure *in vitro* lead to significantly more MBP production by oligodendrocytes through an unknown posttranscriptional mechanism [295, 296]. Some evidence suggests that NT-3 weakly induces the maturation of neural precursor cells into myelinating oligodendrocytes [297], yet other reports have shown NT-3 promotes quiescence or even Schwann cell differentiation of neural precursor cells[183, 208, 298, 299]. These differences could indicate concentration dependent effects or vary with surrounding interactions with other factors. We observed that IL-10 delivery had significantly more oligodendrocyte-derived myelin relative to control. IL-10 polarization of immune cells enhances the ability of neural precursor cells to promote oligodendrocyte differentiation and supports mature oligodendrocyte survival [300]. Our results are consistent with this observation that IL-10 promoted the survival of myelinating oligodendrocytes, which can synergize with the expression of NT-3 to potentiate their myelin production to ensheath more axons. This mechanism has been suggested in other work combining IL-10 and NT-3 delivery for treatment of multiple sclerosis [301]. We did not observe an increase in oligodendrocyte myelination

for NT-3 delivery alone, possibly due to lack of surviving oligodendrocytes and weak effects of NT-3 on their proliferation and differentiation[297].

Oligodendrocyte myelination significantly correlated with increased functional recovery. We assessed locomotor recovery on the ladder beam walking task over the course of 12 weeks. All treatment conditions had significant improvements in functional recovery relative to control, yet IL-10+NT-3 delivery was substantially improved relative to all other conditions. A significant correlation between ladder beam score and oligodendrocyte myelinated axon density was observed, suggesting that oligodendrocyte myelination of axons is a limiting step in functional recovery for our model. The functional benefit of oligodendrocyte myelin versus Schwann cell myelin have been debated in the literature, yet any conclusion remains nebulous. Some reports suggest oligodendrocyte myelin is not necessary in spontaneous functional recovery [302]; however, prolonged recovery as seen in these studies may require oligodendrocyte myelin for restoration of function. The various injury models may differentially impact oligodendrocytes as oligodendrocyte have been seen as less important in contusion models [302]. Our hemisection model severs and removes existing axons and cells in the lesion, while contusion models retain the damaged tissue.

A decrease in hypersensitivity was observed with IL-10 delivery while NT-3 delivery alone increased hypersensitivity. IL-10 has been shown to ameliorate neuropathic pain but the role played by neurotrophins and NT-3 has been nebulous [136]. NT-3 can be involved in a long-term change of neuronal excitability[303]. NT-3 also promotes an extensive growth of lesioned axons in the dorsal columns which contain mostly sensory projections. Furthermore, the effects of NT-3 on neuropathic pain may be concentration or receptor dependent[304-306]. Our results suggest NT-3 exacerbates neuropathic pain. However, there exists a tradeoff of positive and negative effects. We

observed the highest degree of functional recovery when combining IL-10+NT-3, yet we also observed increased neuropathic pain compared to IL-10 alone.

Conclusion

Overall our results show that the combination of IL-10+NT-3 enhanced axonal growth and oligodendrocyte myelinated axon density, and with increased locomotor functional recovery compared to IL-10 or NT-3 alone. Hypersensitivity with the combination was increased compared to IL-10 alone yet decreased relative to NT-3 alone. Furthermore, a positive correlation was observed between oligodendrocyte myelinated axon density and functional recovery, suggesting oligodendrocyte myelination as a target to further improve functional recovery. Poly-cistronic vectors provide a mechanism for expression of multiple transgenes that can simultaneously address multiple aspects that limit regeneration. Multichannel PLG bridges provide a growth supportive substrate and a platform to deliver bioactive agents as well as a defined space to investigate the SCI microenvironment and to assess the biological impact of treatments.

Chapter 7. PLG Bridge Implantation in Chronic SCI Promotes Axonal Elongation and Myelination

Authors

Dominique R. Smith, Courtney M. Dumont, Andrew J. Ciciriello, Amina Guo, Ravindra Tatineni, Mary K. Munsell, Brian J. Cummings, Aileen J. Anderson, Lonnie D. Shea

Abstract

Spinal cord injury (SCI) is a devastating condition that may cause permanent functional loss below the level of injury, including paralysis and loss of bladder, bowel, and sexual function. Patients are rarely treated immediately, and this delay is associated with tissue loss and scar formation that can make regeneration at chronic time points more challenging. Herein, we investigated regeneration using a poly(lactide-co-glycolide) (PLG) multi-channel bridge implanted into a chronic SCI following surgical resection of necrotic tissue. We characterized the dynamic injury response and noted that scar formation decreased at 4 and 8 weeks post injury (wpi), yet macrophage infiltration increased between 4 and 8 wpi. Subsequently, scar tissue was resected and bridges were implanted at 4 and 8 wpi. We observed robust axon growth into the bridge and remyelination at 6 months post initial injury. Axon densities were increased for 8 week bridge implantation relative to 4 week bridge implantation, whereas greater myelination, particularly by Schwann cells, was observed with 4 week bridge implantation. The process of bridge implantation did not significantly decrease the post injury function. Collectively, this chronic model follows the pathophysiology of human SCI and bridge implantation allows for clear demarcation of regenerated tissue. These data demonstrate that bridge implantation into chronic

SCI supports regeneration and provides a platform to investigate strategies to buttress and expand regeneration of neural tissue at chronic time points.

Introduction

The United States has approximately one million patients with spinal cord injury (SCI), costing roughly $40.5 billion annually.[307] SCI is a devastating condition that may cause permanent paralysis below the level of injury and loss of bladder, bowel, and sexual function. SCI is divided into three phases: acute (hours to days), subacute (days to weeks), and chronic (months to years).[308] Our previous work and most other repair strategies focus on acute and sub-acute SCI using biomaterial, tissue/cell transplantation, neurotrophic factors, or neuroprotective strategies. However, acute models of SCI are not clinically translatable treatments because patients are rarely treated immediately due to uncertainties surrounding the functional deficits, injury parameters, and microenvironment. Additionally, due to people currently living with SCI, the prevalence of chronic SCI is more than 20 fold the incidence of acute SCI.[4] The development of therapies for chronic SCI could significantly impact quality of life and alleviate the financial burdens associated with this condition.

SCI produces a complex, dynamic, inhibitory microenvironment after the injury that limits regeneration. During the chronic phase, an established glial and fibrotic scar deters regenerating axons from penetrating into the lesion site.[53, 163] The lesion area also contains myelin-associated proteins that inhibit regeneration, and evidences persistent inflammation; for example, macrophage infiltration and microglial activation.[44, 309] In clinical trials as well as animal models, chronic treatments are increasingly being investigated following resection of the scar.[56, 310] Scar resection aims to remove dense connective tissue that can limit regeneration, though potential concerns are functional deficits from scar removal or the creation of a gap. Gaps created by

penetrating injuries or surgical resection have little to no regeneration into the defect; however, studies over the past decade have identified biomaterials that can bridge defects. These bridges can be designed with a permissive environment that physically stabilizes the spinal cord and supports regeneration through topographical cues and delivery of cells or proteins[308].

Previously, we have reported that poly(lactide-co-glycolide) (PLG) multi-channel bridges are an effective substrate for robust axonal regeneration and investigation of the microenvironment during the acute phase of SCI.[83] PLG has been widely used as a material for spinal cord repair or peripheral nerve conduits. PLG is biodegradable, bioresorbable, and its degradation products are readily cleared by the body.[206] In addition, the bridge features an architecture that encourages axon growth through channels and infiltration of supporting cells into interconnected pores.[83, 137] Regenerating axons have been observed growing through the bridge and into tissue caudal to the injury,[181] but to be clinically feasible, these effects must be shown in the chronic space.

In the present study, we investigated axonal growth into PLG bridges implanted into a chronic model of SCI. The goals of this investigation were to create a reproducible chronic injury model and to show PLG bridges are a growth permissive substrate for axonal elongation and tissue reformation after chronic spinal cord injury. In this model, the bridge is implanted into a hemisection created by surgical resection and allows for clear demarcation of sparing versus regeneration, as all axons and cells found within the bridge must enter it after implantation. We examined the pathophysiology of the injury including inflammatory cell infiltration, inhibitory extracellular matrix (ECM) deposition, and glial scarring. Two time points were analyzed for implantation of the bridge (4 weeks post injury (wpi) or 8 wpi), with analysis of axonal growth, myelination, and source of myelination measured 6 months post-SCI. The goal of these studies is

to establish PLG bridges as a growth supportive substrate in chronic SCI and provide a platform to investigate strategies to buttress and expand regeneration of neural tissue at chronic time points.

Materials and Methods

Fabrication of multi-channel bridges

PLG (75:25 lactide:glycolide; i.v. 0.76 dL/g; Lakeshore Biomaterials, Birmingham, AL, USA) was dissolved in dichloromethane (6% w/w) and emulsified in 1% poly (vinyl alcohol) using a homogenizer (PolyTron 3100; Kinematica AG, Littau, Switzerland) to create microspheres (z-average diameter ~1µm). D-sucrose (Sigma Aldrich), D-glucose (Sigma Aldrich), and dextran MW 100,000 (Sigma Aldrich) were mixed at a ratio of 5.3:2.5:1 respectively by mass. The mixture was caramelized, cooled, and drawn from solution with a Pasteur pipette to make sugar fibers. Fibers were drawn to 150 – 250 µm, coated with a 1:1 mixture of PLG microspheres and salt (63-

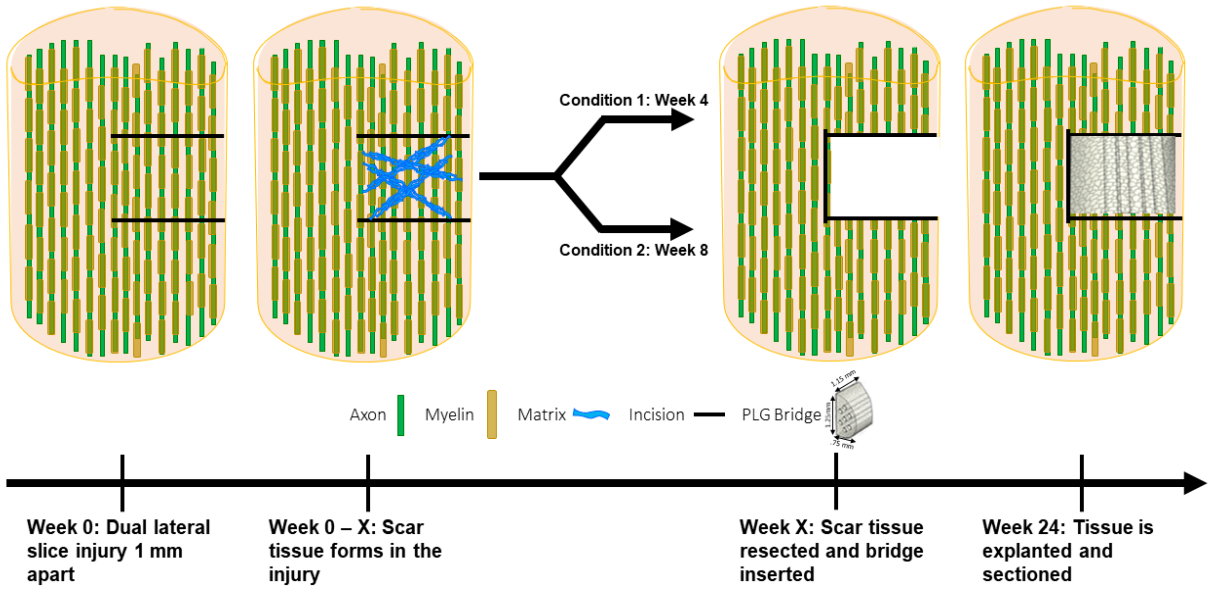

Figure 7.1 Chronic spinal cord injury model. A laminectomy was performed at C5 to allow for two lateral slices 1 mm apart on the spinal cord. The lateral slices were cut from the midline to lateral. Animals were randomly assigned for bridge implantation at either 4 or 8 weeks post injury (wpi). At 4 or 8 wpi, the surgical site was reopened to expose the injured spinal cord. The two lateral slices were located and connected with a third incision along the midline to remove the injured spinal tissue. A 1.15 mm bridge was then implanted into the lesion space.

106 μm) and pressed into a salt-lined aluminum mold. Once dissolved, the sugar strands create 9 channels and the salt creates a micro-porous structure. The molds were then equilibrated and foamed with CO_2 gas (800 psi) for 16 h. The newly formed bridges were subsequently cut into 1.15 mm sections and leached for 2 h to remove the salt. The bridges were dried overnight and stored in a desiccator. The final dimensions of the bridge were 1.15 mm in length, .75 mm in width, and 1.25 mm in height.

Chronic mouse SCI model

All animal procedures were approved and in accordance with the Institutional Animal Care and Use Committee at the University of Michigan. There were 42 C57BL/6 mice used in these studies. After administration of bupivacaine (.8 ml/kg), a laminectomy was performed at C5 to allow for two lateral slices 1 mm apart on the spinal cord (**Figure 7.1**). The lateral slices were cut from the midline to lateral using a micro-feather to transect the gray and white matter. The injury site was covered using Gelfoam (Pfizer, New York, NY, USA) followed by suturing together of the muscle and stapling of the skin. Animals were randomly assigned for bridge implantation at either 4 or 8 wpi. At 4 or 8 wpi, the surgical site was reopened to expose the injured spinal cord. Residual Gelfoam was removed from the dorsal surface of the spinal column. The two lateral slices were located and connected with a third incision along the midline to remove the injured spinal tissue. A 1.15 mm bridge was then implanted into the lesion space. The injury site was covered using a new piece of Gelfoam. Postoperative care consisted of administration of enrofloxacin (2.5 mg/kg; daily for 2 weeks), buprenorphine (0.05 mg/kg; twice daily for 3 days), and Lactated Ringer's solution (5 mL/100 g; daily for 5 days) after both surgeries. Bladders were expressed twice daily until function recovered. Two mice were lost due to weight loss with this injury

paradigm resulting in 11 mice per bridge implantation group. Animals spinal cords were extracted at 6 months post initial injury.

Immunohistochemistry and quantitative analysis

Spinal cords were extracted 2, 4, or 8 weeks post primary SCI without bridge implantation or 6 months post primary SCI with bridge implantation at 4 or 8 weeks post primary SCI and flash frozen in isopentane. Six animals were used at 2, 4, and 8 weeks post primary injury (N=18). Ten animals were used for each bridge implantation condition at 4 and 8 wpi (N=20). For immunofluorescence, spinal cord segments were embedded in Tissue Tek O.C.T. Compound (Sakura Finetek, Torrance, CA, USA) with 30% sucrose. Tissues extracted at 2, 4, and 8 wpi were cryo-sectioned longitudinally into 12 μm sections. Tissues extracted at 6 months post bridge implantation were cryo-sectioned transversely into 12 μm sections. We followed standard immunohistochemistry (IHC) techniques including fixing tissues in 4% paraformaldehyde and blocking with serum before staining for our structures of interest. Primary antibodies against the following antigens were used for immunofluorescence: F4/80 (Abcam, Cambridge, UK), Arginase 1 (Arg1, Santa Cruz Biotech, Dallas, TX, USA), Fibronectin (Sigma Aldrich, St. Louis, MO, USA), CSPG4 (Millipore, Burlington, MA, USA), Glial fibrillary acidic protein (GFAP, Aves Labs, Tigard, OR, USA), Neurofilament 200 (NF200, Sigma Aldrich), myelin basic protein (MBP, Santa Cruz Biotech), Protein-zero myelin protein (P0, Aves Labs), Choline Acetyltransferase (ChAT, Abcam, Cambridge, UK) and Calcitonin gene-related peptide (CGRP, Abcam, Cambridge, UK). Tissues were imaged at multiple focal lengths to obtain z-stacks on an Axio Observer Z1 (Zeiss, Oberkochen, Germany) using a 10x/0.45 or 20x/0.75 M27 apochromatic objective and an ORCA-Flash 4.0 V2 Digital CMOS camera (C11440-22CU, Hamamatsu Photonics, Hamamatsu City, Shizuoka, Japan).

Histological Analysis of Longitudinal Sections: For quantification of immune cells, nine 12 μm thick longitudinal tissues were randomly selected from each animal (N=18). All immunopositive cell events were counterstained with Hoechst 33342 to indicate cell bodies. $F4/80^+$ cells and $F4/80^+$/arginase1^+ ($Arg1^+$) were quantified to determine inflammatory macrophages and non-inflammatory macrophages respectively. Immunopositive cells were counted within the bridge area by 2 blinded researchers independently. Co-staining for multiple markers was assessed by evaluating overlap of z-stacked different channels in Image J (NIH, Bethesda, MD, USA). To quantify cell density, the total number of immunopositive cells was divided by the area of the injury. For quantification of ECM deposition and glial scarring, nine 12 μm thick longitudinal tissues were selected from each animal (N=18). Immunopositive area was outlined, quantified, and averaged by thresholding for the brightest 20% of pixels using the default thresholding technique in each image within a 3mm x 2mm box centered on the lesion site using Image J by 2 blinded researchers. This approach allowed for consistent evaluation of the lesion borders and ECM areas. Fibronectin and CSPG4 were used to assess ECM. Glial scarring was assessed by dense GFAP area staining around the lesion site.

Histological Analysis of Transverse Sections: To assess the number of infiltrating macrophages, $F4/80^+$ cells and $F4/80^+$/arginase1^+ ($Arg1^+$) were quantified to determine inflammatory macrophages and non-inflammatory macrophages respectively. To assess the numbers of regenerated and myelinated axons within the PLG bridge area, NF200 was used to identify axons, $NF200^+/MBP^+$ to determine the number of myelinated axons, and $NF200^+/MBP^+/P0^+$ to determine the amount of myelin derived from infiltrating Schwann cells.[183] Twenty 12 μm thick transverse tissues distributed between conditions were counted by 2 blinded counters to calibrate software for automated counting as previously described.[135, 224, 226, 269] In

short, images were imported into MATLAB (Mathworks, Natick, MA, USA) and the area of the section corresponding to PLG bridge was outlined. A Hessian matrix was created by convolution filtering using second derivative of the Gaussian function in the x, y, and xy directions. Following filtering, positive NF200 events were identified by intensity thresholding, single pixel events were removed, and the number of continuous objects were identified. This ensures high branching axons are counted as a single object. For calibration, the software will output a matrix of predicted axon counts based on filtering parameters inputted by the user. These values are directly compared to manual counts for the twenty tissues used for calibrating the software. The appropriate filter size and threshold sensitivity are selected based on the lowest mean percentage error between the manual and automated counts. Furthermore, predicted values were subjected to standard curve interpolation and Pearson's r to determine derivation from model and correlation. Once calibration was complete, nine 12 μm thick transverse tissues per animal (N=20) were quantified to obtain presented results. To obtain axon densities, total NF200 counts were divided by the area of the PLG bridge. MBP and P0 events were identified similarly as described above. NF200 objects containing pixel locations overlapping with positive MBP or P0 staining were counted and compared to total NF200 counts to determine percentages of axons populations. To assess motor or sensory axons within the PLG bridge area, NF200 was used to identify axons, ChAT to determine motor axons, and CGRP to determine sensory axons.

Behavioral analysis

The ladder beam walking task was used to evaluate locomotor recovery over period of 6 months post the primary SCI as previously described.[270] Briefly, animals were trained to walk across a ladder beam of 50 rungs into an enclosure over the course of 2 weeks before injury. Baseline scores were determined to separate animals in equal groups prior to SCI. The mice were

tested at 2 weeks to separate animals into equal groups across bridge implantation timepoints. Observations were recorded and scored were by 2 blinded observers for 3 trials per animal. Animals were scored by average left forepaw full placements on the ladder beam during the task.

Statistical analysis

For multiple comparisons, statistical significance between groups was determined by two-way ANOVA with Tukey's post-hoc. For single comparisons, the statistical significance between conditions was determined by unpaired dual-tailed t-test. Linear regression analysis was used to determine significance of trendlines. All statistics test significance used an α value of 0.05. * denotes $p<.05$, ** denotes $p<.01$, *** denotes $p<.001$, and **** denotes $p<0.0001$ in all figures unless otherwise stated. Error bars represent standard error in all figures. Prism 7 (GraphPad Software, La Jolla, CA, USA) software was used for all data analysis.

Data Availability

The datasets generated during and/or analyzed during the current study are available from the corresponding author on reasonable request.

Results

Fibrotic and glial scarring is partially resolved in the chronic injury

We assessed changes in deposition of ECM following SCI, as the ECM can contribute to failure of neural tissue regeneration by forming a physical and biochemical barrier. The impact of the dual lateral hemisection injury on matrix expression and deposition was assessed by examining fibronectin and CSPG4 staining at 2, 4, and 8 wpi (**Figure 7.2**). Fibronectin and CSPG4 were localized to the lesion at all time points. The fibronectin area of staining exhibited a 3-fold decrease at 4 and 8 wpi compared to 2 wpi ($p<0.0001$) (**Figure 7.2K**). For the area of CSPG4 staining, there

was a significant reduction between the 2 wpi and 8 wpi (**Figure 7.2J**). The glial scar was visualized by GFAP-positive area at 2 (**Figure 7.3B**), 4 (**Figure 7.3E**), and 8 wpi (Figure 7.3H) and quantified, as GFAP-positive astrocytes contribute to physical and biochemical barriers to tissue regeneration. The GFAP+ area was measured by outlining dense GFAP staining around the border of the lesion as previously described [137]. The area of glial scarring decreased significantly at 4 and 8 wpi compared to 2 wpi (p<0.0001) (Figure 7.3J), with no difference in scar area between

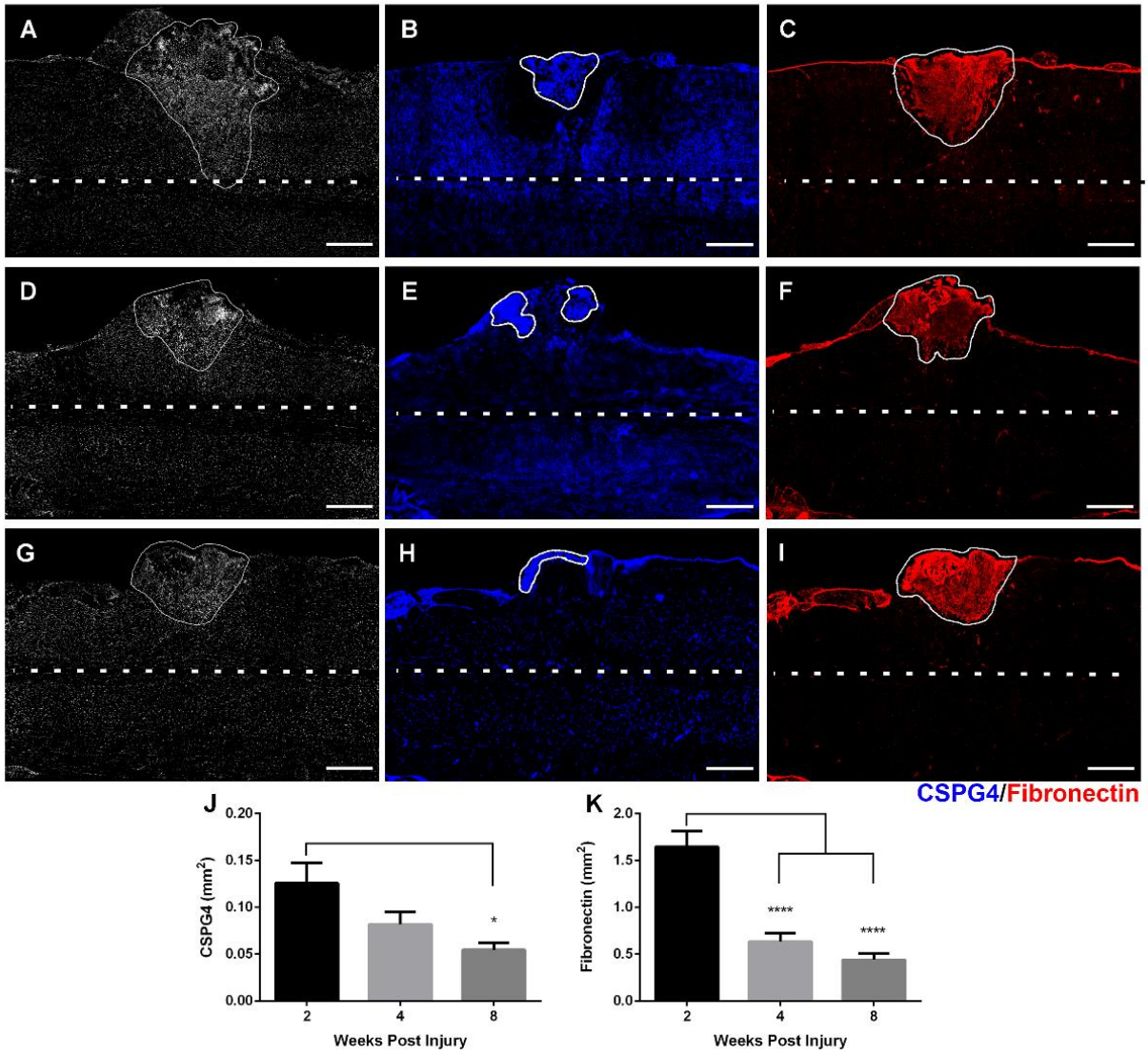

Figure 7.2 Cellular matrix deposition decreases post injury. The lesion site visualized by aggregation of cells (A, D, G). Cellular matrix including CSPG (B, E, H) and fibronectin (C, F, I) localized to the injury site at 2, 4, and 8 wpi. White border denotes injury area. CSPG Area (J) significantly decreased at 8 wpi compared to 2 wpi. Fibronectin Area (K) significantly decreased at 4 and 8 wpi compared to 2 wpi. Scale: 250 µm. * denotes p<.05. **** denotes p<0.0001. n=6 mice per timepoint. Data are presented as mean ± SEM.

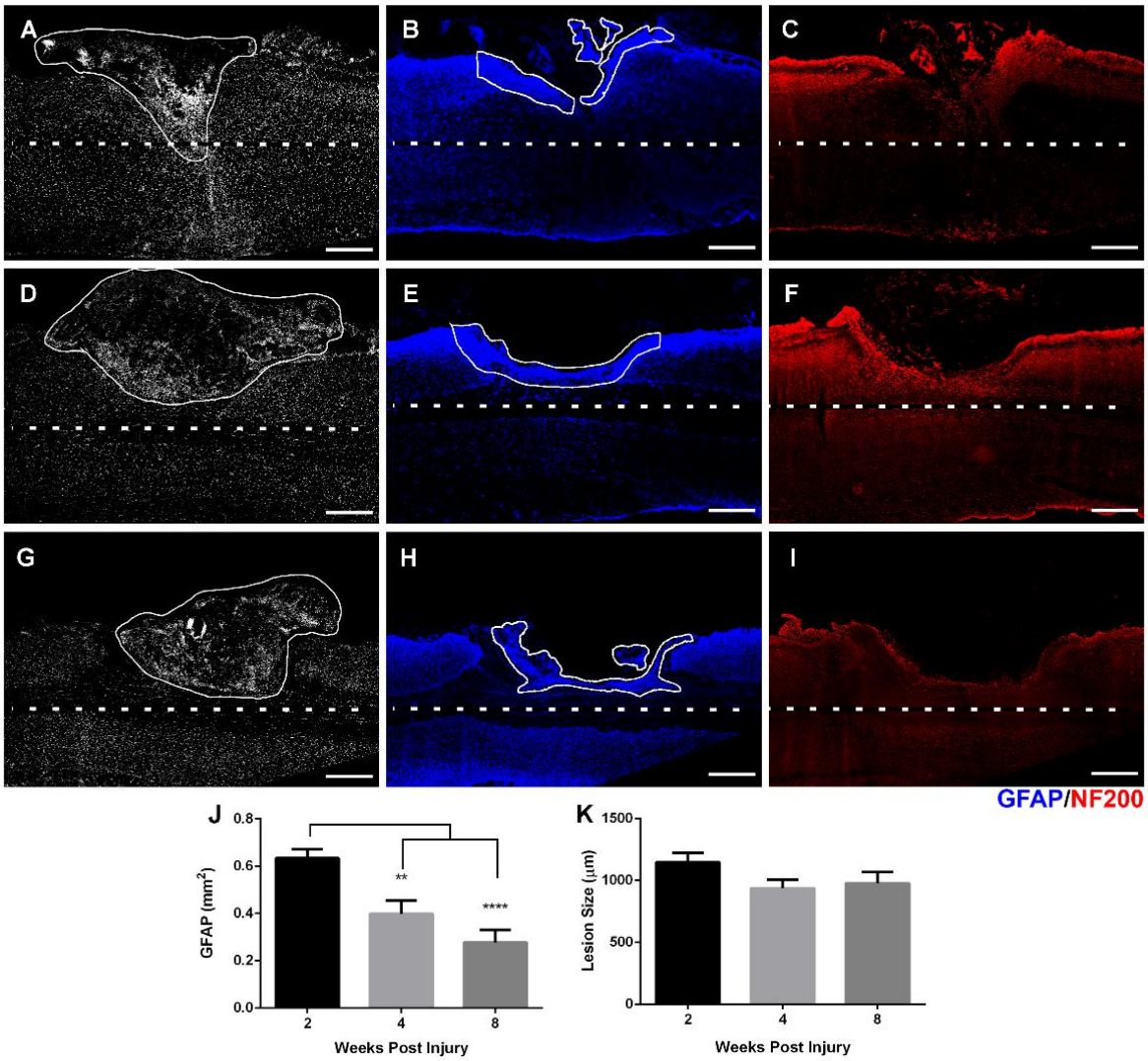

Figure 7.3 Glial scar area resolves post injury. The lesion site visualized by aggregation of cells (A, D, G). The glial scar bordered the lesion area and inhibited axonal growth at 2 (B), 4 (E), and 8 (H) wpi. The lesion space is void of axons at 2 (C) ,4 (F), and 8 (I) wpi. White border denotes the lesion area. White dashed line denotes midline of the spinal cord. Glial scarring (J) decreased significantly at 4 and 8 weeks compared to 2 wpi. The lesion size is consistent across all timepoints. Scale: 250 µm. ** denotes p<.01 ****. denotes p<0.0001. n=6 mice per timepoint. Data are presented as mean ± SEM

4 and 8 wpi. The lesion size was measured by the gap in axon staining at 2 (**Figure 7.3C**), 4 (**Figure 7.3F**), and 8 wpi (**Figure 7.3I**). There was no significant difference in lesion size at any time point. The injury was consistently ~ 1 mm.

Chronic infiltration of macrophages

We initially investigated the extent and timing of macrophage infiltration after the penetrating SCI, as the macrophages are indicators of ongoing inflammation and repair in the injury based on

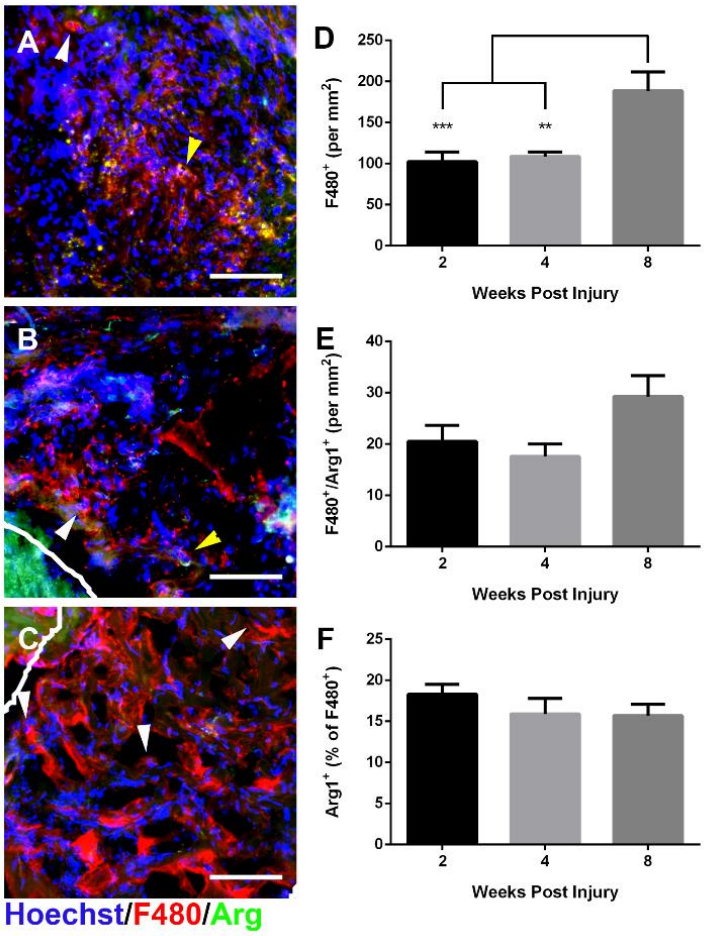

Figure 7.4 F480$^+$ macrophages accumulate in the lesion site at 8 weeks post injury. Macrophages localized to the injury site at 2 (A), 4 (B), and 8 (C) weeks post-SCI. White arrows denote F480$^+$ cells. Yellow arrows denote F480$^+$/Arg1$^+$ cells. (D) Increased density of F480$^+$ at 8 wpi. No difference in density (E) or percentage (F) of F480$^+$/Arg$^+$ macrophages. Scale: 100 µm (A, B, C). ** denotes p<.01 v. 8 weeks, *** denotes p<.001 v. 8 weeks, n=6 mice per timepoint. Data are presented as mean ± SEM.

their phenotype. The number of F4/80$^+$ macrophages in the lesion epicenter was analyzed at 2 (**Figure 7.4A**), 4 (**Figure 7.4B**), and 8 wpi (**Figure 7.4C**) without bridge implantation and divided by the area of the injury for expression as density (cells/mm^2). Macrophage density significantly increased at 8 wpi compared to 2 and 4 wpi (p=0.0007) (**Figure 7.4D**). Macrophage phenotypes exist on a spectrum of cytotoxic to regenerative and we have previously shown that Arg1$^+$ macrophages have a regenerative phenotype in SCI.[135, 260] Therefore, for the purposes of this paper, regenerative macrophages were assessed by co-localization of F4/80$^+$ and Arg1$^+$. No significant

difference in the density of F4/80^{+}/Arg1^{+} cells were observed between 2, 4, and 8 wpi (**Figure 7.4F**). Based on a decrease in glial scarring and the significant difference in macrophage infiltration at 4 and 8 wpi, these time points were the focus of subsequent studies to quantify axonal regeneration at chronic time points.

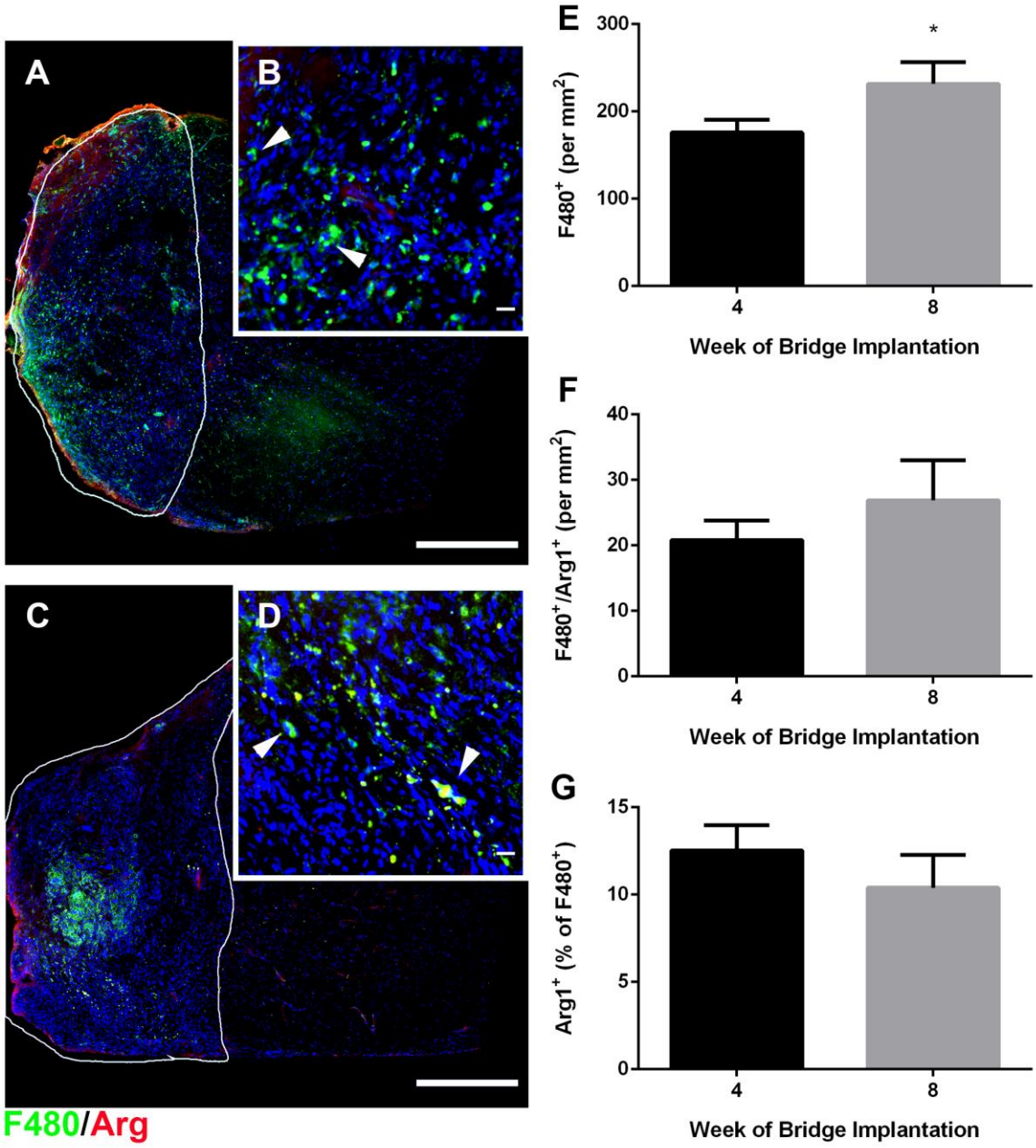

Figure 7.5 Chronic implantation of PLG bridges does not exacerbate immune response at 6 months post injury. Macrophages infiltrated the bridges implanted at 4 (A-B) and 8 (C-D) wpi. White border denotes bridge area. (E) Macrophage density is increased in 8 week bridge implantation compared to 4. No difference in density (F) or percentage (G) of F480^{+}/Arg^{+} macrophages. Scale: 500 µm (A, C). Scale: 20 µm (B, D). **** denotes $p<0.0001$. n=6 mice per timepoint. Data are presented as mean ± SEM.

Bridge implantation does not exacerbate macrophage infiltration

Bridges were implanted at 4 or 8 wpi and explanted for analysis at 6 months post primary SCI. Infiltrating macrophages were found in the bridge for both implantation timepoints (**Figure 7.5**). We observed compaction and degradation of the bridge at 6 months, as evidenced by a reduced bridge area (**Figure 7.10**) with greater reduced area observed in bridges implanted at 4 weeks compared to 8 weeks as these had more time for degradation. However, for bridges implanted at 8 wpi, macrophages were found in clusters rather than evenly distributed as in the 4 wpi condition. There was a higher density of infiltrating macrophages for bridges implanted at 8 wpi compared to 4 wpi (**Figure 7.5E**). As previously stated, we assessed regenerative macrophages by co-localization of $F4/80^{+}$ and $Arg1^{+}$. There were no significant differences in density or percentages of regenerative macrophages (**Figure 7.5F, G**). Furthermore, we observed similar macrophage activity pre- (**Figure 7.4D-F**) and post-bridge (**Figure 7.5E-G**) implantation.

Bridge implantation promotes axonal regeneration into the injury

Bridges were implanted at 4 or 8 wpi and explanted for analysis at 6 months post-SCI. We have previously demonstrated that acutely implanted PLG bridges promote injured axons to grow through the lesion [83, 152, 181, 269], but this is the first time we have reported axon regeneration into the bridge after chronic SCI. We did not observe any axon infiltration into the lesion area before bridge implantation (**Figure 7.3**).

We observed robust axonal growth into bridges implanted at 4 wpi and 8 wpi (**Figure 7.6E**). Furthermore, $CGRP^+$ (sensory) and $ChAT^+$ (motor) axons were observed in the bridge at both implantation timepoints (**Figure 7.11**).

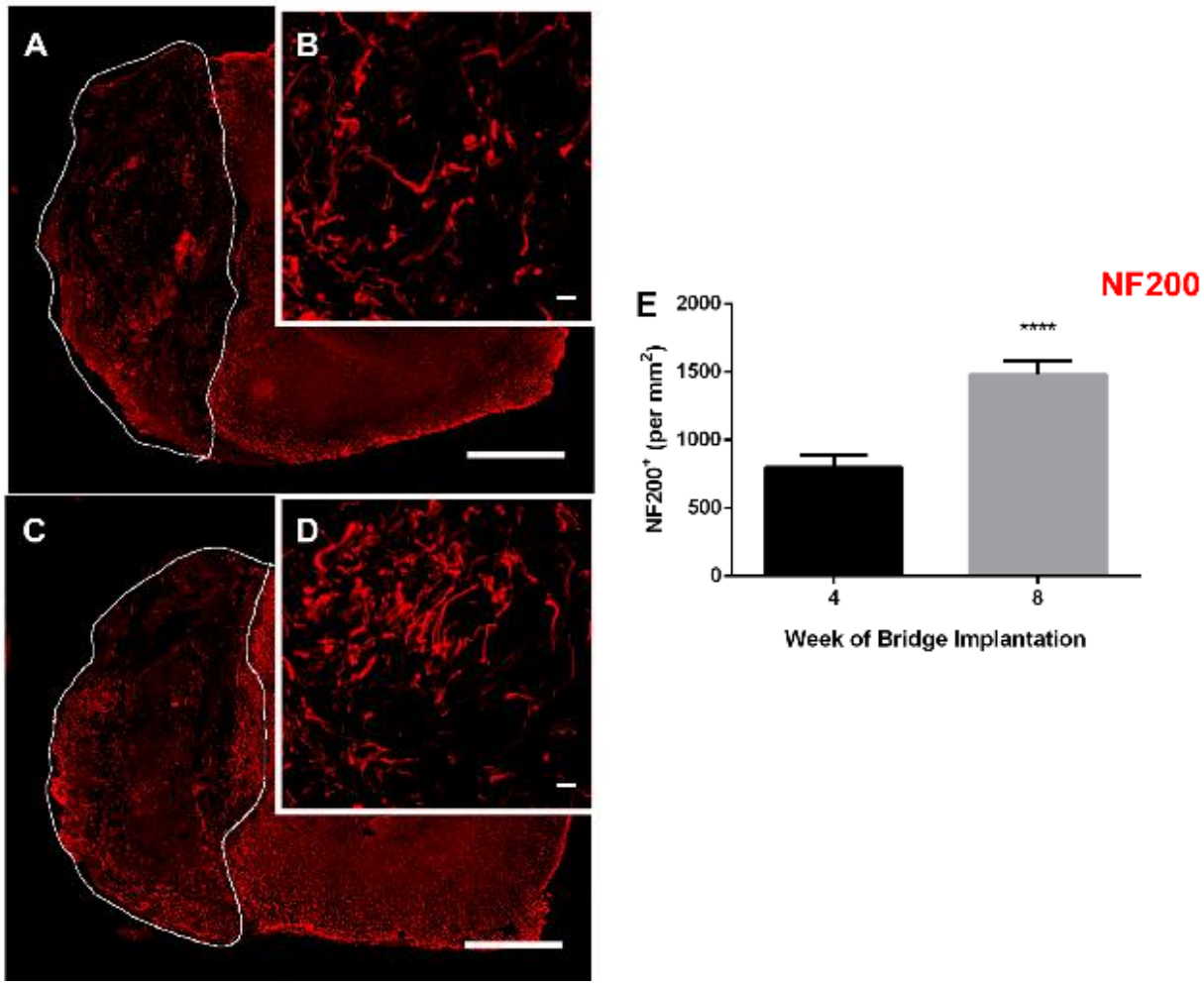

Figure 7.6 Chronic implantation of PLG bridges supports axon elongation at 6 months post injury. Regenerating axons were present throughout bridges implanted at 4 (A-B) and 8 (C-D) wpi. White border denotes bridge area. (E) Axon density is increased in 8 week bridge implantation compared to 4. Scale: 500 µm (A, C). Scale: 20 µm (B, D). **** denotes $p<0.0001$. n=6 mice per timepoint. Data are presented as mean ± SEM.

Chronically regenerated axons are myelinated

Myelinated axons ($NF200^+/MBP^+$) were present throughout the bridges. (**Figure 7.7**). Myelinated axons in bridges implanted at 4 wpi (**Figure 7.7A-B**) were distributed throughout the bridge. However, for bridges implanted at 8 wpi (**Figure 7.7C-D**), myelinated axons were localized to the periphery of the bridge. No significant difference in myelinated axon density was observed between conditions (**Figure 7.7E**). However, a significantly higher percentage, almost

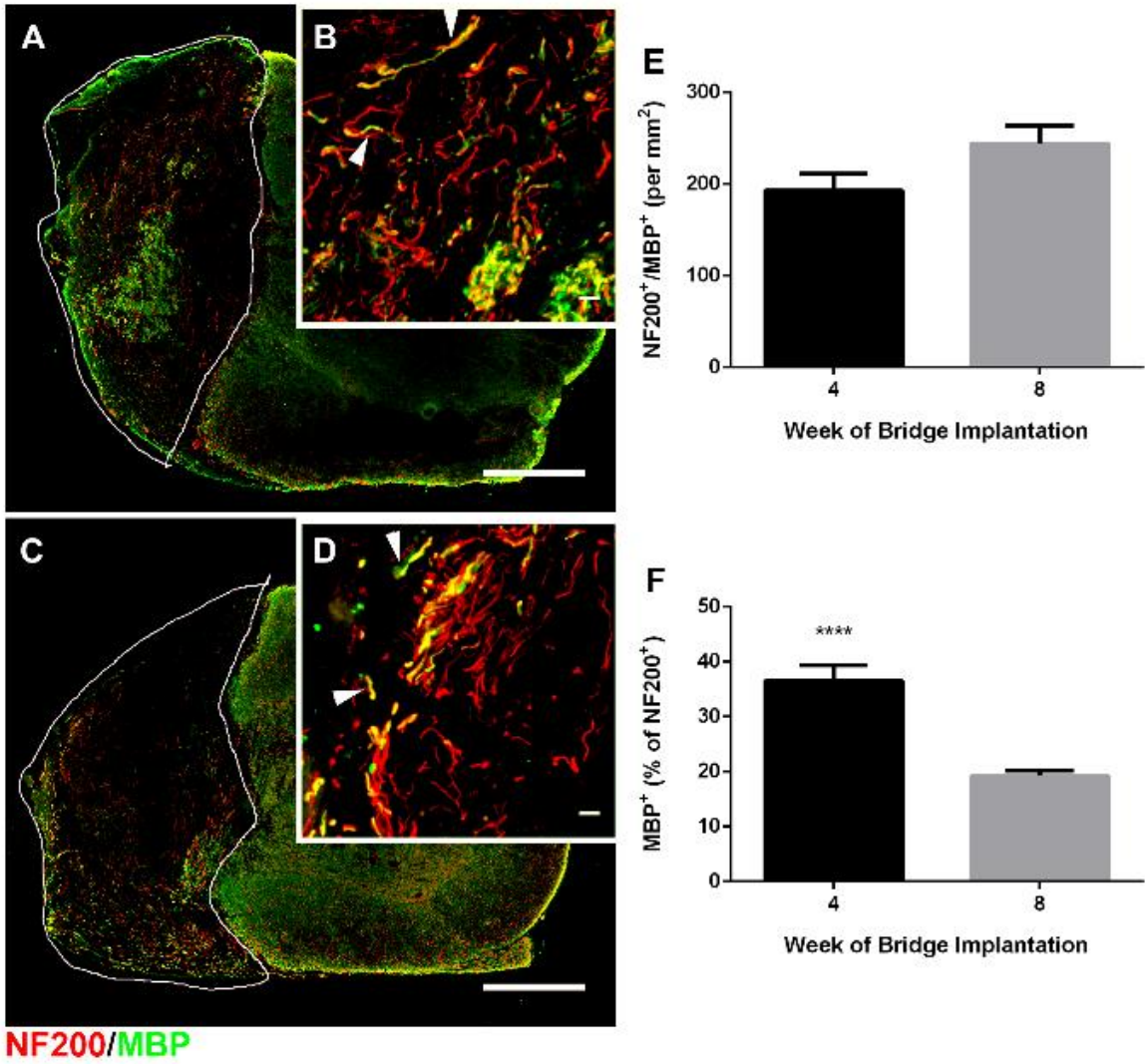

Figure 7.7 Chronically regenerated axons are myelinated at 6 months post injury. Myelinated axons were present throughout bridges implanted at 4 (A-B) and 8 (C-D) wpi. White border denotes bridge area. White arrows denote $NF200^+/MBP^+$ axons. Although myelinated axon density (E) was not significantly different between 4- and 8-week bridge implantation conditions, myelinated axon percentage (F) was significantly greater at 4 week bridge implantation. Scale: 500 µm (A, C). Scale: 20 µm (B, D). **** denotes $p<0.0001$. n=6 mice per timepoint. Data are presented as mean ± SEM

2-fold, of myelinated axons within bridges implanted at 4 wpi compared to 8 wpi (36% vs 19%)

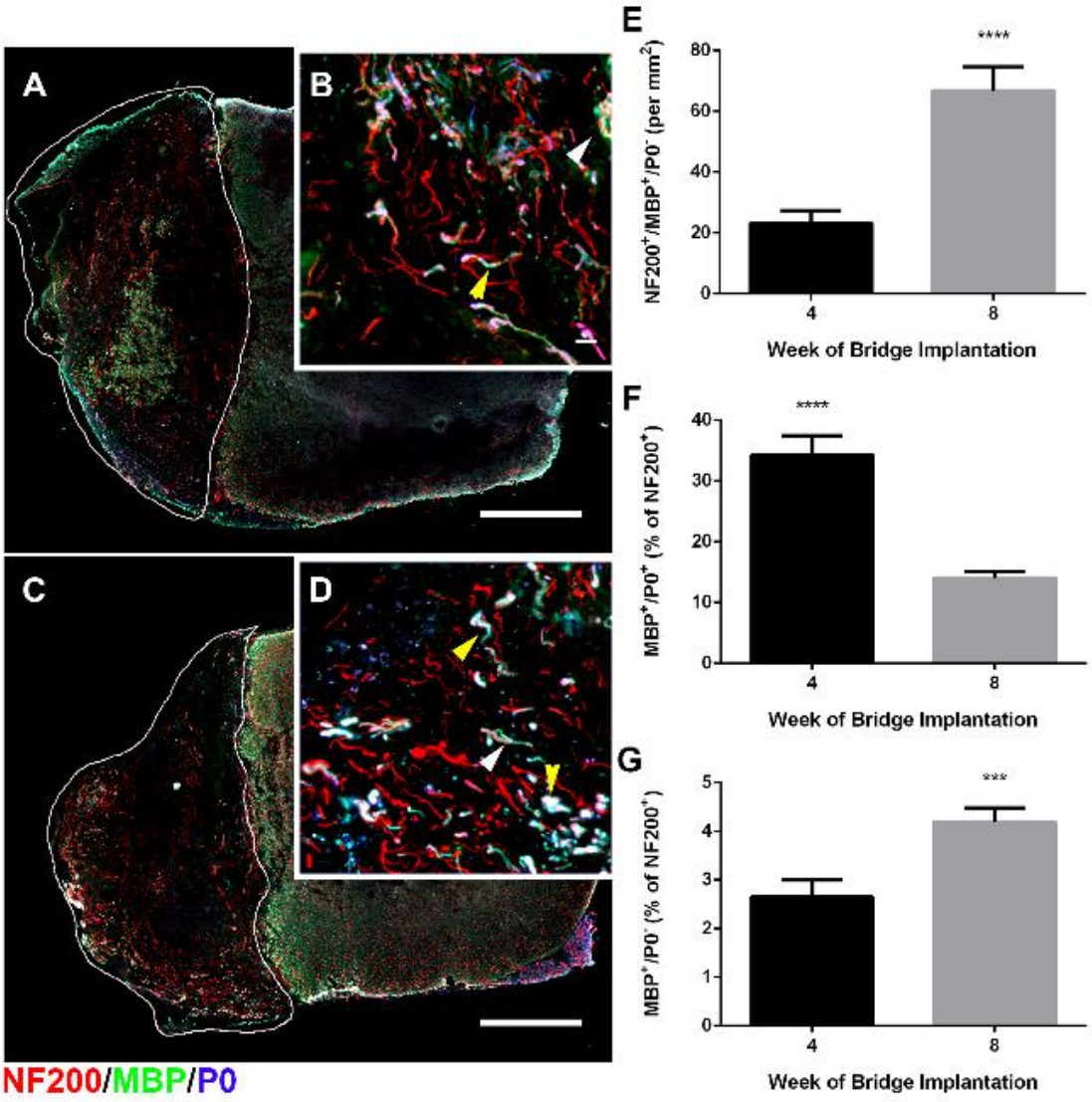

Figure 7.8 Chronically regenerated axons are myelinated primarily by Schwann cells at 6 months post injury. Myelinated axons were present throughout bridges implanted at 4 (A-B) and 8 (C-D) wpi. White border denotes bridge area. White arrows denote $NF200^+/MBP^+$ axons. Yellow arrows denote $NF200^+/MBP^+/P0^+$ axons. $NF200^+/MBP^+/P0^-$ axon density (E) was significantly increased for 8 wbi although the density was low. (F) A significantly larger percentage of axons were myelinated by Schwann cells ($MBP^+/P0^+$) at 4 week bridge implantation condition compared to 8. However, a significantly higher percentage of axons were myelinated by oligodendrocytes ($MBP^+/P0^-$) at 8 wpi bridge implants compared to 4. although the percentages were very low. Scale: 500 µm (A, C). Scale: 20 µm (B, D). *** denotes $p<.001$, **** denotes $p<0.0001$. n=6 mice per timepoint. Data are presented as mean ± SEM.

was observed ($p<0.0001$) (**Figure 7.7F**), with the percentage of myelinated axons defined as the number of $NF200^+/MBP^+$ axons divided by total $NF200^+$ axons. Myelinated axons were separated into Schwann cell myelin ($NF200^+/MBP^+/P0^+$) and oligodendrocyte-derived myelin

($NF200^+/MBP^+/P0^-$) (**Figure 7.8)** to determine their relative contribution to total myelination. A significant increase in the density of oligodendrocyte-derived myelinated axons was observed for bridges implanted at 8 wpi compared to 4 wpi ($p<0.0001$) (**Figure 7.8E**). For bridges implanted at 4 wpi, the percentage of Schwann cell-myelinated axons was increased almost 2.5-fold relative to bridges implanted 8 wpi (34% vs 14%) ($p=0.0009$) (**Figure 7.8F**). However, a significantly increased percentage of oligodendrocyte-derived myelin was observed for bridges at 8 wpi compared to bridges implanted at 4 wpi ($p<0.0001$) (**Figure 7.8G**), although the percentage in both conditions was low, 4.2% and 2.6% of total axons respectively, compared to acute studies[269].

Bridge implantation does not significantly decrease functional outcomes

The ladder beam task was used to evaluate functional recovery before bridge implantation and after bridge implantation (**Figure 7.9**). No significant difference in positive left placement events before bridge implantation compared to after bridge implantation was observed for either group. We performed a linear regression for both conditions to determine if the slope of recovery deviated from zero. Bridges implanted at 4 wpi (**Figure 7.9A**) or 8 wpi (**Figure 7.9B**) did not deviate significantly from zero slope indicating no significant differences in recovery or decrease in function. Overall, the average number of left placements for both conditions across all timepoints

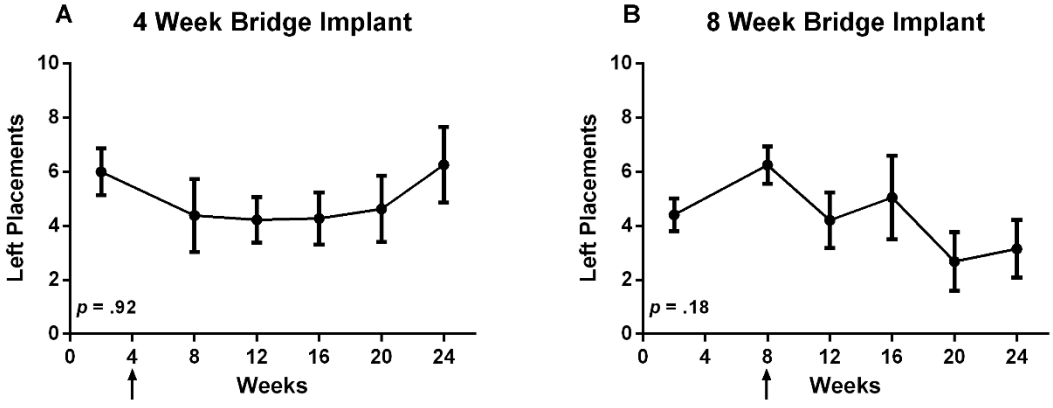

Figure 7.9 Chronic bridge implantation does not decrease functional outcome at 6 months post injury. Ladder beam task was evaluated over the course of 6 months post primary injury for 4 week bridge implantation group (A) and 8 week bridge implantation group (B). p values denote significance from zero slope. n=12 mice per timepoint. Data are presented as mean ± SEM. Furthermore, there was no significant difference between the conditions (p=.84)

were relatively low at 4.9 for bridges implanted at 4 wpi and 4.3 for bridges implanted at 8 wpi. Additionally, the functional outcome of animals receiving bridge implants at 4 weeks versus 8 weeks were not significantly different (p=0.84). We also used the cylinder task to determine dissimilarity index pre- and post-injury (**Figure 7.13**). The animals did not regain use of the impaired forelimb for weight supported full rearing.

Discussion

Currently, no clinically translated strategies exist for treatment of chronic SCI. While researchers acknowledge the need for chronic treatments, there are relatively few investigations compared to acute studies. However, most patients recruited for clinical trials are in the chronic phase and the barriers to regeneration in the chronic lesion are different from those of the acute lesion. Chronic SCI models commonly employ a contusion injury and treatments generally combine exogenous cell transplantation with the digestion of the glial scar and some neurotrophic support. Similar cellular and biochemical events occur in both contusion/compressive and transection models. The glial scar is formed by reactive astrocytes, which become hypertrophic and greatly increase their expression of intermediate filament proteins such as vimentin and glial fibrillary acidic protein (GFAP). The expression of both growth-inhibitory and growth-promoting ECM increases in reactive astroglia and invading immune cells, but the inhibitory ECM components, such as fibronectin, GFAP, and CSPGs are more markedly upregulated.[311] When severed axons meet the scar, the growth cones form ‘dystrophic endbulbs’ and stop growing. However, differences in the spatial distribution of ECM and cellular infiltration are observed. In contusion models, ECM such as fibronectin or CSPGs fill the lesion site while in transection models, these materials reside at the borders of the lesion.[84, 137] In contusion models, this injury results in a necrotic core of tissue; while in transection models of injury, a necrotic core is not

observed. Furthermore, transection models are easier to reproduce and implement and do not suffer from variability in lesion size and location. A transection chronic injury model allows for biomaterial implantation of a permissive substrate for improved responsive of treatment paradigms. Biomaterials have been used extensively in acute studies of SCI but have been relatively absent in chronic SCI due to irregular injury boundaries from contusion or penetrating injuries and formation of dense scar tissue in the lesion site. However, resection of the scar is being investigated in animal and clinical treatment strategies to remove the dense connective tissue that can inhibit regeneration.[56, 310] Our bridge has served as an effective platform to study the acute space, but we have not investigated its efficacy in chronic SCI. The goals of this investigation were to create a reproducible chronic injury model that combines the benefits of contusion and transection models and to show PLG bridges are a growth permissive substrate for axonal elongation and tissue reformation after chronic spinal cord injury.

The chronic injury model was based on our previous acute penetrating lateral hemisection model and other models of chronic SCI.[269, 310] We performed two lateral slices 1 mm apart for reproducibility in locating the boundaries of our lesion site. The tissue was not resected immediately to mimic a central aspect of human SCI and pathophysiology, in which the injured tissue becomes necrotic, which can be anticipated to modulate both the immune response and scar formation in the host spinal cord. At 4 or 8 wpi, the lateral slices were located and connected along the midline to resect the necrotic tissue. The necrotic tissue was evident by its stiff texture and discoloration.[312] We did not resect tissue past our lesion area defined by the two lateral slices or recreate the initial two lateral slices. The bridge was then implanted at two timepoints, at 4 or 8 wpi, and evaluated at 6 month post injury. The goal of this model was to capture the pathophysiology of human SCI and scar resection while elucidating differences in

pathophysiological considerations for biomaterial invention by using two different timepoints. In our model, surgical resection of the scar following the initial injury creates a gap into which a bridge is implanted. Bridge implantation demarcates an area that allows analysis of the extent of axon regeneration into the injury as axons present within the bridge could not have been spared.

The glial scar and fibrotic scar that forms at the interface between the injury and intact host tissue acts both as a physical barrier and as a set of cellular and biochemical signals that instruct axonal ends to become dystrophic and stop growing.[58-60] This scar forms within days of SCI but is stabilized after 4 – 8 weeks in rodents[312]. We chose to investigate biomaterial intervention after the scar stabilized to assess the ability of axons to regenerate through this scar and into our bridge in this model. The scar is comprised of potent inhibitory ECM components including fibronectin and CSPG4 as well as cellular components such as reactive astrocytes. These components are thought to be the most potent inhibitors of axonal regeneration. Fibronectin scarring was significantly decreased, almost 3-fold, at 4 and 8 wpi compared to 2 wpi. However, no difference was observed between 4 and 8 wpi. Fibronectin has been reported to develop and stabilize over a 28 day period into a dense scar and decline significantly after 28 days in contusive models of SCI.[313] Similarly, CSPG4 expression decreased significantly at 8 wpi compared to 2 wpi. CSPG4 expression is temporally related to inflammation within the CNS and its resolution suggests there was no ongoing destruction of CNS tissue past the initial 2 weeks of high expression.[314] We also saw a significant decrease at 4 and 8 wpi compared to 2 wpi in reactive astrocytes evidenced by GFAP area. The components of the glial scar condensed and localized to the lesion site over time. This is consistent with other chronic models of SCI.[235, 315] The functions of glial scar formation remain nebulous; however, lack of glial scar formation presents deleterious effects on spontaneous regrowth of transected axons.[26, 56] The process of axonal dieback was immediate. $NF200^{+}$ axons

initially retracted from the scar, but then gathered near the scar border. This observation is consistent with other studies showing that majority of axonal dieback has ceased by 4 wpi.[316] However, they did not penetrate the lesion site before bridge implantation**.** The condensing of the glial scar to the injury site and accumulation of axons near the lesion borders may facilitate axon entry into our bridge once implanted by expression of growth supporting molecules at the injury site [56]. The spinal cord may have more growth potential at 4 week bridge implantation rather than 8 week bridge implantation. However, the transition of acute to chronic has been identified by the density of glial and fibrotic scaring by many researchers, and these densities are not statistically different between 4 and 8 weeks. However, a consistent metric that delineates the transition of acute to chronic injury has not been determined, as many chronic models have ranged from 4 – 8 weeks.[91, 317, 318] Some studies have sought to characterize the transition to chronic injury using combined MRI, electrophysiological, and histological guidelines.[312] These strategies targets 4 – 8 weeks as the transition into chronic injury, which reflects our choice of time points.

We observed accumulation of macrophages into the lesion at long time points, which is consistent with chronic SCI[319]. Macrophage density was significantly increased at 8 wpi compared to other time points. Previous studies have reported a second wave of macrophage infiltration at 60 days post-SCI in a contusion model.[319] The phenotype of these macrophages is unclear because their invasion has not been associated with increased improvements or decrements of motor function. We observed a ~44% (20.52 cells/mm^2 vs. 29.53 cells/mm^2) increase in Arg1$^+$ macrophage density at 8 wpi vs 2 wpi. F480$^+$/Arg1$^+$ macrophages have been associated with a pro-regenerative phenotype[135, 224]. Interestingly, the percentage of Arg1$^+$ macrophages was consistent at all time points. This result is also consistent with previous reports of Arg1 expression levels returning to baseline shortly after the initial contusion injury.[260] The net effect of infiltrating

macrophages at chronic timepoints remains undefined. They have been associated with encouraging remyelination by upregulating differentiation of oligodendrocyte progenitors, upregulating factors that inhibit remyelination, and reactivating regenerating properties of the axons.[319-321] The accumulation of macrophages and the nebulous nature of their activity make them an attractive target to investigate chronic modulation of these cells to alter the percentage of regenerative macrophages in future studies. Taken together, this model recapitulates several aspects of the pathophysiology of traditional chronic models and enables generation of a reproducible defined space for investigation of regenerative medicine interventions.

The bridge features aligned channels to support axonal growth and provides a porous structure for cellular infiltration and ultimately supports axon growth into the injury at chronic time points.[83, 137, 178] Axons entering the implant must be attributed to either regeneration of injured axons or sprouting of new axons from spared or contralateral tissue. This bridge provides a defined space for histological analysis at and near the lesion. Sufficient evidence exists that demonstrates a lack of substantial axonal ingrowth without intervention.[310] Moreover, without biomaterial intervention there is no precise way to delineate between sparing, regeneration, or local axon sprouting in the ipsilateral tissue. The bridge alone has supported robust axon ingrowth, myelination, and recovery of some motor function at acute timepoints,[181] but we have not investigated its efficacy in a chronic injury. Bridges were implanted at 4 or 8 wpi to investigate if the substrate alone could support ingrowth at chronic timepoints. The spinal cord tissue was explanted at 6 months post primary SCI. The PLG bridge scaffold has degraded significantly at this timepoint, however the general structure such as its porosity was still observed in histological sections as previously reported.[137] First, we determined if bridge implantation caused increased infiltrating of macrophages into the lesion space. Although macrophages were observed within the bridges, the number of

macrophages were similar to before bridge implantation suggesting bridge implantation does not cause increased inflammation. There were also similar percentages of anti-inflammatory macrophages present in the bridge post implantation compared to macrophage phenotypes in the lesion space before bridge implantation. This buttresses the bridge as tool to observe the chronic spinal cord microenvironment and capture the residing cells without influencing the inflammatory environment.

PLG bridges were able to support ingrowth of sensory and motor axons at both implantation timepoints without added bioactive agents. Similarly, poly(ethylene glycol) (PEG) gel injection has been shown to support axonal ingrowth at chronic timepoints but, we cannot readily compare our results due to a difference in method of quantification.[103] Furthermore, the PLG bridge offers a topographical benefit over bulk PEG injection. Interestingly, there was higher infiltration of axons for bridges implanted 8 wpi compared to 4 wpi. This suggests axonal regeneration can occur through our bridges at up to 8 wpi. Studies have shown axonal growth at chronic timepoints with the aid of cell transplantation and factor delivery, but this result is novel because the PLG bridge alone without added bioactive agents supported robust ingrowth. Future studies will focus on identification of specific tracts using genetically modified mice to reveal differences in spinal tract specific regeneration potential in the chronic period post-SCI.

While no difference in the density of myelinated axons was observed, a significantly higher percentage of axons were myelinated for bridges implanted at 4 wpi. This lack of myelination for bridges implanted at 8 wpi could be the result of overall lower mobilization of glial cells at chronic timepoints.[322] The percentage of myelinated axons is consistent with previous data using PLG bridges.[183, 269] Axons after injury can be myelinated oligodendrocytes or Schwann cells. Therefore, we investigated the source of the myelin at chronic time points. A higher density and percentage

of oligodendrocyte myelin was observed for bridges implanted at 8 wpi compared to bridges implanted at 4 wpi. There was a 3-fold increase in density and 2-fold increase in percentage. This suggests higher activity of oligodendrocytes at later timepoints possibly due to differentiation of progenitor cells. However, oligodendrocyte myelin density and percentage were low at both time points suggesting low availability or differentiation of oligodendrocytes at chronic timepoints. Oligodendrogenesis can occur up to at least 80 days post injury.[323] While there is evidence for negligible demyelination of spared axons and remyelination of intact or spared axons at chronic timepoints, the ability of newly formed oligodendrocytes to myelinate large numbers of regenerating axons has not investigated and quantified at chronic time points.[221, 222] The failure of oligodendrocytes to myelinate these regenerating axons may contribute to the lack to functional recovery.[187, 238] A 3-fold increase in Schwann cell myelin percentage was observed within bridges implanted at 4 wpi compared to 8 wpi. Although Schwann cells are highly migratory and invade the lesion site immediately after injury.[184] they can also be differentiated from oligodendrocyte progenitor cells (OPCs).[299] Future studies will focus on pushing these OPCs to adopt an oligodendrocyte fate as previously described.[269]

We employed the ladder beam task to assess functional recovery before bridge implantation and after bridge implantation for both implant paradigms. Few studies have noted functional improvements in chronic spinal cord even with the additions of cells or bioactive factors.[91, 324] Studies that have seen functional improvements typically were completed with milder injuries, pre-treatments with biological agents, or stem cell delivery with added factors.[76, 103, 163, 256, 325] However, our model reflects more severe injuries and allows for the assessment of regeneration in a more controlled environment using only a multiple channel bridge. While the bridge alone did not improve functional outcomes for either implantation time point, importantly, the process of

bridge implantation did not significantly decrease the post injury function. These studies establish that axons can regenerate into the bridge and can be myelinated with implantation at chronic time points. However, the bridge alone is limited in its ability to foster regeneration. We have used these bridges as a substrate to deliver multiple treatments aimed at repopulation of resident cells,[152] remyelination,[269] modulating inflammation,[135, 224] and treating neuropathic pain.[136] The studies discussed herein provide a baseline for future studies with bridges combined with strategies we have developed previously for acute SCI intervention.

Conclusions

We have demonstrated a chronic SCI model that follows emerging clinical practices and the pathophysiology of most patients and other models. We have also shown that resection of necrotic tissue and implantation of multi-channel PLG bridges without added bioactive agents as a promising building block for axonal regrowth and myelination during chronic implantation. The bridges also serve as a tool to delineate between regenerating and spared tissue at several implantation timepoints. There are three essential factors for axons growth; neuron intrinsic growth capacity, growth supportive substrate, and chemoattraction.[326] These studies establish PLG bridges as a growth supportive substrate and will serve as a baseline for future studies focusing on utilization of the bridge as a platform to deliver bioactive agents to promote neuron intrinsic growth and chemoattraction as well as a defined space to investigate the chronic tissue microenvironment.

Supplementary Figures

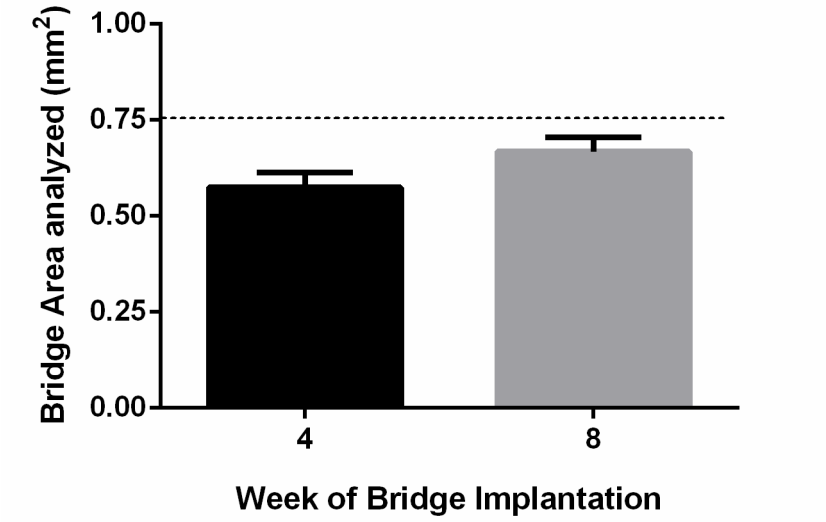

Figure 7.10 Bridge area 6 months post injury. Dashed line indicates cross sectional bridge area at time of implantation. While there was significant degradation from initial implantation, there was not a significant difference between 4 and 8 week bridge implantation timepoints. Note that the bridges implanted at 4 weeks post injury exhibit a lower area, most likely due to being inside the animals longer than the bridges implanted at 8 week post injury.

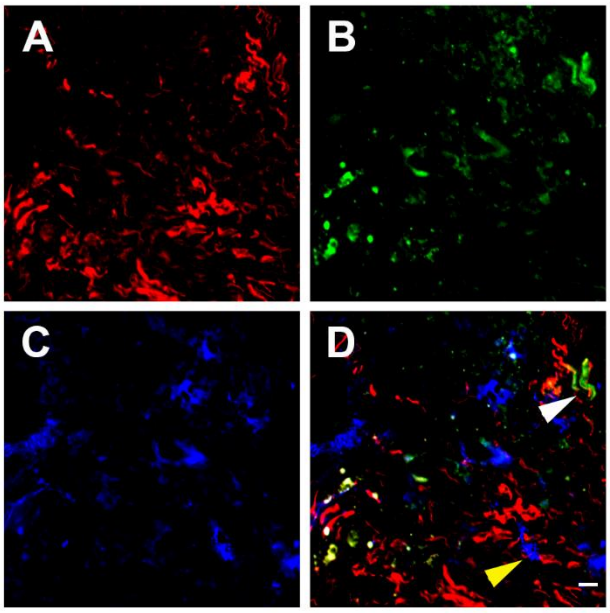

Figure 7.11 CGRP and ChAT axons regenerate into the bridge at 6 months post injury. (A) $NF200^+$ axons colocalized with ChAT (B) and CGRP (C) (D) White arrows denote $NF200^+/ChAT^+$ axons. Yellow arrows denote $NF200^+/CGRP^+$ axons. Scale: 20 µm.

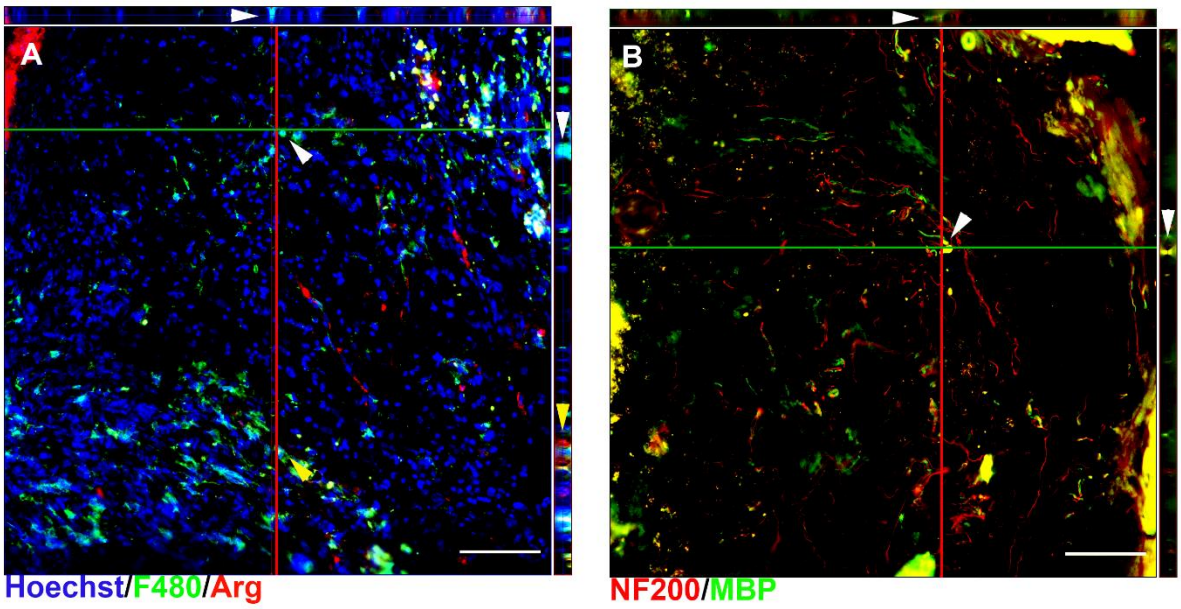

Figure 7.12 Z-stack images showing 3 dimensional overlap of (A) Hoechst^{+}/F480^{+}/Arg $^{+}$ and (B) NF200^{+}/MBP^{+}. White arrows denote areas of overlap. Yellow arrows denote Hoechst^{+}/F480^{+}/Arg $^{+}$ cells. Scale: 100 µm.

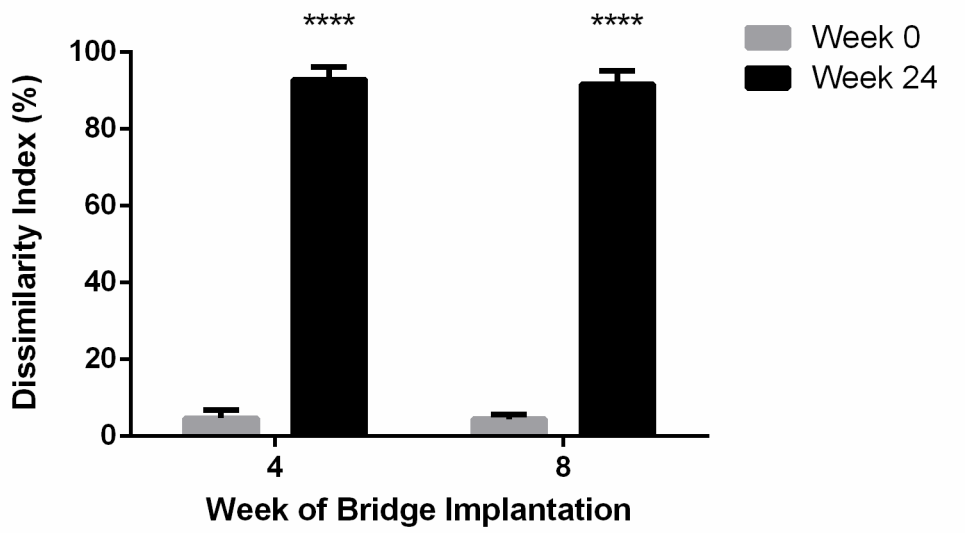

Figure 7.13 Cylinder Test. Asymmetry in the mice was evaluated over 6 months. Animals predominantly used the non-impaired forelimb for weight supported full rearing which is indicated by high dissimilarity index at 6 month post injury. **** denotes $p<0.0001$.

Chapter 8. Conclusions and Future Directions

Summary of findings

Taken together, the work presented in this dissertation describes development of a biomaterial scaffold implant for spinal cord regeneration and as a tool to understand the spinal cord microenvironment post injury. The implant was formed from PLG into a multi-channel, porous bridge that allows the recruitment of host cells and regeneration of axons across the lesion site. We combined the bridge with gene therapy strategies to elucidate how exogenous factor delivery impact the tissue microenvironment. Pro-oligodendrogenic factors were used to study the effect of recruitment, proliferation, and differentiation of endogenous progenitor cells on myelination of regenerating axons and subsequent functional recovery. We identified oligodendrocyte myelin as a key factor in determining functional recovery. Additionally, the bridge platform was used to deliver an immunomodulatory factor combined with a neurotrophic factor to evaluate how spared tissue and regenerating tissue differ in their tissue formation and functional recovery. We found neurotrophic factors and immunomodulatory factors can have synergistic effects on axonal growth, myelination, and functional recovery. The bridge was also evaluated in a chronic SCI. We found that bridge implantation alone can promote axon elongation and myelination at chronic timepoints, providing further evidence for biomaterials being translated to human patients. The research described in this dissertation builds on the previous work in this field and advances the utility of biomaterials as a platform SCI regeneration and tissue regeneration broadly.

Significance and Impact of findings

The work presented in this dissertation addresses an unmet clinical need for development of spinal cord injury treatments. Nationally, the incidence of cervical SCI exceeds thoracic (51% vs. 36%), and the incidence of contusion/compression trauma exceeds penetrating injuries due to violence (e.g. gunshot or stab wounds). However, penetrating SCI accounts for 14% of cases annually in the general population, and astonishingly 28% of cases in the military [7], largely due to the contribution of blast injuries. Penetrating injuries directly sever descending motor and ascending sensory tracts, so they offer many opportunities to study strategies that encourage formation of new axons and myelination. Moreover, while spontaneous recovery within the first days and months post-SCI is a significant component of the final outcome in individuals with contusion/compression injuries [8], the initial deficits resulting from penetrating SCI exhibit substantially less improvement, if any, over time [9]. There are minimal therapeutic strategies for penetrating SCI, in which there may be little opportunity to ameliorate the initial damage, and reconnection of spinal pathways require a bridge to support true axonal regeneration. This work aimed to use the bridge as a platform to investigate the spinal cord microenvironment and determine the most germane barriers to regeneration for any potential treatment strategies. In **Chapter 5** we use the PLG bridges as a platform to investigate the role of pro-oligodendrogenic factors in promoting remyelination of regenerating axons. The combination of noggin + PDGF enhanced total myelination of regenerating axons relative to either factor alone, and importantly, enhanced functional recovery relative to the control condition. The increase in myelination was consistent with an increase in oligodendrocyte-derived myelin, which was also associated with a greater density of cells of an oligodendroglial lineage relative to each factor individually and control conditions. These findings demonstrate that myelination of regenerating axons, specifically

by oligodendrocytes is important to functional recovery and should be a part of any potential clinically translatable treatment for SCI. In **Chapter 6** we build upon the success of the multiple channel PLG bridges by delivering 2 distinct transgenes targeting immunomodulation and neurotropism in combination to observe synergistic or possibly antagonistic effects on spinal cord regeneration. Our results show that the combination of IL-10+NT-3 enhanced axonal growth and oligodendrocyte myelinated axon density. This resulted in increased locomotor functional recovery compared to IL-10 or NT-3 alone but increased hypersensitivity compared to IL-10 alone. Furthermore, we observed a strong positive correlation between oligodendrocyte myelinated axon density and functional recovery. This suggests oligodendrocyte myelin as an important area of future of research to improve functional recovery. For these therapies to be clinically translatable, they must be investigated in a chronic injury model. Therefore, in **Chapter 7** we investigate tissue regeneration into PLG bridges implanted into a chronic model of SCI. Two time points were analyzed for implantation of the bridge (4 wpi or 8 wpi). We observed robust axon growth into the bridge and remyelination at 6 months post initial injury. Axon densities were increased for 8 week bridge implantation relative to 4 week bridge implantation, whereas greater myelination was observed with 4 week bridge implantation. While the bridge alone did not improve functional outcomes for either implantation time point, importantly, the process of bridge implantation did not significantly decrease the post injury function. This chapter demonstrates implantation of PLG bridges without added bioactive agents as a promising building block for axonal regrowth and myelination during chronic implantation and further demonstrates the clinical translatability of the bridge.

Future Directions

The follow sections propose future studies that will enhance the significance and impact of the work presented herein.

Temporal regulation of pro-regenerative signaling

In **Chapter 5**, we delivered pro-oligodendrogenic factors to promote remyelination of regenerating axons. We delivered these factors simultaneously, but each factor affects a different stage along the cell lineage. PDGF affects the proliferation of NSCs while noggin impacts the differentiation of NSCs along the oligodendrocyte lineage. This dissertation shows that when delivered together, these factors can increase the total number of oligodendrocytes and increase remyelination. However, there is an opportunity to investigate sequential delivery of these factors to increase the number of differentiating oligodendrocytes, subsequent myelination, and functional recovery. We can temporally regulate transgene expression with the use of tetracycline (TET)-inducible systems, which modulate gene expression with the doxycycline administration [327, 328]. The TET system can turn on the expression of PDGF with doxycycline administration called TET-on and subsequently turning on noggin expression and turning off PDGF expression with removal of doxycycline (TET-off). This system combined with sophisticated tracking of cell fates using BrdU can elucidate the differentiation potential of endogenous NSCs and how they contribute to myelination of regenerating axons. The TET system can be used for temporal delivery of other sequential processes such as axonal extension through the lesion and then encouraging synapse formation or reducing inflammation and then promoting regeneration. Furthermore, cells may behave differently in a temporally regulated system rather than constant gene expression [329]. Temporal regulation of signaling is of vast importance to future therapies and our understanding of tissue regeneration because it has the potential to recreate the temporal signaling used during

development and avoid the pitfalls of receptor downregulation and depression. Currently, there are many in vitro models that attempt to recreate the conditions of oligodendrocyte development, but for these models to be translatable, they must be applied in vivo [248]. While the TET system is well known and easy to implement, there are other temporally inducible systems such as the tamoxifen (TAM) system [330]. There must be more investigation into which system is the most appropriate for use in our models.

Improved understanding of the cytokine/neurotrophin axis

In **Chapter 6,** we investigated the cytokine/neurotrophin axis which a complicated feedback and crosstalk system between invading immune cells and CNS tissue that can inhibit or promote regeneration. This dissertation suggests there can be additive effects when delivering IL-10 and NT-3 simultaneously on myelination and functional recovery. However, there are remaining questions related to the mechanism of the interactions and the phenotype of the immune cells. We employed arginase to label regenerative macrophages, but at the time of completion of this study, there was no avenue for distinguishing microglia and macrophages. Macrophages are invading immune cells differentiated from circulating monotype after injury. Microglia are resident macrophages in the CNS. Currently, these cells can be differentiated by TMEM119[331]. Separation of these two cells will allow us to determine the relative importance of contribution of macrophages versus microglia in the regenerating spinal cord. Furthermore, these cells express several phenotypes and may behave differently in response to neurotrophins and cytokines. Single cell RNAseq experiments will be able to distinguish phenotypes and elucidate beneficial cell types and targets for perturbing immune cells to adopt the preferred phenotypes.

Improved understanding of the role of oligodendrocyte myelin in functional recovery

One aim of this dissertation was to determine the most germane barriers to functional recovery post-SCI. Lack of myelination has been demonstrated to be a significant hindrance to recovery of function to regenerating axons [187, 238]. We analyzed remyelination of regenerating axons **Chapters 5, 6, and 7** and we employed metrics of functional recovery to elucidate how myelination contributed to motor recovery. This dissertation suggests the difference in myelination density and percentage may contribute in part to improved functional outcomes. This dissertation also suggests that oligodendrocyte-derived myelin is pivotal for return of function. We observed a significant correlation between functional recovery and oligodendrocyte myelinated axon density when performing a linear regression analysis on our results. However, the exact impact of oligodendrocytes and their myelination remains nebulous. Differences in injury models may determine the impact of oligodendrocytes as oligodendrocyte have been seen as less important in contusion models [302]. Our hemisection model severs and removes existing axons and cells in the lesion while contusion models leave the damaged tissue. There is an opportunity to investigate this difference in the impact of oligodendrocytes on functional recovery. Oligodendrocytes perform many functions in the developing and stable CNS including; promoting vascularization, modulating neuroinflammation, modulating synaptic efficacy, remodeling myelin, regulating neuronal excitability, conduction velocity, and synchronicity, and providing metabolic and survival support to axons and neurons [332]. We must investigate these functions of oligodendrocytes in the regenerating spinal cord. We and others have investigated MBP expression in the myelin sheath but, while critical for action potential conduction, other factors are required for neuron and axon survival [294]. In addition to understanding the function of oligodendrocytes in supporting axonal growth, we must investigate how functional recovery is related to regenerated axons. We

must understand the spinal circuitry changes that enable recovery by applying new approaches to trace network remodeling and circuit remapping to identify whether functional recovery results from regenerating axons, spared axons, or a combination of both. This goal can be achieved using complex synaptic tracing involving G-protein deleted rabies virus and electrophysiological recording from the spinal cord and muscle at several timepoints to correlated tissue regeneration and electrophysiological metrics. Further investigation into this area will facilitate a greater understanding of a chief supporting cell in the CNS and provide insights into axon/myelin interactions beyond conduction velocity to enhance functional recovery post-SCI.

Chronic implantation of bridges combined with other bioactive agents

Currently, there are no widespread clinical treatments for chronic SCI. In **Chapter 7**, we employed the PLG bridge in a chronic SCI to determine if the bridges are a suitable substrate for tissue regeneration in the chronic environment. We found the bridge is a suitable substrate for axonal regeneration and myelination. We have set a baseline for expected regeneration and there is an opportunity to build on the PLG substrate. There is little understanding of how early injury interventions affect later regeneration. While, methylprednisolone has previously been employed to treat SCI, it is no longer the standard of therapy due to mixed results [10]. It is also unclear if axon growth promoting factors remain effective during the chronic phase of SCI. These questions can be investigated by combining acute delivery of anti-inflammatory factors after injury such as IL-4 or IL-10 to reduce the initial tissue destruction and promote tissue sparing with chronic treatments[135, 224]. Additionally, the glial scar can be dissolved prior to bridge implantation using Ch'ase or ADAMTS-5. ADAMTS-5 presents a better option because it is less immunogenic as its source is mammalian and not bacterial[333]. Chronically, we can deliver axon growth promoting factors such as EpoD to drive axons through the inhibitory environment and myelinating factors

such as PDGF and noggin to myelinate the regenerating axons. The stabilization of axons, combined with the directional cues supplied by the bridge, may lead to more robust regeneration. However, chronic SCI studies have been hampered by lack of sustained motor recovery due to elimination and re-apposition of presynaptic terminals leading to unsynchronized action potential initiation and propagation that reduces recovery of locomotor function and promotes nociceptive hypersensitivity [334]. In order to achieve functional recovery chronically, our approach must induce appropriate plasticity. To this goal, it is imperative that we move toward identifying the circuits that are beneficial to plasticity. These studies will lay the groundwork for transition into larger animal studies and possible clinical translation.

Clinical translation of bridge technology

There are several considerations for transitioning into larger animals and patient trials. Larger animal studies will require modifications to the bridge structure, but the pathophysiology of injury and recovery is conserved across mammals. Second, we must determine a reliable way to identify the lesion border and where to implant the bridge. This can be achieved by using a combination of MRI and nanoparticles. MRI can distinguish the healthy tissue from necrotic tissue using fractional anisotropy. Additionally, we can use labeled nanoparticles to invade the lesion site by taking advantage of the injured BBB. This would give us a visual indication of the lesion borders. Third, we must identify if there is a critical period for bridge implantation. This dissertation shows that there are remarkable differences between implanting a bridge at 4 wpi compared to 8 wpi. We must determine how different implantation times translates to larger animals and humans. Last, as spinal cord lesions can span several laminae, we must determine if there is a critical implantation area or if all the affected tissue should be replaced with a bridge structure. This will allow us to determine the optimal bridge implantation area. The pitfall of most experimental clinically

translated approaches is determining trials receive less favorable patients because the risk/benefit ratio more reasonable. However, these patients have often undergone complete sensory and motor failure (American Spinal Injury Association (ASIA) impairment scale A/B). While some trials have seen some success, rarely are patients upgraded in the ASIA impairment scale [308, 335]. Enhanced understanding of circuit reorganization during chronic injury and how early intervention impact motor recovery may help improve the outcomes seen when these therapies are translated to human patients.

Appendix

Peptide modification of PLG bridges for viral loading

Introduction

Delivery of therapeutic substances to the spinal cord presents a challenging engineering problem. The blood-spinal cord barrier prevents entry using systemic approaches and cerebral spinal fluid could transport the therapeutic from the site. The Shea Lab has developed multi-channel PLG bridges to combat this problem. The bridges provide a vehicle for lentiviral delivery resulting in long-term, localized transgene expression with the delivery of multiple factors which is difficult to achieve and generally requires the use of osmotic pumps[83, 183]. Osmotic pumps can clog, require surgery for removal, and cause further tissue damage. Other reports have used direct injection of vectors which does not allow localized delivery to the injury. Unlike other viral vectors, lentivirus does not influence the phenotype of progenitors[230] or cause significant inflammation[128]. Lentiviral vectors physical properties are also independent of the encoding gene making them the ideal system to deliver multiple vectors encoding various inductive factors without modification to the base biomaterial. Previously, we have delivered single viral vectors with great results, but the delivery of multiple vectors has presented a challenge. Single factors cannot address the multiple barriers to regeneration. We have investigated coating the bridge with heparin, but these interactions are not specific and fail to consistently bind and release the virus[182]. Therefore, we have investigated an alternative strategy based on specific interactions. Toward this goal, we have used phage display technology to identify specific peptides that can reversibly bind

and stabilize lentiviral vector[336]. We have identified several candidate peptides (**Table A.1**) that can be immobilized to a material.

Table A.1 Candidate peptides

Peptide	Occurrence
HLKHTHNTHYKT	4
HWKPHSNLHLSR	8
STQHHHHSKQSR	32
WPGHHNHSMKHK	6

We proposed immobilization that lentivirus onto PLG bridges modified with specific peptides would allow for consistency, efficiency, and reproducibility of lentiviral loading to have a more pronounced effect on the spinal cord microenvironment when delivering genes of interest.

Preliminary Results

Modification of PLG microparticles

Microspheres were made by dissolving PLG (75:25-mole ratio of D, L-lactide to glycolide,

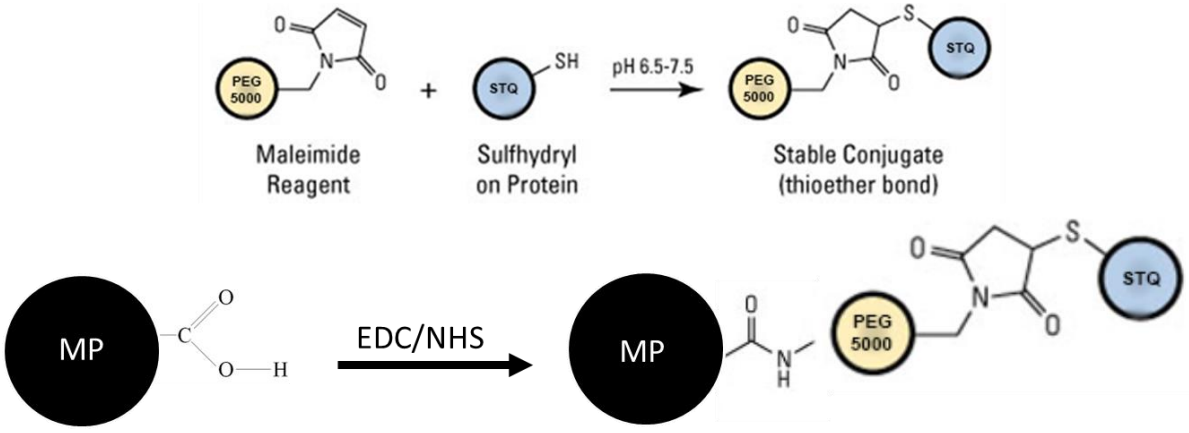

Figure A.1 EDC/NHS chemistry to create STQ PLG microparticles. STQ particles were made to determine their ability to retain lentiviral particles. PEG 5000 linker was used to allow flexibility for STQ active region

M.W. 99000) in dichloromethane (2% w/w) and then emulsified in 1% poly (ethylene-alt-maleic anhydride) to create microspheres (**Figure A.1**). STQ (GenScript, Piscataway, NJ) was conjugated

to the surface of PLG microspheres using N-ethyl-N′-(3-(dimethylamino) propyl) carbodiimide/N-hydroxysuccinimide (EDC/NHS) chemistry in a 1:5 molar ratio PLG to peptide. Unmodified microspheres were used as a negative control. We observed a modest change in the size of the microparticles, but a significant change in the charge of the particles (**Table A.2**). Furthermore, we were able to couple 6.77 µg of STQ peptide per mg of PLG microparticles. This was the maximum loading efficiency achieved.

Table A.2 Properties of modified particles

Sample	Size (um)	Charge	Protein Loading (µg/mg)
Control Particles	9.039 ± .011	-38.1 ± 2.35	-------
STQ - Particles	10.491 ± .073	11.2 ± 4.62	6.77

STQ modification improves virus retention in vitro, but not in vivo

We investigated STQ modified microparticles' ability to retain more lentivirus. We formed STQ particles into bridges and seeded them with various amounts of Fluc lentivirus. Fluc is a control virus that allows us to quantify its expression using radiance. All lentivirus in these studies was concentrated at 2E9 IU/ml. The bridges were seeded with 2, 4, or 6 µl of lentivirus. The control condition was unmodified PLG bridges seeded with 8 µl as this was our current standard. The bridges were seeded with human embryonic kidney cells and observed at 24 hours using the IVIS (**Figure A.2A**). There was no significant difference between control and 6 µl conditions indicating fewer viral particles were needed to observe the same total flux in the STQ modified bridges *in vitro*. We translated these results into an *in vivo* study. STQ and unmodified control bridges were seeded with 8 µl of Fluc lentivirus, implanted into spinal cord injured mice, and observed for 8 weeks post injury (**Figure A.2B**). There was a modest but not statistically significant increase in Fluc expression at 2 and 4 wpi, but this difference disappeared at 6 and 8 wpi. Since STQ modification increased viral loading, but did not lead to increased expression, we

determined the limiting factor in expression was the number of cells in the lesion site. Therefore, we focused on optimizing expression of multiple proteins by innovative viral constructs rather than increased viral loading.

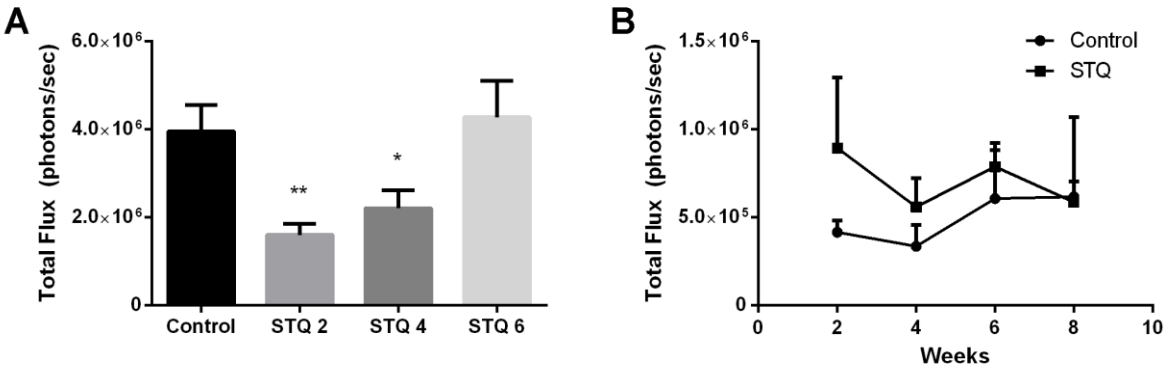

Figure A.2 Firefly Luciferase flux from PLG bridges. We analyzed lentivirus retention by using Fluc expression as a metric. Fluc expression was measured by radiance (total flux). (A) The total flux from bridges seeded with 6 µL was not significantly different from control bridges in. (B) The total flux from control bridges and STQ modified bridges are not significantly different in vivo* denotes $p<0.05$, ** denotes $p<.01$, *** denotes $p<.001$

Real time electrophysiological recordings from PLG bridge

Introduction

We have previously shown our ability to enhance axonal regeneration and myelination in an acute mouse model using multichannel PLG bridges[183]. This strategy supports regeneration of axons across the hemisection to reach distal spared tissue. However, these regenerating axons must form functional synaptic contacts to improve function outcomes. Synapse formation provides confirmation that biochemical and cellular processes necessary for neurotransmitter release, post-synaptic detection, and network transmission of neuronal impulses, all of which are vital for functional improvement, have been appropriately expressed and coordinated among cells. NT-3 supports the survival of existing neurons promotes synapse formation post-SCI by providing guidance cues to direct regenerating axons to targets[273]. Several rodent studies have shown electrical activity of regenerating axons post-SCI but are done ex vivo at the end of treatment and thus cannot be correlated to returning function over time[337-341]. Therefore, our goal is to investigate the formation of new neural circuits over time by electrophysiological recording from electrodes integrated into PLG bridges. This study will inform the correlation of electrophysiological measurements, synapse formation, and locomotor recovery.

Preliminary Results

We manufactured bridges with 25 μm platinum iridium inserted into 3 separate channels. The wires were held in the bridge with animal grade glue (**Figure A.3**). The wires were attached to a micro-connector and then to a computer for recording. We encountered many technical difficulties during the course of this project. The first problem was inserting the wires into the bridge channels reliably. We tried to accomplish this by using a micro manipulator but since we could only insert

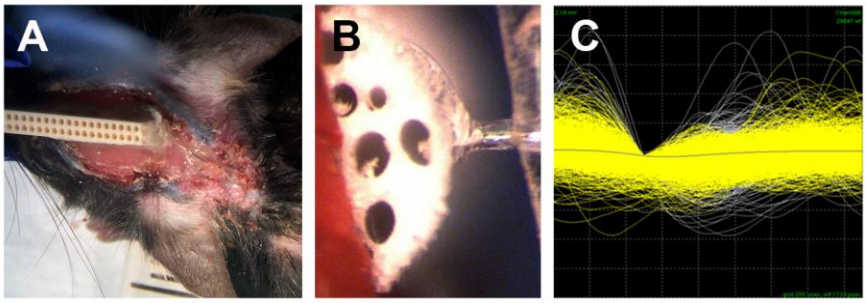

Figure A.3 Electrophysiological recording from mouse spinal cord. (A) Headmount glued to mouse skull. (B) Pt-Ir wires glued into bridge channel before implantation into mouse. (C) Sample recording from PLG bridge implanted in spinal showing no observable signal

a small number of wires and axons grow throughout the bridge, we could not reliably predict which channel would be best for recording. We assumed the most axons would grow into the bridge nearest the contralateral tissue, but when recording from these channels we could not reliability record a signal. The second problem was the weight of the micro-connector and headcap on the mouse. We could not source high channel micro-connectors for mice, rather most micro-connectors were made for rats. The weight of these rat connectors on the mouse skull combined with functional deficits of the spinal cord injury caused the mice to not be able to properly walk for real-time electrophysiological recordings. The third problem we faced was micromotion of the wires in the bridge which caused early degradation of bridge and occluded axonal and tissue ingrowth. This problem was insurmountable and forced the conclusion of this specific strategy for real-time electrophysiological recordings. Other strategies have begun in our lab to gather similar data using EMG instead of recording from the spinal cord and optogenetics for stimulated recordings instead of ambulatory recording.

MRI for spinal cord tissue structure and function

Introduction

Traumatic spinal cord injuries have a devastating effect on patients' quality of life. Although current treatments are largely ineffective in recovery of function, recent developments in tissue regeneration may lead to significant improvements in the recovery of patients with spinal cord injury. A major challenge to the development and optimization of spinal cord regeneration therapy is the need for non-invasive methods to evaluate the effectiveness of the treatment or to characterize the regeneration process in animal models over time. Currently, this is carried out by measuring functional locomotor recovery, histology, or electrophysiology. Functional measurements are not very informative about tissue structure and cellular processes. Histology and electrophysiology require multiple groups of animals to be sacrificed at different time points, thus increasing the variance of the results, as well as the resources required for the study, significantly. More importantly, as spinal cord regeneration therapy matures and becomes adopted clinically, there will be a strong need for non-invasive procedures to assess damage and treatment strategy in human patients.

To this end, non-invasive imaging technologies can be leveraged beyond simple structural imaging to obtain quantitative biomarkers of spinal cord regeneration. These can be used to optimize therapy by allowing the investigator to conduct longitudinal studies throughout the course of recovery on the same animal. These technologies must be readily translatable to the clinical setting for use in human patients. Magnetic resonance imaging (MRI) can be a useful tool post-SCI, providing detailed information about the status of ligaments, intervertebral discs, and surrounding soft tissue [342]. A limitation of using MRI to characterize and monitor regenerative therapies is that, in its current state of the art, MRI is limited in its ability to identify the presence

of specific cell types. MRI reveals only the bulk properties of the tissue, rather than showing the detail and morphology of specific cells, as histological samples can. However, there exist many MRI techniques that can be used to make inferences about specific parameters of the cellular milieu. MRI can readily cover a large field of view in a single scan, rather than requiring analysis over extremely small regions that are chosen based on macroscopic properties. MRI is also completely non-invasive and thus can be used *in vivo* with relative frequency throughout the therapeutic process, without disturbing it or damaging the tissue. This allows for characterization the temporal characteristics of the regeneration process, including edema, inflammation, cellular infiltration and the degradation of the implants. Furthermore, recent work in anesthetized monkeys has shown that resting state functional connectivity as measured with MRI can serve as a biomarker of spinal cord integrity [343]. The goals of this investigation were to design, optimize, and implement an imaging protocol for the longitudinal study of spinal cord regeneration using PLG implanted bridges in mice. We will scrutinize the utility of several quantitative imaging techniques for studying spinal cord regeneration. We plan to quantify several endpoints including: (1) the rate of axonal formation, (2) re-myelination (3) axonal formation, (4) inflammation and (5) functional connectivity.

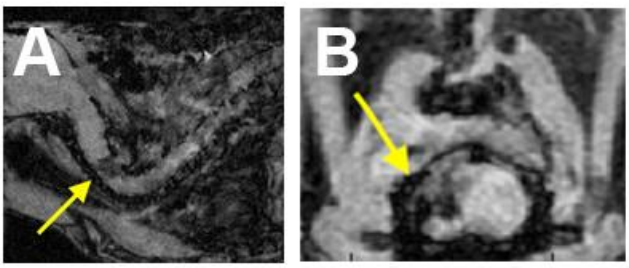

Figure A.4 T1 weighted images of the SCI. (A) Sagittal view of the SCI. (B) Axial view of the SCI with bridge implanted

Preliminary Results

We were able to identify the injury site (**Figure A.4**) in sagittal and axial planes. These images were collected to determine the consistency of our surgery and reliability of finding the injury site for further characterization of the lesion. We used these injury sites to test diffusion weighted imaging techniques as a biomarker of axonal regeneration and density (**Figure A.5**). We collected fast spin echo images and applied a standard diffusion curve at every pixel to obtain apparent diffusion coefficient (ADC) maps in the principal cartesian axes. These maps were then used to calculate fractional anisotropy maps. Fractional anisotropy allows us to determine the tissue structure using the anisotropy of water diffusion as a proxy. The maps indicate a clear difference in the diffusion movement of water between the white and gray matter as evidenced by the differences in ADC in the x,y, and z axes. The goal was to use these metrics as a prognosis for behavioral recovery, correlate them axonal growth and density, and correlate them to myelin fraction. This project is very promising and should be continued pending adequate funding.

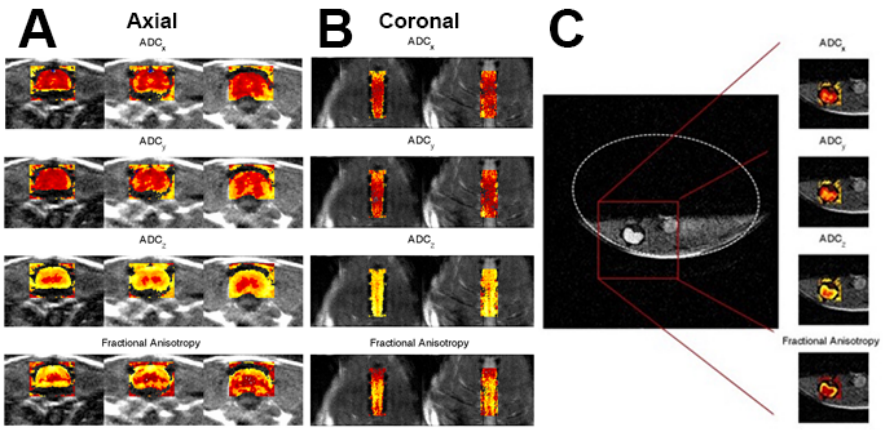

Figure A.5 Axial and coronal measurements of ADC and fractional anisotropy. (A) Axial fast spin echo images of ADC and fractional anisotropy map. (B) Coronal fast spin echo images of ADC and fractional anisotropy map. (C) Diffusion weighted ZOOM images excluding the lungs and heart. Yellow indicates areas of high water diffusion. Red indicates areas of low water diffusion.

PEG hydrogel tubes and neural stem cells for spinal cord regeneration

Neural stem cells (NSCs) promote nerve regeneration by release of neurotrophic factors, repopulation CNS cell populations, and immune cell modulation. Numerous growth factors [171, 173, 344-346] and extracellular matrix proteins [347-351] are released by NSCs in the tissue following delivery to a CNS injury site [352-356]. However, survival of exogenous NSCs without co-delivery of other pharmacological or biochemical factors has been seen as high as 12% using bioluminescence assessment [357] but is typically less than 1-5% [87, 358-360]. Typically, poor survival is attributed to the highly inflammatory microenvironment rather than immune cell-mediated rejection [361, 362].

Delivery method of the NSCs may also affect survival, as most methods deliver the cells via direct injection. Direct injection of cells into a highly inflammatory injury microenvironment results in limited survival of the NSCs [363] and increasing the number of transplanted NSCs does not results in a commensurate increase in survival or proliferation [364]. We have previously employed IL-10 delivery to reduce inflammation in the spinal cord post-injury with amazing results. IL-10 promoted M2 macrophage polarization, reduction in inflammatory cytokine production, and upregulated pro-regenerative genes glial cells [135, 224]. Additionally, using a biomaterial as a NSC delivery platform would provide a substrate for NSC attachment leading to an up-regulation of downstream survival pathways [347, 365]. Biomaterial delivery of NSCs may also be beneficial to cell survival and subsequent engraftment as these materials limit inflammation and scarring following SCI by filling the injury site and preventing cavitation.

Biomaterials platforms such as soft hydrogels and highly organized bridges have been evaluated for NSC delivery following SCI. Hydrogels can conform to the shape of injury site to promote regeneration and limit scar formation after SCI [87, 90, 105]. Current hydrogel technologies offer a vehicle to deliver NSCs in high doses, however, current hydrogels employed in spinal cord

repair lack topographical cues to guide axon extension. We have previously developed modular aligned PEG tubes that conform to the injury and provide an orientation that guides axons through the injury [78]. In this study, we evaluated the utility of PEG tubes to deliver IL-10 lentivirus immediately after a lateral hemisection spinal cord injury. At 2 wpi, embryonic day 14 (E14) mouse spinal cord EGFP-NSCs were transplanted into the injury by injection into the PEG material to promote regeneration. We plan to evaluate immune cell infiltration, NSC survival, exogenous and endogenous cell differentiation, axon elongation, axon myelination, and functional recovery.

Preliminary Results

First, we evaluated PEG tubes as a suitable substrate for lentiviral delivery. We seeded PEG tube with lentiviral particles encoding FLuc and implanted the tubes in our mouse SCI model. We used bioluminescence imaging to visualize the viral expression over 12 weeks (**Figure A.6**). Luciferase expression was significantly higher than background at several times points for 12 weeks post-SCI.

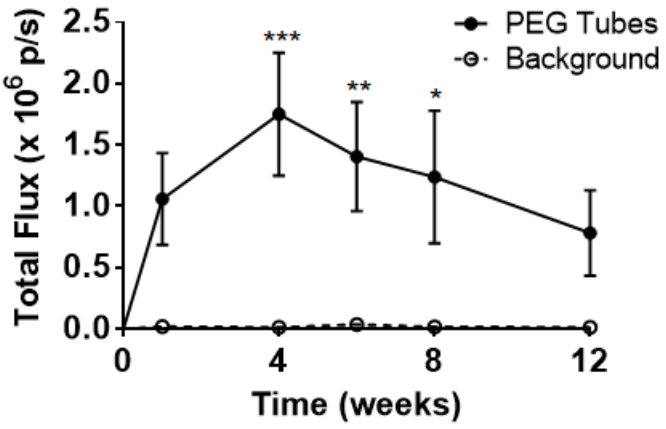

Figure A.6 Lentiviral expression is sustained when delivered with PEG tubes. Bioluminescence of luciferase was significantly higher than background for 12 weeks post-SCI. * denotes p<0.05, ** denotes p<.01, *** denotes p<.001

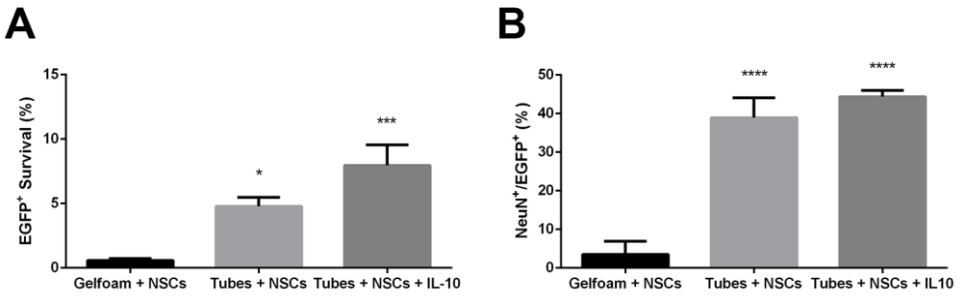

Figure A.7 NSC survival and differentiation is increased with PEG tubes. (A) NSC survival is significantly increased with PEG tubes and PEG tubes + IL-10. (B) Differentiation of NSC into $NeuN^+$ cells are significantly increase with PEG tubes and PEG tubes + IL-10. * denotes $p<0.05$, ** denotes $p<.01$, *** denotes $p<.001$

Subsequently, we used the PEG tubes to deliver IL-10 in combination with NSCs to determine their survival. NSCs were also delivered with PEG tubes without IL-10 and collagen Gelfoam as controls. We evaluated NSC survival at 2 weeks post transplantation (4 wpi). NSC survival was significantly higher with PEG tube delivery compared to Gelfoam delivery (**Figure A.7A**). While, NSC transplantation combined with IL-10 delivery and PEG tubes trended towards higher survival percentage than PEG tubes alone, this difference was not significant. We also evaluated the differentiation of the transplanted NSCs. A significantly higher percentage of NSCs delivered with PEG tubes or PEG tubes + IL-10 differentiated into $NeuN^+$ cells, denoting a neural lineage (**Figure A.7B**). We plan to evaluate the differentiation of transplanted NSCs into other glial cell lineages. We also investigated the functional recovery of animals receiving NSCs using the ladder beam test (**Figure A.8**). There was no significant difference in the ladder beam scores between the groups over 8 wpi, but the groups are beginning to separate. We will continue to monitor functional recovery until 12 wpi. We will also conduct thermal and mechanical hypersensitivity tests to determine NSCs effect on thermal hyperalgesia and allodynia.

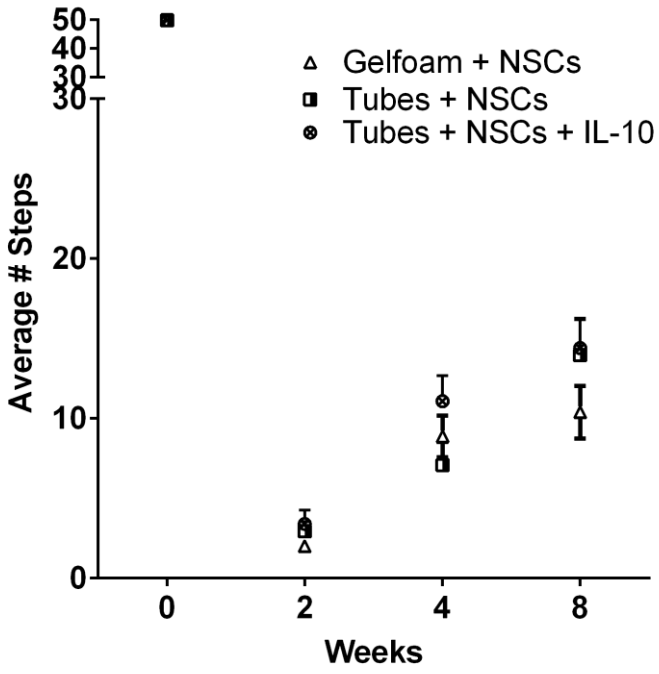

Figure A.8 NSC delivery does not significantly improve functional recovery.

Bibliography

1. Richardson, P.M., U.M. McGuinness, and A.J. Aguayo, *Axons from CNS neurons regenerate into PNS grafts.* Nature, 1980. **284**(5753): p. 264-5.
2. Bunge, M.B., *Novel combination strategies to repair the injured mammalian spinal cord.* J Spinal Cord Med, 2008. **31**(3): p. 262-9.
3. Tuinstra, H.M., D.J. Margul, A.G. Goodman, R.M. Boehler, S.J. Holland, M.L. Zelivyanskaya, B.J. Cummings, A.J. Anderson, and L.D. Shea, *Long-term characterization of axon regeneration and matrix changes using multiple channel bridges for spinal cord regeneration.* Tissue Eng Part A, 2014. **20**(5-6): p. 1027-37.
4. Center, N.S.C.I.S., *Facts and Figures at a Glance*, U.o.A.a. Birmingham, Editor. 2018: Birmingham, AL.
5. Anderson, K.D., *Targeting recovery: priorities of the spinal cord-injured population.* J Neurotrauma, 2004. **21**(10): p. 1371-83.
6. (U.S.), N.S.C.I.S.C. *Spinal Cord Injury Facts and Figures at a Glance*

2012.
7. Blair, J.A., D.R. Possley, J.L. Petfield, A.J. Schoenfeld, R.A. Lehman, and J.R. Hsu, *Military penetrating spine injuries compared with blunt.* Spine J, 2012. **12**(9): p. 762-8.
8. Fawcett, J.W., A. Curt, J.D. Steeves, W.P. Coleman, M.H. Tuszynski, D. Lammertse, P.F. Bartlett, A.R. Blight, V. Dietz, J. Ditunno, B.H. Dobkin, L.A. Havton, P.H. Ellaway, M.G. Fehlings, A. Privat, R. Grossman, J.D. Guest, N. Kleitman, M. Nakamura, M. Gaviria, and D. Short, *Guidelines for the conduct of clinical trials for spinal cord injury as developed by the ICCP panel: spontaneous recovery after spinal cord injury and statistical power needed for therapeutic clinical trials.* Spinal Cord, 2007. **45**(3): p. 190-205.
9. Rhee, P., E.J. Kuncir, L. Johnson, C. Brown, G. Velmahos, M. Martin, D. Wang, A. Salim, J. Doucet, S. Kennedy, and D. Demetriades, *Cervical spine injury is highly dependent on the mechanism of injury following blunt and penetrating assault.* J Trauma, 2006. **61**(5): p. 1166-70.
10. Silva, N.A., N. Sousa, R.L. Reis, and A.J. Salgado, *From basics to clinical: a comprehensive review on spinal cord injury.* Prog Neurobiol, 2014. **114**: p. 25-57.
11. Fehlings, M.G., A. Vaccaro, J.R. Wilson, A. Singh, W.C. D, J.S. Harrop, B. Aarabi, C. Shaffrey, M. Dvorak, C. Fisher, P. Arnold, E.M. Massicotte, S. Lewis, and R. Rampersaud, *Early versus delayed decompression for traumatic cervical spinal cord injury: results of the Surgical Timing in Acute Spinal Cord Injury Study (STASCIS).* PLoS One, 2012. **7**(2): p. e32037.
12. Bracken, M.B., M.J. Shepard, W.F. Collins, T.R. Holford, W. Young, D.S. Baskin, H.M. Eisenberg, E. Flamm, L. Leo-Summers, J. Maroon, and et al., *A randomized, controlled trial of methylprednisolone or naloxone in the treatment of acute spinal-cord injury. Results of the Second National Acute Spinal Cord Injury Study.* N Engl J Med, 1990. **322**(20): p. 1405-11.

13. Bracken, M.B., M.J. Shepard, T.R. Holford, L. Leo-Summers, E.F. Aldrich, M. Fazl, M. Fehlings, D.L. Herr, P.W. Hitchon, L.F. Marshall, R.P. Nockels, V. Pascale, P.L. Perot, Jr., J. Piepmeier, V.K. Sonntag, F. Wagner, J.E. Wilberger, H.R. Winn, and W. Young, *Administration of methylprednisolone for 24 or 48 hours or tirilazad mesylate for 48 hours in the treatment of acute spinal cord injury. Results of the Third National Acute Spinal Cord Injury Randomized Controlled Trial. National Acute Spinal Cord Injury Study.* Jama, 1997. **277**(20): p. 1597-604.
14. Hurlbert, R.J. and M.G. Hamilton, *Methylprednisolone for Acute Spinal Cord Injury: 5-Year Practice Reversal.* Canadian Journal of Neurological Sciences / Journal Canadien des Sciences Neurologiques, 2014. **35**(1): p. 41-45.
15. Dietz, V. and K. Fouad, *Restoration of sensorimotor functions after spinal cord injury.* Brain, 2014. **137**(Pt 3): p. 654-67.
16. Ahuja, C.S., A.R. Martin, and M. Fehlings, *Recent advances in managing a spinal cord injury secondary to trauma [version 1; referees: 2 approved].* F1000Research, 2016. **5**.
17. Bamford, J.A., K.G. Todd, and V.K. Mushahwar, *The effects of intraspinal microstimulation on spinal cord tissue in the rat.* Biomaterials, 2010. **31**(21): p. 5552-5563.
18. Hamid, S. and R. Hayek, *Role of electrical stimulation for rehabilitation and regeneration after spinal cord injury: an overview.* Eur Spine J, 2008. **17**(9): p. 1256-69.
19. Harkema, S., Y. Gerasimenko, J. Hodes, J. Burdick, C. Angeli, Y. Chen, C. Ferreira, A. Willhite, E. Rejc, R.G. Grossman, and V.R. Edgerton, *Effect of epidural stimulation of the lumbosacral spinal cord on voluntary movement, standing, and assisted stepping after motor complete paraplegia: a case study.* Lancet, 2011. **377**(9781): p. 1938-47.
20. Rejc, E., C.A. Angeli, D. Atkinson, and S.J. Harkema, *Motor recovery after activity-based training with spinal cord epidural stimulation in a chronic motor complete paraplegic.* Scientific Reports, 2017. **7**(1): p. 13476.
21. Abbott, N.J., L. Ronnback, and E. Hansson, *Astrocyte-endothelial interactions at the blood-brain barrier.* Nat Rev Neurosci, 2006. **7**(1): p. 41-53.
22. Bradl, M. and H. Lassmann, *Oligodendrocytes: biology and pathology.* Acta Neuropathol, 2010. **119**(1): p. 37-53.
23. Newman, E.A., *New roles for astrocytes: regulation of synaptic transmission.* Trends Neurosci, 2003. **26**(10): p. 536-42.
24. Rose, C.R. and A. Verkhratsky, *Principles of sodium homeostasis and sodium signalling in astroglia.* Glia, 2016.
25. McKeon, R.J., R.C. Schreiber, J.S. Rudge, and J. Silver, *Reduction of neurite outgrowth in a model of glial scarring following CNS injury is correlated with the expression of inhibitory molecules on reactive astrocytes.* J Neurosci, 1991. **11**(11): p. 3398-411.
26. Sofroniew, M.V. and H.V. Vinters, *Astrocytes: biology and pathology.* Acta Neuropathol, 2010. **119**(1): p. 7-35.
27. Risau, W. and H. Wolburg, *Development of the blood-brain barrier.* Trends Neurosci, 1990. **13**(5): p. 174-8.
28. Graeber, M.B., *Changing face of microglia.* Science, 2010. **330**(6005): p. 783-8.
29. Hughes, V., *Microglia: The constant gardeners.* Nature, 2012. **485**(7400): p. 570-2.
30. Kettenmann, H., U.K. Hanisch, M. Noda, and A. Verkhratsky, *Physiology of microglia.* Physiol Rev, 2011. **91**(2): p. 461-553.
31. Olson, J.K. and S.D. Miller, *Microglia initiate central nervous system innate and adaptive immune responses through multiple TLRs.* J Immunol, 2004. **173**(6): p. 3916-24.

32. Martinez, F.O., A. Sica, A. Mantovani, and M. Locati, *Macrophage activation and polarization.* Front Biosci, 2008. **13**: p. 453-61.
33. Fleming, J.C., M.D. Norenberg, D.A. Ramsay, G.A. Dekaban, A.E. Marcillo, A.D. Saenz, M. Pasquale-Styles, W.D. Dietrich, and L.C. Weaver, *The cellular inflammatory response in human spinal cords after injury.* Brain, 2006. **129**(Pt 12): p. 3249-69.
34. Yang, L., P.C. Blumbergs, N.R. Jones, J. Manavis, G.T. Sarvestani, and M.N. Ghabriel, *Early expression and cellular localization of proinflammatory cytokines interleukin-1beta, interleukin-6, and tumor necrosis factor-alpha in human traumatic spinal cord injury.* Spine (Phila Pa 1976), 2004. **29**(9): p. 966-71.
35. Pineau, I. and S. Lacroix, *Proinflammatory cytokine synthesis in the injured mouse spinal cord: multiphasic expression pattern and identification of the cell types involved.* J Comp Neurol, 2007. **500**(2): p. 267-85.
36. Nguyen, H.X., T.J. O'Barr, and A.J. Anderson, *Polymorphonuclear leukocytes promote neurotoxicity through release of matrix metalloproteinases, reactive oxygen species, and TNF-alpha.* J Neurochem, 2007. **102**(3): p. 900-12.
37. Trivedi, A., A.D. Olivas, and L.J. Noble-Haeusslein, *Inflammation and Spinal Cord Injury: Infiltrating Leukocytes as Determinants of Injury and Repair Processes.* Clin Neurosci Res, 2006. **6**(5): p. 283-292.
38. Anderson, A.J., *Mechanisms and pathways of inflammatory responses in CNS trauma: spinal cord injury.* J Spinal Cord Med, 2002. **25**(2): p. 70-9; discussion 80.
39. Donnelly, D.J. and P.G. Popovich, *Inflammation and its role in neuroprotection, axonal regeneration and functional recovery after spinal cord injury.* Exp Neurol, 2008. **209**(2): p. 378-88.
40. Qin, L., G. Li, X. Qian, Y. Liu, X. Wu, B. Liu, J.S. Hong, and M.L. Block, *Interactive role of the toll-like receptor 4 and reactive oxygen species in LPS-induced microglia activation.* Glia, 2005. **52**(1): p. 78-84.
41. Liu, D., G.Y. Xu, E. Pan, and D.J. McAdoo, *Neurotoxicity of glutamate at the concentration released upon spinal cord injury.* Neuroscience, 1999. **93**(4): p. 1383-1389.
42. Filbin, M.T., *Myelin-associated inhibitors of axonal regeneration in the adult mammalian CNS.* Nat Rev Neurosci, 2003. **4**(9): p. 703-13.
43. Yiu, G. and Z. He, *Glial inhibition of CNS axon regeneration.* Nat Rev Neurosci, 2006. **7**(8): p. 617-27.
44. Baldwin, K.T. and R.J. Giger, *Insights into the physiological role of CNS regeneration inhibitors.* Front Mol Neurosci, 2015. **8**: p. 23.
45. Fournier, A.E., B.T. Takizawa, and S.M. Strittmatter, *Rho kinase inhibition enhances axonal regeneration in the injured CNS.* Journal of Neuroscience, 2003. **23**(4): p. 1416-1423.
46. Vourc'h, P. and C. Andres, *Oligodendrocyte myelin glycoprotein (OMgp): evolution, structure and function.* Brain Res Brain Res Rev, 2004. **45**(2): p. 115-24.
47. Li, J., E.R. Ramenaden, J. Peng, H. Koito, J.J. Volpe, and P.A. Rosenberg, *Tumor necrosis factor alpha mediates lipopolysaccharide-induced microglial toxicity to developing oligodendrocytes when astrocytes are present.* J Neurosci, 2008. **28**(20): p. 5321-30.
48. Liu, K., Y. Lu, J.K. Lee, R. Samara, R. Willenberg, I. Sears-Kraxberger, A. Tedeschi, K.K. Park, D. Jin, B. Cai, B. Xu, L. Connolly, O. Steward, B. Zheng, and Z. He, *PTEN deletion enhances the regenerative ability of adult corticospinal neurons.* Nature Neuroscience, 2010. **13**(9): p. 1075-1081.

49. Kurihara, D. and T. Yamashita, *Chondroitin sulfate proteoglycans down-regulate spine formation in cortical neurons by targeting tropomyosin-related kinase B (TrkB) protein.* J Biol Chem, 2012. **287**(17): p. 13822-8.
50. Zhou, Z., X. Peng, P. Chiang, J. Kim, X. Sun, D.J. Fink, and M. Mata, *HSV-mediated gene transfer of C3 transferase inhibits Rho to promote axonal regeneration.* Experimental Neurology, 2012. **237**(1): p. 126-133.
51. Nicolas, C.S., M. Amici, Z.A. Bortolotto, A. Doherty, Z. Csaba, A. Fafouri, P. Dournaud, P. Gressens, G.L. Collingridge, and S. Peineau, *The role of JAK-STAT signaling within the CNS.* JAK-STAT, 2013. **2**(1): p. e22925-e22925.
52. Park, K.W., C.Y. Lin, E.N. Benveniste, and Y.S. Lee, *Mitochondrial STAT3 is negatively regulated by SOCS3 and upregulated after spinal cord injury.* Exp Neurol, 2016. **284**(Pt A): p. 98-105.
53. Okada, S., M. Hara, K. Kobayakawa, Y. Matsumoto, and Y. Nakashima, *Astrocyte reactivity and astrogliosis after spinal cord injury.* Neuroscience Research, 2017.
54. Fitch, M.T., C. Doller, C.K. Combs, G.E. Landreth, and J. Silver, *Cellular and molecular mechanisms of glial scarring and progressive cavitation: in vivo and in vitro analysis of inflammation-induced secondary injury after CNS trauma.* J Neurosci, 1999. **19**(19): p. 8182-98.
55. Rhodes, K.E., G. Raivich, and J.W. Fawcett, *The injury response of oligodendrocyte precursor cells is induced by platelets, macrophages and inflammation-associated cytokines.* Neuroscience, 2006. **140**(1): p. 87-100.
56. Anderson, M.A., J.E. Burda, Y. Ren, Y. Ao, T.M. O'Shea, R. Kawaguchi, G. Coppola, B.S. Khakh, T.J. Deming, and M.V. Sofroniew, *Astrocyte scar formation aids central nervous system axon regeneration.* Nature, 2016. **advance online publication**.
57. Wanner, I.B., M.A. Anderson, B. Song, J. Levine, A. Fernandez, Z. Gray-Thompson, Y. Ao, and M.V. Sofroniew, *Glial scar borders are formed by newly proliferated, elongated astrocytes that interact to corral inflammatory and fibrotic cells via STAT3-dependent mechanisms after spinal cord injury.* J Neurosci, 2013. **33**(31): p. 12870-86.
58. Fitch, M.T. and J. Silver, *CNS injury, glial scars, and inflammation: Inhibitory extracellular matrices and regeneration failure.* Exp Neurol, 2008. **209**(2): p. 294-301.
59. Silver, J. and J.H. Miller, *Regeneration beyond the glial scar.* Nature Reviews Neuroscience, 2004. **5**(2): p. 146-156.
60. Tom, V.J., M.P. Steinmetz, J.H. Miller, C.M. Doller, and J. Silver, *Studies on the development and behavior of the dystrophic growth cone, the hallmark of regeneration failure, in an in vitro model of the glial scar and after spinal cord injury.* Journal of Neuroscience, 2004. **24**(29): p. 6531-9.
61. Smith-Thomas, L.C., J. Fok-Seang, J. Stevens, J.S. Du, E. Muir, A. Faissner, H.M. Geller, J.H. Rogers, and J.W. Fawcett, *An inhibitor of neurite outgrowth produced by astrocytes.* J Cell Sci, 1994. **107 (Pt 6)**: p. 1687-95.
62. Wanner, I.B., A. Deik, M. Torres, A. Rosendahl, J.T. Neary, V.P. Lemmon, and J.L. Bixby, *A new in vitro model of the glial scar inhibits axon growth.* Glia, 2008. **56**(15): p. 1691-709.
63. Tuinstra, H.M., M.M. Ducommun, W.E. Briley, and L.D. Shea, *Gene delivery to overcome astrocyte inhibition of axonal growth: an in vitro model of the glial scar.* Biotechnol Bioeng, 2013. **110**(3): p. 947-57.

64. Cholas, R., H.P. Hsu, and M. Spector, *Collagen scaffolds incorporating select therapeutic agents to facilitate a reparative response in a standardized hemiresection defect in the rat spinal cord.* Tissue Eng Part A, 2012. **18**(19-20): p. 2158-72.
65. Cholas, R.H., H.P. Hsu, and M. Spector, *The reparative response to cross-linked collagen-based scaffolds in a rat spinal cord gap model.* Biomaterials, 2012. **33**(7): p. 2050-9.
66. Yoshii, S., M. Oka, M. Shima, M. Akagi, and A. Taniguchi, *Bridging a spinal cord defect using collagen filament.* Spine (Phila Pa 1976), 2003. **28**(20): p. 2346-51.
67. Cheng, H., Y.C. Huang, P.T. Chang, and Y.Y. Huang, *Laminin-incorporated nerve conduits made by plasma treatment for repairing spinal cord injury.* Biochem Biophys Res Commun, 2007. **357**(4): p. 938-44.
68. Menezes, K., J.R. de Menezes, M.A. Nascimento, S. Santos Rde, and T. Coelho-Sampaio, *Polylaminin, a polymeric form of laminin, promotes regeneration after spinal cord injury.* Faseb j, 2010. **24**(11): p. 4513-22.
69. Zhang, Q., S. Yan, R. You, D.L. Kaplan, Y. Liu, J. Qu, X. Li, M. Li, and X. Wang, *Multichannel silk protein/laminin grafts for spinal cord injury repair.* J Biomed Mater Res A, 2016. **104**(12): p. 3045-3057.
70. King, V.R., A. Alovskaya, D.Y. Wei, R.A. Brown, and J.V. Priestley, *The use of injectable forms of fibrin and fibronectin to support axonal ingrowth after spinal cord injury.* Biomaterials, 2010. **31**(15): p. 4447-56.
71. Lewandowski, G. and O. Steward, *AAVshRNA-mediated suppression of PTEN in adult rats in combination with salmon fibrin administration enables regenerative growth of corticospinal axons and enhances recovery of voluntary motor function after cervical spinal cord injury.* J Neurosci, 2014. **34**(30): p. 9951-62.
72. Fuhrmann, T., J. Obermeyer, C.H. Tator, and M.S. Shoichet, *Click-crosslinked injectable hyaluronic acid hydrogel is safe and biocompatible in the intrathecal space for ultimate use in regenerative strategies of the injured spinal cord.* Methods, 2015. **84**: p. 60-9.
73. Wen, Y., S. Yu, Y. Wu, R. Ju, H. Wang, Y. Liu, Y. Wang, and Q. Xu, *Spinal cord injury repair by implantation of structured hyaluronic acid scaffold with PLGA microspheres in the rat.* Cell Tissue Res, 2016. **364**(1): p. 17-28.
74. Chedly, J., S. Soares, A. Montembault, Y. von Boxberg, M. Veron-Ravaille, C. Mouffle, M.N. Benassy, J. Taxi, L. David, and F. Nothias, *Physical chitosan microhydrogels as scaffolds for spinal cord injury restoration and axon regeneration.* Biomaterials, 2017. **138**: p. 91-107.
75. Yang, Z., A. Zhang, H. Duan, S. Zhang, P. Hao, K. Ye, Y.E. Sun, and X. Li, *NT3-chitosan elicits robust endogenous neurogenesis to enable functional recovery after spinal cord injury.* Proc Natl Acad Sci U S A, 2015. **112**(43): p. 13354-9.
76. Brazda, N., V. Estrada, C. Voss, K. Seide, H.K. Trieu, and H.W. Muller, *Experimental Strategies to Bridge Large Tissue Gaps in the Injured Spinal Cord after Acute and Chronic Lesion.* J Vis Exp, 2016(110): p. e53331.
77. Koffler, J., W. Zhu, X. Qu, O. Platoshyn, J.N. Dulin, J. Brock, L. Graham, P. Lu, J. Sakamoto, M. Marsala, S. Chen, and M.H. Tuszynski, *Biomimetic 3D-printed scaffolds for spinal cord injury repair.* Nature Medicine, 2019. **25**(2): p. 263-269.
78. Dumont, C.M., M.A. Carlson, M.K. Munsell, A.J. Ciciriello, K. Strnadova, J. Park, B.J. Cummings, A.J. Anderson, and L.D. Shea, *Aligned hydrogel tubes guide regeneration following spinal cord injury.* Acta Biomaterialia, 2019. **86**: p. 312-322.

79. Hejcl, A., J. Ruzicka, V. Proks, H. Mackova, S. Kubinova, D. Tukmachev, J. Cihlar, D. Horak, and P. Jendelova, *Dynamics of tissue ingrowth in SIKVAV-modified highly superporous PHEMA scaffolds with oriented pores after bridging a spinal cord transection.* J Mater Sci Mater Med, 2018. **29**(7): p. 89.
80. Pertici, V., T. Trimaille, J. Laurin, M.S. Felix, T. Marqueste, B. Pettmann, J.P. Chauvin, D. Gigmes, and P. Decherchi, *Repair of the injured spinal cord by implantation of a synthetic degradable block copolymer in rat.* Biomaterials, 2014. **35**(24): p. 6248-58.
81. Zamani, F., M. Amani-Tehran, M. Latifi, M.A. Shokrgozar, and A. Zaminy, *Promotion of spinal cord axon regeneration by 3D nanofibrous core-sheath scaffolds.* J Biomed Mater Res A, 2014. **102**(2): p. 506-13.
82. Moore, M.J., J.A. Friedman, E.B. Lewellyn, S.M. Mantila, A.J. Krych, S. Ameenuddin, A.M. Knight, L. Lu, B.L. Currier, R.J. Spinner, R.W. Marsh, A.J. Windebank, and M.J. Yaszemski, *Multiple-channel scaffolds to promote spinal cord axon regeneration.* Biomaterials, 2006. **27**(3): p. 419-429.
83. Tuinstra, H.M., M.O. Aviles, S. Shin, S.J. Holland, M.L. Zelivyanskaya, A.G. Fast, S.Y. Ko, D.J. Margul, A.K. Bartels, R.M. Boehler, B.J. Cummings, A.J. Anderson, and L.D. Shea, *Multifunctional, multichannel bridges that deliver neurotrophin encoding lentivirus for regeneration following spinal cord injury.* Biomaterials, 2012. **33**(5): p. 1618-26.
84. Fitch, M.T. and J. Silver, *CNS injury, glial scars, and inflammation: Inhibitory extracellular matrices and regeneration failure.* Experimental Neurology, 2008. **209**(2): p. 294-301.
85. Silva, N.A., R.A. Sousa, J.S. Fraga, M. Fontes, H. Leite-Almeida, R. Cerqueira, A. Almeida, N. Sousa, R.L. Reis, and A.J. Salgado, *Benefits of spine stabilization with biodegradable scaffolds in spinal cord injured rats.* Tissue Engineering - Part C: Methods, 2013. **19**(2): p. 101-108.
86. Tam, R.Y., M.J. Cooke, and M.S. Shoichet, *A covalently modified hydrogel blend of hyaluronan-methyl cellulose with peptides and growth factors influences neural stem/progenitor cell fate.* Journal of Materials Chemistry, 2012. **22**(37): p. 19402-19411.
87. Mothe, A.J., R.Y. Tam, T. Zahir, C.H. Tator, and M.S. Shoichet, *Repair of the injured spinal cord by transplantation of neural stem cells in a hyaluronan-based hydrogel.* Biomaterials, 2013. **34**(15): p. 3775-3783.
88. Caicco, M.J., T. Zahir, A.J. Mothe, B.G. Ballios, A.J. Kihm, C.H. Tator, and M.S. Shoichet, *Characterization of hyaluronan-methylcellulose hydrogels for cell delivery to the injured spinal cord.* Journal of Biomedical Materials Research - Part A, 2013. **101 A**(5): p. 1472-1477.
89. He, Z., H. Zang, L. Zhu, K. Huang, T. Yi, S. Zhang, and S. Cheng, *An anti-inflammatory peptide and brain-derived neurotrophic factor-modified hyaluronan-methylcellulose hydrogel promotes nerve regeneration in rats with spinal cord injury.* Int J Nanomedicine, 2019. **14**: p. 721-732.
90. Tsai, E.C., P.D. Dalton, M.S. Shoichet, and C.H. Tator, *Matrix inclusion within synthetic hydrogel guidance channels improves specific supraspinal and local axonal regeneration after complete spinal cord transection.* Biomaterials, 2006. **27**(3): p. 519-33.
91. Ruzicka, J., N. Romanyuk, K. Jirakova, A. Hejcl, O. Janouskova, L.U. Machova, M. Bochin, M. Pradny, L. Vargova, and P. Jendelova, *The Effect of iPS-Derived Neural Progenitors Seeded on Laminin-Coated pHEMA-MOETACl Hydrogel with Dual Porosity in a Rat Model of Chronic Spinal Cord Injury.* Cell Transplant, 2019. **28**(4): p. 400-412.

92. Crompton, K.E., D. Tomas, D.I. Finkelstein, M. Marr, J.S. Forsythe, and M.K. Horne, *Inflammatory response on injection of chitosan/GP to the brain.* J Mater Sci Mater Med, 2006. **17**(7): p. 633-9.
93. Lee, J.Y., C.A. Bashur, A.S. Goldstein, and C.E. Schmidt, *Polypyrrole-Coated Electrospun PLGA Nanofibers for Neural Tissue Applications.* Biomaterials, 2009. **30**(26): p. 4325-4335.
94. Lee, J.Y., C.A. Bashur, C.A. Milroy, L. Forciniti, A.S. Goldstein, and C.E. Schmidt, *Nerve growth factor-immobilized electrically conducting fibrous scaffolds for potential use in neural engineering applications.* IEEE Trans Nanobioscience, 2012. **11**(1): p. 15-21.
95. Li, W.J., C.T. Laurencin, E.J. Caterson, R.S. Tuan, and F.K. Ko, *Electrospun nanofibrous structure: A novel scaffold for tissue engineering.* Journal of Biomedical Materials Research, 2002. **60**(4): p. 613-621.
96. Pritchard, C.D., J.R. Slotkin, D. Yu, H. Dai, M.S. Lawrence, R.T. Bronson, F.M. Reynolds, Y.D. Teng, E.J. Woodard, and R.S. Langer, *Establishing a model spinal cord injury in the African green monkey for the preclinical evaluation of biodegradable polymer scaffolds seeded with human neural stem cells.* Journal of Neuroscience Methods, 2010. **188**(2): p. 258-269.
97. Haggerty, A.E. and M. Oudega, *Biomaterials for spinal cord repair.* Neurosci Bull, 2013. **29**(4): p. 445-59.
98. Bakshi, A., O. Fisher, T. Dagci, B.T. Himes, I. Fischer, and A. Lowman, *Mechanically engineered hydrogel scaffolds for axonal growth and angiogenesis after transplantation in spinal cord injury.* J Neurosurg Spine, 2004. **1**(3): p. 322-9.
99. Nomura, H., Y. Katayama, M.S. Shoichet, and C.H. Tator, *Complete spinal cord transection treated by implantation of a reinforced synthetic hydrogel channel results in syringomyelia and caudal migration of the rostral stump.* Neurosurgery, 2006. **59**(1): p. 183-192.
100. Tsai, E.C., P.D. Dalton, M.S. Shoichet, and C.H. Tator, *Matrix inclusion within synthetic hydrogel guidance channels improves specific supraspinal and local axonal regeneration after complete spinal cord transection.* Biomaterials, 2006. **27**(3): p. 519-533.
101. Shi, R. and R.B. Borgens, *Acute repair of crushed guinea pig spinal cord by polyethylene glycol.* Journal of Neurophysiology, 1999. **81**(5): p. 2406-2414.
102. Frith, J.E., D.J. Menzies, A.R. Cameron, P. Ghosh, D.L. Whitehead, S. Gronthos, A.C. Zannettino, and J.J. Cooper-White, *Effects of bound versus soluble pentosan polysulphate in PEG/HA-based hydrogels tailored for intervertebral disc regeneration.* Biomaterials, 2014. **35**(4): p. 1150-62.
103. Estrada, V., N. Brazda, C. Schmitz, S. Heller, H. Blazyca, R. Martini, and H.W. Müller, *Long-lasting significant functional improvement in chronic severe spinal cord injury following scar resection and polyethylene glycol implantation.* Neurobiology of Disease, 2014. **67**: p. 165-179.
104. Clarke, E.C., *Spinal Cord Mechanical Properties*, in *Neural Tissue Biomechanics*, L.E. Bilston, Editor. 2011, Springer Berlin Heidelberg: Berlin, Heidelberg. p. 25-40.
105. Belkas, J.S., C.A. Munro, M.S. Shoichet, M. Johnston, and R. Midha, *Long-term in vivo biomechanical properties and biocompatibility of poly(2-hydroxyethyl methacrylate-co-methyl methacrylate) nerve conduits.* Biomaterials, 2005. **26**(14): p. 1741-9.
106. Blakney, A.K., M.D. Swartzlander, and S.J. Bryant, *The effects of substrate stiffness on the in vitro activation of macrophages and in vivo host response to poly(ethylene glycol)-based hydrogels.* J Biomed Mater Res A, 2012. **100**(6): p. 1375-86.

107. Dadsetan, M., T.E. Hefferan, J.P. Szatkowski, P.K. Mishra, S.I. Macura, L. Lu, and M.J. Yaszemski, *Effect of hydrogel porosity on marrow stromal cell phenotypic expression.* Biomaterials, 2008. **29**(14): p. 2193-202.
108. Thomas, A.M., M.B. Kubilius, S.J. Holland, S.K. Seidlits, R.M. Boehler, A.J. Anderson, B.J. Cummings, and L.D. Shea, *Channel density and porosity of degradable bridging scaffolds on axon growth after spinal injury.* Biomaterials, 2013. **34**(9): p. 2213-20.
109. Straley, K.S., C.W.P. Foo, and S.C. Heilshorn, *Biomaterial design strategies for the treatment of spinal cord injuries.* Journal of neurotrauma, 2010. **27**(1): p. 1-19.
110. Ziemba, A.M. and R.J. Gilbert, *Biomaterials for Local, Controlled Drug Delivery to the Injured Spinal Cord.* Front Pharmacol, 2017. **8**: p. 245.
111. Koppes, A.N., N.W. Zaccor, C.J. Rivet, L.A. Williams, J.M. Piselli, R.J. Gilbert, and D.M. Thompson, *Neurite outgrowth on electrospun PLLA fibers is enhanced by exogenous electrical stimulation.* J Neural Eng, 2014. **11**(4): p. 046002.
112. Zuidema, J.M., G.P. Desmond, C.J. Rivet, K.R. Kearns, D.M. Thompson, and R.J. Gilbert, *Nebulized solvent ablation of aligned PLLA fibers for the study of neurite response to anisotropic-to-isotropic fiber/film transition (AFFT) boundaries in astrocyte-neuron co-cultures.* Biomaterials, 2015. **46**: p. 82-94.
113. Houchin-Ray, T., L.A. Swift, J.H. Jang, and L.D. Shea, *Patterned PLG substrates for localized DNA delivery and directed neurite extension.* Biomaterials, 2007. **28**(16): p. 2603-11.
114. Dull, T., R. Zufferey, M. Kelly, R.J. Mandel, M. Nguyen, D. Trono, and L. Naldini, *A Third-Generation Lentivirus Vector with a Conditional Packaging System.* Journal of Virology, 1998. **72**(11): p. 8463-8471.
115. Walthers, C.M. and S.K. Seidlits, *Gene delivery strategies to promote spinal cord repair.* Biomark Insights, 2015. **10**(Suppl 1): p. 11-29.
116. Ruitenberg, M.J., G.W. Plant, F.P.T. Hamers, J. Wortel, B. Blits, P.A. Dijkhuizen, W.H. Gispen, G.J. Boer, and J. Verhaagen, *Adenoviral Vector-Mediated Neurotrophin Gene Transfer to Olfactory Ensheathing Glia: Effects on Rubrospinal Tract Regeneration, Lesion Size, and Functional Recovery after Implantation in the Injured Rat Spinal Cord.* The Journal of Neuroscience, 2003. **23**(18): p. 7045.
117. Ruitenberg, M.J., D.B. Levison, S.V. Lee, J. Verhaagen, A.R. Harvey, and G.W. Plant, *NT-3 expression from engineered olfactory ensheathing glia promotes spinal sparing and regeneration.* Brain, 2005. **128**(4): p. 839-853.
118. Facchiano, F., E. Fernandez, S. Mancarella, G. Maira, M. Miscusi, D. D'Arcangelo, G. Cimino-Reale, M.L. Falchetti, M.C. Capogrossi, and R. Pallini, *Promotion of regeneration of corticospinal tract axons in rats with recombinant vascular endothelial growth factor alone and combined with adenovirus coding for this factor.* Journal of Neurosurgery, 2002. **97**(1): p. 161-168.
119. Zhang, Y., P.A. Dijkhuizen, P.N. Anderson, A.R. Lieberman, and J. Verhaagen, *NT-3 delivered by an adenoviral vector induces injured dorsal root axons to regenerate into the spinal cord of adult rats.* Journal of Neuroscience Research, 1998. **54**(4): p. 554-562.
120. Snyder, B.R., S.J. Gray, E.T. Quach, J.W. Huang, C.H. Leung, R.J. Samulski, N.M. Boulis, and T. Federici, *Comparison of adeno-associated viral vector serotypes for spinal cord and motor neuron gene delivery.* Hum Gene Ther, 2011. **22**(9): p. 1129-35.

121. Klaw, M.C., C. Xu, and V.J. Tom, *Intraspinal AAV Injections Immediately Rostral to a Thoracic Spinal Cord Injury Site Efficiently Transduces Neurons in Spinal Cord and Brain.* Mol Ther Nucleic Acids, 2013. **2**: p. e108.
122. Manservigi, R., R. Argnani, and P. Marconi, *HSV Recombinant Vectors for Gene Therapy.* The open virology journal, 2010. **4**: p. 123-156.
123. Zhou, Z., X. Peng, D.J. Fink, and M. Mata, *HSV-mediated Transfer of Artemin Overcomes Myelin Inhibition to Improve Outcome After Spinal Cord Injury.* Mol Ther, 2009. **17**(7): p. 1173-1179.
124. Hao, S., M. Mata, J.C. Glorioso, and D.J. Fink, *HSV-mediated expression of interleukin-4 in dorsal root ganglion neurons reduces neuropathic pain.* Mol Pain, 2006. **2**: p. 6.
125. Zhou, Z., X. Peng, R. Insolera, D.J. Fink, and M. Mata, *IL-10 promotes neuronal survival following spinal cord injury.* Exp Neurol, 2009. **220**(1): p. 183-90.
126. Zhou, Z., X. Peng, R. Insolera, D.J. Fink, and M. Mata, *Interleukin-10 provides direct trophic support to neurons.* J Neurochem, 2009. **110**(5): p. 1617-27.
127. Baum, C., O. Kustikova, U. Modlich, Z. Li, and B. Fehse, *Mutagenesis and oncogenesis by chromosomal insertion of gene transfer vectors.* Hum Gene Ther, 2006. **17**(3): p. 253-63.
128. Abdellatif, A.A., J.L. Pelt, R.L. Benton, R.M. Howard, P. Tsoulfas, P. Ping, X.M. Xu, and S.R. Whittemore, *Gene delivery to the spinal cord: comparison between lentiviral, adenoviral, and retroviral vector delivery systems.* J Neurosci Res, 2006. **84**(3): p. 553-67.
129. Baumgartner, B.J. and H.D. Shine, *Targeted transduction of CNS neurons with adenoviral vectors carrying neurotrophic factor genes confers neuroprotection that exceeds the transduced population.* J Neurosci, 1997. **17**(17): p. 6504-11.
130. Cameron, A.A., G.M. Smith, D.C. Randall, D.R. Brown, and A.G. Rabchevsky, *Genetic manipulation of intraspinal plasticity after spinal cord injury alters the severity of autonomic dysreflexia.* J Neurosci, 2006. **26**(11): p. 2923-32.
131. Nakajima, H., K. Uchida, T. Yayama, S. Kobayashi, A.R. Guerrero, S. Furukawa, and H. Baba, *Targeted retrograde gene delivery of brain-derived neurotrophic factor suppresses apoptosis of neurons and oligodendroglia after spinal cord injury in rats.* Spine (Phila Pa 1976), 2010. **35**(5): p. 497-504.
132. Zhou, L., B.J. Baumgartner, S.J. Hill-Felberg, L.R. McGowen, and H.D. Shine, *Neurotrophin-3 expressed in situ induces axonal plasticity in the adult injured spinal cord.* J Neurosci, 2003. **23**(4): p. 1424-31.
133. Gros, T., J.S. Sakamoto, A. Blesch, L.A. Havton, and M.H. Tuszynski, *Regeneration of long-tract axons through sites of spinal cord injury using templated agarose scaffolds.* Biomaterials, 2010. **31**(26): p. 6719-29.
134. Boehler, R.M., R. Kuo, S. Shin, A.G. Goodman, M.A. Pilecki, R.M. Gower, J.N. Leonard, and L.D. Shea, *Lentivirus delivery of IL-10 to promote and sustain macrophage polarization towards an anti-inflammatory phenotype.* Biotechnol Bioeng, 2014. **111**(6): p. 1210-21.
135. Park, J., J.T. Decker, D.J. Margul, D.R. Smith, B.J. Cummings, A.J. Anderson, and L.D. Shea, *Local Immunomodulation with Anti-inflammatory Cytokine-Encoding Lentivirus Enhances Functional Recovery after Spinal Cord Injury.* Molecular Therapy, 2018.
136. Park, J., J.T. Decker, D.R. Smith, B.J. Cummings, A.J. Anderson, and L.D. Shea, *Reducing inflammation through delivery of lentivirus encoding for anti-inflammatory cytokines attenuates neuropathic pain after spinal cord injury.* Journal of Controlled Release, 2018. **290**: p. 88-101.

137. Tuinstra, H.M., D.J. Margul, A.G. Goodman, R.M. Boehler, S.J. Holland, M.L. Zelivyanskaya, B.J. Cummings, A.J. Anderson, and L.D. Shea, *Long-Term Characterization of Axon Regeneration and Matrix Changes Using Multiple Channel Bridges for Spinal Cord Regeneration.* Tissue Engineering. Part A, 2014. **20**(5-6): p. 1027-1037.
138. Hayakawa, K., S. Uchida, T. Ogata, S. Tanaka, K. Kataoka, and K. Itaka, *Intrathecal injection of a therapeutic gene-containing polyplex to treat spinal cord injury.* Journal of Controlled Release, 2015. **197**: p. 1-9.
139. Yao, L., S. Yao, W. Daly, W. Hendry, A. Windebank, and A. Pandit, *Non-viral gene therapy for spinal cord regeneration.* Drug Discov Today, 2012. **17**(17-18): p. 998-1005.
140. Uchida, K., H. Nakajima, A.R. Guerrero, W.E. Johnson, W.E. Masri, and H. Baba, *Gene therapy strategies for the treatment of spinal cord injury.* Ther Deliv, 2014. **5**(5): p. 591-607.
141. Liu, Y., D. Kim, B.T. Himes, S.Y. Chow, T. Schallert, M. Murray, A. Tessler, and I. Fischer, *Transplants of fibroblasts genetically modified to express BDNF promote regeneration of adult rat rubrospinal axons and recovery of forelimb function.* Journal of Neuroscience, 1999. **19**(11): p. 4370-4387.
142. Tuszynski, M.H., D.A. Peterson, J. Ray, A. Baird, Y. Nakahara, and F.H. Gages, *Fibroblasts genetically modified to produce nerve growth factor induce robust neuritic ingrowth after grafting to the spinal cord.* Experimental Neurology, 1994. **126**(1): p. 1-14.
143. Xu, X.M., V. Guenard, N. Kleitman, and M.B. Bunge, *Axonal regeneration into Schwann cell-seeded guidance channels grafted into transected adult rat spinal cord.* J Comp Neurol, 1995. **351**(1): p. 145-60.
144. Xu, X.M., A. Chen, V. Guenard, N. Kleitman, and M.B. Bunge, *Bridging Schwann cell transplants promote axonal regeneration from both the rostral and caudal stumps of transected adult rat spinal cord.* J Neurocytol, 1997. **26**(1): p. 1-16.
145. Keyvan-Fouladi, N., G. Raisman, and Y. Li, *Delayed repair of corticospinal tract lesions as an assay for the effectiveness of transplantation of Schwann cells.* GLIA, 2005. **51**(4): p. 306-311.
146. Gomez, V.M., S. Averill, V. King, Q. Yang, E. Doncel Perez, S.C. Chacon, R. Ward, M. Nieto-Sampedro, J. Priestley, and J. Taylor, *Transplantation of olfactory ensheathing cells fails to promote significant axonal regeneration from dorsal roots into the rat cervical cord.* J Neurocytol, 2003. **32**(1): p. 53-70.
147. Oudega, M., *Schwann cell and olfactory ensheathing cell implantation for repair of the contused spinal cord.* Acta Physiol (Oxf), 2007. **189**(2): p. 181-9.
148. Li, L., H. Adnan, B. Xu, J. Wang, C. Wang, F. Li, and K. Tang, *Effects of transplantation of olfactory ensheathing cells in chronic spinal cord injury: a systematic review and meta-analysis.* European Spine Journal, 2015. **24**(5): p. 919-930.
149. Ekberg, J.A.K. and J.A. St John, *Olfactory ensheathing cells for spinal cord repair: Crucial differences between subpopulations of the glia.* Neural Regeneration Research, 2015. **10**(9): p. 1395-1396.
150. Li, Y., P.M. Field, and G. Raisman, *Regeneration of adult rat corticospinal axons induced by transplanted olfactory ensheathing cells.* Journal of Neuroscience, 1998. **18**(24): p. 10514-10524.
151. Li, Y., P.M. Field, and G. Raisman, *Repair of adult rat corticospinal tract by transplants of olfactory ensheathing cells.* Science, 1997. **277**(5334): p. 2000-2002.

152. Dumont, C., M. Munsell, M. Carlson, B. Cummings, A. Anderson, and L. Shea, *Spinal Progenitor-Laden Bridges Support Earlier Axon Regeneration Following Spinal Cord Injury.* Tissue Engineering Part A, 2018. **24**(21-22): p. 1588-1602.
153. Karimi-Abdolrezaee, S., E. Eftekharpour, J. Wang, D. Schut, and M.G. Fehlings, *Synergistic effects of transplanted adult neural stem/progenitor cells, chondroitinase, and growth factors promote functional repair and plasticity of the chronically injured spinal cord.* J Neurosci, 2010. **30**(5): p. 1657-76.
154. Karimi-Abdolrezaee, S., E. Eftekharpour, J. Wang, C.M. Morshead, and M.G. Fehlings, *Delayed transplantation of adult neural precursor cells promotes remyelination and functional neurological recovery after spinal cord injury.* J Neurosci, 2006. **26**(13): p. 3377-89.
155. Swartzlander, M.D., A.K. Blakney, L.D. Amer, K.D. Hankenson, T.R. Kyriakides, and S.J. Bryant, *Immunomodulation by mesenchymal stem cells combats the foreign body response to cell-laden synthetic hydrogels.* Biomaterials, 2015. **41**: p. 79-88.
156. Bessout, R., A. Semont, C. Demarquay, A. Charcosset, M. Benderitter, and N. Mathieu, *Mesenchymal stem cell therapy induces glucocorticoid synthesis in colonic mucosa and suppresses radiation-activated T cells: New insights into MSC immunomodulation.* Mucosal Immunology, 2014. **7**(3): p. 656-669.
157. Cui, X., L. Chen, Y. Ren, Y. Ji, W. Liu, J. Liu, Q. Yan, L. Cheng, and Y.E. Sun, *Genetic modification of mesenchymal stem cells in spinal cord injury repair strategies.* Biosci Trends, 2013. **7**(5): p. 202-8.
158. Katoh, H., K. Yokota, and M.G. Fehlings, *Regeneration of Spinal Cord Connectivity Through Stem Cell Transplantation and Biomaterial Scaffolds.* Front Cell Neurosci, 2019. **13**: p. 248.
159. Assuncao-Silva, R.C., E.D. Gomes, N. Sousa, N.A. Silva, and A.J. Salgado, *Hydrogels and Cell Based Therapies in Spinal Cord Injury Regeneration.* Stem Cells Int, 2015. **2015**: p. 948040.
160. Keirstead, H.S. and W.F. Blakemore, *The role of oligodendrocytes and oligodendrocyte progenitors in CNS remyelination.* Adv Exp Med Biol, 1999. **468**: p. 183-97.
161. Sharp, J. and H.S. Keirstead, *Therapeutic applications of oligodendrocyte precursors derived from human embryonic stem cells.* Curr Opin Biotechnol, 2007. **18**(5): p. 434-40.
162. Cummings, B.J., N. Uchida, S.J. Tamaki, D.L. Salazar, M. Hooshmand, R. Summers, F.H. Gage, and A.J. Anderson, *Human neural stem cells differentiate and promote locomotor recovery in spinal cord-injured mice.* Proc Natl Acad Sci U S A, 2005. **102**(39): p. 14069-74.
163. Suzuki, H., C.S. Ahuja, R.P. Salewski, L. Li, K. Satkunendrarajah, N. Nagoshi, S. Shibata, and M.G. Fehlings, *Neural stem cell mediated recovery is enhanced by Chondroitinase ABC pretreatment in chronic cervical spinal cord injury.* 2017. **12**(8): p. e0182339.
164. Yokota, K., K. Kobayakawa, K. Kubota, A. Miyawaki, H. Okano, Y. Ohkawa, Y. Iwamoto, and S. Okada, *Engrafted Neural Stem/Progenitor Cells Promote Functional Recovery through Synapse Reorganization with Spared Host Neurons after Spinal Cord Injury.* Stem Cell Reports, 2015. **5**(2): p. 264-77.
165. Drukker, M., *Immunogenicity of embryonic stem cells and their progeny.* Methods Enzymol, 2006. **420**: p. 391-409.

166. Drukker, M., G. Katz, A. Urbach, M. Schuldiner, G. Markel, J. Itskovitz-Eldor, B. Reubinoff, O. Mandelboim, and N. Benvenisty, *Characterization of the expression of MHC proteins in human embryonic stem cells.* Proc Natl Acad Sci U S A, 2002. **99**(15): p. 9864-9.
167. Nagoshi, N., O. Tsuji, M. Nakamura, and H. Okano, *Cell therapy for spinal cord injury using induced pluripotent stem cells.* Regenerative therapy, 2019. **11**: p. 75-80.
168. Barbeau, D.J., K.T. La, D.S. Kim, S.S. Kerpedjieva, G.V. Shurin, and K. Tamama, *Early growth response-2 signaling mediates immunomodulatory effects of human multipotential stromal cells.* Stem Cells Dev, 2014. **23**(2): p. 155-66.
169. English, K., *Mechanisms of mesenchymal stromal cell immunomodulation.* Immunol Cell Biol, 2013. **91**(1): p. 19-26.
170. Yan, Z., Y. Zhuansun, R. Chen, J. Li, and P. Ran, *Immunomodulation of mesenchymal stromal cells on regulatory T cells and its possible mechanism.* Exp Cell Res, 2014. **324**(1): p. 65-74.
171. Bonnamain, V., E. Mathieux, R. Thinard, P. Thebault, V. Nerriere-Daguin, X. Leveque, I. Anegon, B. Vanhove, I. Neveu, and P. Naveilhan, *Expression of heme oxygenase-1 in neural stem/progenitor cells as a potential mechanism to evade host immune response.* Stem Cells, 2012. **30**(10): p. 2342-53.
172. Gao, L., Q. Lu, L.J. Huang, L.H. Ruan, J.J. Yang, W.L. Huang, W.S. ZhuGe, Y.L. Zhang, B. Fu, K.L. Jin, and Q.C. ZhuGe, *Transplanted neural stem cells modulate regulatory T, gammadelta T cells and corresponding cytokines after intracerebral hemorrhage in rats.* Int J Mol Sci, 2014. **15**(3): p. 4431-41.
173. Wang, L., J. Shi, F.W. van Ginkel, L. Lan, G. Niemeyer, D.R. Martin, E.Y. Snyder, and N.R. Cox, *Neural stem/progenitor cells modulate immune responses by suppressing T lymphocytes with nitric oxide and prostaglandin E2.* Exp Neurol, 2009. **216**(1): p. 177-83.
174. Hill, C.E., L.D. Moon, P.M. Wood, and M.B. Bunge, *Labeled Schwann cell transplantation: cell loss, host Schwann cell replacement, and strategies to enhance survival.* Glia, 2006. **53**(3): p. 338-43.
175. Steward, O., K.G. Sharp, and K. Matsudaira Yee, *Long-distance migration and colonization of transplanted neural stem cells.* Cell, 2014. **156**(3): p. 385-7.
176. Ulery, B.D., L.S. Nair, and C.T. Laurencin, *Biomedical Applications of Biodegradable Polymers.* Journal of polymer science. Part B, Polymer physics, 2011. **49**(12): p. 832-864.
177. Thomas, A., L. Kubilius, S. Holland, S. Seidlits, R. Boehler, A. Anderson, B. Cummings, and L. Shea, *Channel density and porosity of degradable bridging scaffolds on axon growth after spinal injury.* Biomaterials, 2013. **34**(9): p. 2213-2220.
178. Yang, Y., L. De Laporte, M.L. Zelivyanskaya, K.J. Whittlesey, A.J. Anderson, B.J. Cummings, and L.D. Shea, *Multiple channel bridges for spinal cord injury: cellular characterization of host response.* Tissue Eng Part A, 2009. **15**(11): p. 3283-95.
179. De Laporte, L., Y. Yang, M.L. Zelivyanskaya, B.J. Cummings, A.J. Anderson, and L.D. Shea, *Plasmid releasing multiple channel bridges for transgene expression after spinal cord injury.* Mol Ther, 2009. **17**(2): p. 318-26.
180. Bixby, J.L. and W.A. Harris, *Molecular mechanisms of axon growth and guidance.* Annu Rev Cell Biol, 1991. **7**: p. 117-59.
181. Pawar, K., B.J. Cummings, A. Thomas, L.D. Shea, A. Levine, S. Pfaff, and A.J. Anderson, *Biomaterial bridges enable regeneration and re-entry of corticospinal tract axons into the caudal spinal cord after SCI: Association with recovery of forelimb function.* Biomaterials, 2015. **65**: p. 1-12.

182. Thomas, A.M. and L.D. Shea, *Polysaccharide-modified scaffolds for controlled lentivirus delivery in vitro and after spinal cord injury.* J Control Release, 2013. **170**(3): p. 421-9.
183. Thomas, A.M., S.K. Seidlits, A.G. Goodman, T.V. Kukushliev, D.M. Hassani, B.J. Cummings, A.J. Anderson, and L.D. Shea, *Sonic hedgehog and neurotrophin-3 increase oligodendrocyte numbers and myelination after spinal cord injury.* Integr Biol (Camb), 2014. **6**(7): p. 694-705.
184. Zhang, S.-x., F. Huang, M. Gates, and E.G. Holmberg, *Role of endogenous Schwann cells in tissue repair after spinal cord injury.* Neural Regeneration Research, 2013. **8**(2): p. 177-185.
185. Park, J.D., J.T., Margul, D.J., Smith, D.R., Cummings, B.J., Anderson, A.J., Shea, L.D., *Localized immunomodulation with anti-inflammatory cytokine encoding lentivirus enhances functional regeneration after spinal cord injury.* Submitted.
186. Dumont, C.M., Munsell, M. K., Carlson, M. A., Cummings, B. J., Anderson, A. J., Shea, L. D., *Neural stem cell-laden multichannel bridges support axon regeneration and neurogenesis following spinal cord injury. Submitted.*
187. Duncan, I.D., A. Brower, Y. Kondo, J.F. Curlee, and R.D. Schultz, *Extensive remyelination of the CNS leads to functional recovery.* Proceedings of the National Academy of Sciences of the United States of America, 2009. **106**(16): p. 6832-6836.
188. Baumann, N. and D. Pham-Dinh, *Biology of oligodendrocyte and myelin in the mammalian central nervous system.* Physiol Rev, 2001. **81**(2): p. 871-927.
189. Schwab, M.E., *Repairing the injured spinal cord.* Science, 2002. **295**(5557): p. 1029-31.
190. Bunge, M.B., *Bridging areas of injury in the spinal cord.* Neuroscientist, 2001. **7**(4): p. 325-39.
191. Schmidt, C.E. and J.B. Leach, *Neural tissue engineering: strategies for repair and regeneration.* Annu Rev Biomed Eng, 2003. **5**: p. 293-347.
192. Beattie, M.S., G.E. Hermann, R.C. Rogers, and J.C. Bresnahan, *Cell death in models of spinal cord injury.* Prog Brain Res, 2002. **137**: p. 37-47.
193. Kadoya, K., S. Tsukada, P. Lu, G. Coppola, D. Geschwind, M.T. Filbin, A. Blesch, and M.H. Tuszynski, *Combined intrinsic and extrinsic neuronal mechanisms facilitate bridging axonal regeneration one year after spinal cord injury.* Neuron, 2009. **64**(2): p. 165-72.
194. Li, G.L., M. Farooque, A. Holtz, and Y. Olsson, *Apoptosis of oligodendrocytes occurs for long distances away from the primary injury after compression trauma to rat spinal cord.* Acta Neuropathol, 1999. **98**(5): p. 473-80.
195. Casha, S., W.R. Yu, and M.G. Fehlings, *Oligodendroglial apoptosis occurs along degenerating axons and is associated with FAS and p75 expression following spinal cord injury in the rat.* Neuroscience, 2001. **103**(1): p. 203-18.
196. Lytle, J.M. and J.R. Wrathall, *Glial cell loss, proliferation and replacement in the contused murine spinal cord.* Eur J Neurosci, 2007. **25**(6): p. 1711-24.
197. Almad, A., F.R. Sahinkaya, and D.M. McTigue, *Oligodendrocyte fate after spinal cord injury.* Neurotherapeutics, 2011. **8**(2): p. 262-73.
198. Mi, S., R.H. Miller, W. Tang, X. Lee, B. Hu, W. Wu, Y. Zhang, C.B. Shields, Y. Zhang, S. Miklasz, D. Shea, J. Mason, R.J. Franklin, B. Ji, Z. Shao, A. Chedotal, F. Bernard, A. Roulois, J. Xu, V. Jung, and B. Pepinsky, *Promotion of central nervous system remyelination by induced differentiation of oligodendrocyte precursor cells.* Ann Neurol, 2009. **65**(3): p. 304-15.

199. Sellers, D.L., D.O. Maris, and P.J. Horner, *Postinjury niches induce temporal shifts in progenitor fates to direct lesion repair after spinal cord injury.* J Neurosci, 2009. **29**(20): p. 6722-33.
200. Barnabe-Heider, F., C. Goritz, H. Sabelstrom, H. Takebayashi, F.W. Pfrieger, K. Meletis, and J. Frisen, *Origin of new glial cells in intact and injured adult spinal cord.* Cell Stem Cell, 2010. **7**(4): p. 470-82.
201. Chen, B.K., N.N. Madigan, J.S. Hakim, M. Dadsetan, S.S. McMahon, M.J. Yaszemski, and A.J. Windebank, *GDNF Schwann cells in hydrogel scaffolds promote regional axon regeneration, remyelination and functional improvement after spinal cord transection in rats.* 2017.
202. Fortun, J., C.E. Hill, and M.B. Bunge, *Combinatorial strategies with Schwann cell transplantation to improve repair of the injured spinal cord.* Neurosci Lett, 2009. **456**(3): p. 124-32.
203. Pearse, D.D. and D.J. Barakat, *Cellular repair strategies for spinal cord injury.* Expert Opin Biol Ther, 2006. **6**(7): p. 639-52.
204. Tetzlaff, W., E.B. Okon, S. Karimi-Abdolrezaee, C.E. Hill, J.S. Sparling, J.R. Plemel, W.T. Plunet, E.C. Tsai, D. Baptiste, L.J. Smithson, M.D. Kawaja, M.G. Fehlings, and B.K. Kwon, *A systematic review of cellular transplantation therapies for spinal cord injury.* J Neurotrauma, 2011. **28**(8): p. 1611-82.
205. Li, J. and G. Lepski, *Cell transplantation for spinal cord injury: a systematic review.* Biomed Res Int, 2013. **2013**: p. 786475.
206. Wang, M., P. Zhai, X. Chen, D.J. Schreyer, X. Sun, and F. Cui, *Bioengineered Scaffolds for Spinal Cord Repair.* Tissue Engineering Part B: Reviews, 2011. **17**(3): p. 177-194.
207. Marti, E. and P. Bovolenta, *Sonic hedgehog in CNS development: one signal, multiple outputs.* Trends Neurosci, 2002. **25**(2): p. 89-96.
208. Delgado, A.C., S.R. Ferron, D. Vicente, E. Porlan, A. Perez-Villalba, C.M. Trujillo, P. D'Ocon, and I. Farinas, *Endothelial NT-3 delivered by vasculature and CSF promotes quiescence of subependymal neural stem cells through nitric oxide induction.* Neuron, 2014. **83**(3): p. 572-85.
209. Gritli-Linde, A., P. Lewis, A.P. McMahon, and A. Linde, *The whereabouts of a morphogen: direct evidence for short- and graded long-range activity of hedgehog signaling peptides.* Dev Biol, 2001. **236**(2): p. 364-86.
210. Lowry, N., S.K. Goderie, P. Lederman, C. Charniga, M.R. Gooch, K.D. Gracey, A. Banerjee, S. Punyani, J. Silver, R.S. Kane, J.H. Stern, and S. Temple, *The effect of long-term release of Shh from implanted biodegradable microspheres on recovery from spinal cord injury in mice.* Biomaterials, 2012. **33**(10): p. 2892-901.
211. Ribes, V. and J. Briscoe, *Establishing and Interpreting Graded Sonic Hedgehog Signaling during Vertebrate Neural Tube Patterning: The Role of Negative Feedback.* Cold Spring Harbor Perspectives in Biology, 2009. **1**(2): p. a002014.
212. Liu, A. and L.A. Niswander, *Bone morphogenetic protein signalling and vertebrate nervous system development.* Nat Rev Neurosci, 2005. **6**(12): p. 945-54.
213. Enzmann, G.U., R.L. Benton, J.P. Woock, R.M. Howard, P. Tsoulfas, and S.R. Whittemore, *Consequences of noggin expression by neural stem, glial, and neuronal precursor cells engrafted into the injured spinal cord.* Exp Neurol, 2005. **195**(2): p. 293-304.

214. Zhang, H., L. Vutskits, V. Calaora, P. Durbec, and J.Z. Kiss, *A role for the polysialic acid-neural cell adhesion molecule in PDGF-induced chemotaxis of oligodendrocyte precursor cells.* J Cell Sci, 2004. **117**(Pt 1): p. 93-103.
215. Woodruff, R.H., M. Fruttiger, W.D. Richardson, and R.J. Franklin, *Platelet-derived growth factor regulates oligodendrocyte progenitor numbers in adult CNS and their response following CNS demyelination.* Mol Cell Neurosci, 2004. **25**(2): p. 252-62.
216. Chen, Y., V. Balasubramaniyan, J. Peng, E.C. Hurlock, M. Tallquist, J. Li, and Q.R. Lu, *Isolation and culture of rat and mouse oligodendrocyte precursor cells.* Nat Protoc, 2007. **2**(5): p. 1044-51.
217. Hill, R.A., K.D. Patel, J. Medved, A.M. Reiss, and A. Nishiyama, *NG2 cells in white matter but not gray matter proliferate in response to PDGF.* J Neurosci, 2013. **33**(36): p. 14558-66.
218. Asakura, K., S.F. Hunter, and M. Rodriguez, *Effects of transforming growth factor-beta and platelet-derived growth factor on oligodendrocyte precursors: insights gained from a neuronal cell line.* J Neurochem, 1997. **68**(6): p. 2281-90.
219. Hu, J.G., S.L. Fu, Y.X. Wang, Y. Li, X.Y. Jiang, X.F. Wang, M.S. Qiu, P.H. Lu, and X.M. Xu, *Platelet-derived growth factor-AA mediates oligodendrocyte lineage differentiation through activation of extracellular signal-regulated kinase signaling pathway.* Neuroscience, 2008. **151**(1): p. 138-47.
220. Hinks, G.L. and R.J. Franklin, *Distinctive patterns of PDGF-A, FGF-2, IGF-I, and TGF-beta1 gene expression during remyelination of experimentally-induced spinal cord demyelination.* Mol Cell Neurosci, 1999. **14**(2): p. 153-68.
221. Powers, B.E., J. Lasiene, J.R. Plemel, L. Shupe, S.I. Perlmutter, W. Tetzlaff, and P.J. Horner, *Axonal thinning and extensive remyelination without chronic demyelination in spinal injured rats.* The Journal of Neuroscience, 2012. **32**(15): p. 5120-5125.
222. Lasiene, J., L. Shupe, S. Perlmutter, and P. Horner, *No evidence for chronic demyelination in spared axons after spinal cord injury in a mouse.* J Neurosci, 2008. **28**(15): p. 3887-96.
223. Powers, B.E., D.L. Sellers, E.A. Lovelett, W. Cheung, S.P. Aalami, N. Zapertov, D.O. Maris, and P.J. Horner, *Remyelination reporter reveals prolonged refinement of spontaneously regenerated myelin.* Proc Natl Acad Sci U S A, 2013. **110**(10): p. 4075-80.
224. Margul, D.J., J. Park, R.M. Boehler, D.R. Smith, M.A. Johnson, D.A. McCreedy, T. He, A. Ataliwala, T.V. Kukushliev, J. Liang, A. Sohrabi, A.G. Goodman, C.M. Walthers, L.D. Shea, and S.K. Seidlits, *Reducing neuroinflammation by delivery of IL-10 encoding lentivirus from multiple-channel bridges.* Bioengineering & Translational Medicine, 2016: p. n/a-n/a.
225. Li, J., T.A. Rickett, and R. Shi, *Biomimetic nerve scaffolds with aligned intraluminal microchannels: a "sweet" approach to tissue engineering.* Langmuir, 2009. **25**(3): p. 1813-7.
226. McCreedy, D.A., D.J. Margul, S.K. Seidlits, J.T. Antane, R.J. Thomas, G.M. Sissman, R.M. Boehler, D.R. Smith, S.W. Goldsmith, T.V. Kukushliev, J.B. Lamano, B.H. Vedia, T. He, and L.D. Shea, *Semi-automated counting of axon regeneration in poly(lactide co-glycolide) spinal cord bridges.* J Neurosci Methods, 2016. **263**: p. 15-22.
227. Basso, D.M., L.C. Fisher, A.J. Anderson, L.B. Jakeman, D.M. McTigue, and P.G. Popovich, *Basso Mouse Scale for locomotion detects differences in recovery after spinal cord injury in five common mouse strains.* J Neurotrauma, 2006. **23**(5): p. 635-59.

228. Sabelstrom, H., M. Stenudd, and J. Frisen, *Neural stem cells in the adult spinal cord.* Exp Neurol, 2014. **260**: p. 44-9.
229. Lee, H.J., J. Wu, J. Chung, and J.R. Wrathall, *SOX2 expression is upregulated in adult spinal cord after contusion injury in both oligodendrocyte lineage and ependymal cells.* J Neurosci Res, 2013. **91**(2): p. 196-210.
230. Hughes, S.M., F. Moussavi-Harami, S.L. Sauter, and B.L. Davidson, *Viral-mediated gene transfer to mouse primary neural progenitor cells.* Mol Ther, 2002. **5**(1): p. 16-24.
231. Chung, K. and R.E. Coggeshall, *Numbers of axons in lateral and ventral funiculi of rat sacral spinal cord.* The Journal of Comparative Neurology, 1983. **214**(1): p. 72-78.
232. Chung, K. and R.E. Coggeshall, *Propriospinal fibers in the rat.* The Journal of Comparative Neurology, 1983. **217**(1): p. 47-53.
233. Hsu, J.-Y.C., S.A. Stein, and X.-M. Xu, *Development of the corticospinal tract in the mouse spinal cord: A quantitative ultrastructural analysis.* Brain Research, 2006. **1084**(1): p. 16-27.
234. Tan, B.T., L. Jiang, L. Liu, Y. Yin, Z.R. Luo, Z.Y. Long, S. Li, and L.H. Yu, *Local injection of Lenti-Olig2 at lesion site promotes functional recovery of spinal cord injury in rats.* 2017. **23**(6): p. 475-487.
235. Alizadeh, A., S.M. Dyck, H. Kataria, G.M. Shahriary, D.H. Nguyen, K.T. Santhosh, and S. Karimi-Abdolrezaee, *Neuregulin-1 positively modulates glial response and improves neurological recovery following traumatic spinal cord injury.* Glia, 2017. **65**(7): p. 1152-1175.
236. Deng, L.X., P. Deng, Y. Ruan, Z.C. Xu, N.K. Liu, X. Wen, G.M. Smith, and X.M. Xu, *A novel growth-promoting pathway formed by GDNF-overexpressing Schwann cells promotes propriospinal axonal regeneration, synapse formation, and partial recovery of function after spinal cord injury.* J Neurosci, 2013. **33**(13): p. 5655-67.
237. Cao, Q., Q. He, Y. Wang, X. Cheng, R.M. Howard, Y. Zhang, W.H. DeVries, C.B. Shields, D.S. Magnuson, X.M. Xu, D.H. Kim, and S.R. Whittemore, *Transplantation of ciliary neurotrophic factor-expressing adult oligodendrocyte precursor cells promotes remyelination and functional recovery after spinal cord injury.* J Neurosci, 2010. **30**(8): p. 2989-3001.
238. Duncan, I.D., R.L. Marik, A.T. Broman, and M. Heidari, *Thin myelin sheaths as the hallmark of remyelination persist over time and preserve axon function.* Proc Natl Acad Sci U S A, 2017. **114**(45): p. E9685-e9691.
239. Hawryluk, G.W.J. and M.G. Fehlings, *The Center of the Spinal Cord May Be Central to Its Repair.* Cell Stem Cell, 2008. **3**(3): p. 230-232.
240. Horky, L.L., F. Galimi, F.H. Gage, and P.J. Horner, *Fate of endogenous stem/progenitor cells following spinal cord injury.* J Comp Neurol, 2006. **498**(4): p. 525-38.
241. Miron, V.E., T. Kuhlmann, and J.P. Antel, *Cells of the oligodendroglial lineage, myelination, and remyelination.* Biochim Biophys Acta, 2011. **1812**(2): p. 184-93.
242. Xiao, Q., Y. Du, W. Wu, and H.K. Yip, *Bone morphogenetic proteins mediate cellular response and, together with Noggin, regulate astrocyte differentiation after spinal cord injury.* Experimental Neurology, 2010. **221**(2): p. 353-366.
243. Sabo, J.K., T.D. Aumann, D. Merlo, T.J. Kilpatrick, and H.S. Cate, *Remyelination is altered by bone morphogenic protein signaling in demyelinated lesions.* J Neurosci, 2011. **31**(12): p. 4504-10.

244. Chen, Y., V. Balasubramaniyan, J. Peng, E.C. Hurlock, M. Tallquist, J. Li, and Q.R. Lu, *Isolation and culture of rat and mouse oligodendrocyte precursor cells.* Nat. Protocols, 2007. **2**(5): p. 1044-1051.
245. Lutton, C., Y.W. Young, R. Williams, A.C. Meedeniya, A. Mackay-Sim, and B. Goss, *Combined VEGF and PDGF treatment reduces secondary degeneration after spinal cord injury.* J Neurotrauma, 2012. **29**(5): p. 957-70.
246. Wang, Z., H. Colognato, and C. Ffrench-Constant, *Contrasting effects of mitogenic growth factors on myelination in neuron-oligodendrocyte co-cultures.* Glia, 2007. **55**(5): p. 537-45.
247. Butt, A.M., M.F. Hornby, S. Kirvell, and M. Berry, *Platelet-derived growth factor delays oligodendrocyte differentiation and axonal myelination in vivo in the anterior medullary velum of the developing rat.* J Neurosci Res, 1997. **48**(6): p. 588-96.
248. Barateiro, A. and A. Fernandes, *Temporal oligodendrocyte lineage progression: In vitro models of proliferation, differentiation and myelination.* Biochimica et Biophysica Acta (BBA) - Molecular Cell Research, 2014. **1843**(9): p. 1917-1929.
249. Boulanger, J.J. and C. Messier, *From precursors to myelinating oligodendrocytes: Contribution of intrinsic and extrinsic factors to white matter plasticity in the adult brain.* Neuroscience, 2014. **269**: p. 343-366.
250. Zhou, X., M. Vink, B. Klaver, B. Berkhout, and A.T. Das, *Optimization of the Tet-On system for regulated gene expression through viral evolution.* Gene Ther, 2006. **13**(19): p. 1382-90.
251. Lourenço, T. and M. Grãos, *Modulation of Oligodendrocyte Differentiation by Mechanotransduction.* Frontiers in Cellular Neuroscience, 2016. **10**(277).
252. Aizawa, Y., N. Leipzig, T. Zahir, and M. Shoichet, *The effect of immobilized platelet derived growth factor AA on neural stem/progenitor cell differentiation on cell-adhesive hydrogels.* Biomaterials, 2008. **29**(35): p. 4676-4683.
253. Russell, L.N. and K.J. Lampe, *Oligodendrocyte Precursor Cell Viability, Proliferation, and Morphology is Dependent on Mesh Size and Storage Modulus in 3D Poly(ethylene glycol)-Based Hydrogels.* ACS Biomaterials Science & Engineering, 2017. **3**(12): p. 3459-3468.
254. McIver, S.R., M. Muccigrosso, E.R. Gonzales, J.-M. Lee, M.S. Roberts, M.S. Sands, and M.P. Goldberg, *OLIGODENDROCYTE DEGENERATION AND RECOVERY AFTER FOCAL CEREBRAL ISCHEMIA.* Neuroscience, 2010. **169**(3): p. 1364-1375.
255. Nishiyama, A., M. Komitova, R. Suzuki, and X. Zhu, *Polydendrocytes (NG2 cells): multifunctional cells with lineage plasticity.* Nat Rev Neurosci, 2009. **10**(1): p. 9-22.
256. Xiao, Z., F. Tang, J. Tang, H. Yang, Y. Zhao, B. Chen, S. Han, N. Wang, X. Li, S. Cheng, G. Han, C. Zhao, X. Yang, Y. Chen, Q. Shi, S. Hou, S. Zhang, and J. Dai, *One-year clinical study of NeuroRegen scaffold implantation following scar resection in complete chronic spinal cord injury patients.* Science China Life Sciences, 2016. **59**(7): p. 647-655.
257. Milone, M.C. and U. O'Doherty, *Clinical use of lentiviral vectors.* Leukemia, 2018. **32**(7): p. 1529-1541.
258. Foundation, C.a.D.R.a.C.f.D., *One Degree of Separation: Paralysis and Spinal Cord Injury in the United States*. 2009
259. Golz, G., L. Uhlmann, D. Ludecke, N. Markgraf, R. Nitsch, and S. Hendrix, *The cytokine/neurotrophin axis in peripheral axon outgrowth.* Eur J Neurosci, 2006. **24**(10): p. 2721-30.

260. Kigerl, K.A., J.C. Gensel, D.P. Ankeny, J.K. Alexander, D.J. Donnelly, and P.G. Popovich, *Identification of two distinct macrophage subsets with divergent effects causing either neurotoxicity or regeneration in the injured mouse spinal cord.* J Neurosci, 2009. **29**(43): p. 13435-44.
261. Murray, P.J. and T.A. Wynn, *Obstacles and opportunities for understanding macrophage polarization.* J Leukoc Biol, 2011. **89**(4): p. 557-63.
262. Murray, P.J. and T.A. Wynn, *Protective and pathogenic functions of macrophage subsets.* Nat Rev Immunol, 2011. **11**(11): p. 723-37.
263. Porcheray, F., S. Viaud, A.C. Rimaniol, C. Leone, B. Samah, N. Dereuddre-Bosquet, D. Dormont, and G. Gras, *Macrophage activation switching: an asset for the resolution of inflammation.* Clin Exp Immunol, 2005. **142**(3): p. 481-9.
264. Ogden, C.A., J.D. Pound, B.K. Batth, S. Owens, I. Johannessen, K. Wood, and C.D. Gregory, *Enhanced apoptotic cell clearance capacity and B cell survival factor production by IL-10-activated macrophages: implications for Burkitt's lymphoma.* J Immunol, 2005. **174**(5): p. 3015-23.
265. Mokarram, N., A. Merchant, V. Mukhatyar, G. Patel, and R.V. Bellamkonda, *Effect of modulating macrophage phenotype on peripheral nerve repair.* Biomaterials, 2012. **33**(34): p. 8793-801.
266. Boato, F., D. Hechler, K. Rosenberger, D. Ludecke, E.M. Peters, R. Nitsch, and S. Hendrix, *Interleukin-1 beta and neurotrophin-3 synergistically promote neurite growth in vitro.* J Neuroinflammation, 2011. **8**: p. 183.
267. Daneman, R. and A. Prat, *The blood-brain barrier.* Cold Spring Harb Perspect Biol, 2015. **7**(1): p. a020412.
268. Liu, Z., O. Chen, J.B.J. Wall, M. Zheng, Y. Zhou, L. Wang, H. Ruth Vaseghi, L. Qian, and J. Liu, *Systematic comparison of 2A peptides for cloning multi-genes in a polycistronic vector.* Scientific Reports, 2017. **7**(1): p. 2193.
269. Smith, D.R., D.J. Margul, C.M. Dumont, M.A. Carlson, M.K. Munsell, M. Johnson, B.J. Cummings, A.J. Anderson, and L.D. Shea, *Combinatorial lentiviral gene delivery of pro-oligodendrogenic factors for improving myelination of regenerating axons after spinal cord injury.* Biotechnology and bioengineering, 2019. **116**(1): p. 155-167.
270. Cummings, B.J., C. Engesser-Cesar, G. Cadena, and A.J. Anderson, *Adaptation of a ladder beam walking task to assess locomotor recovery in mice following spinal cord injury.* Behavioural Brain Research, 2007. **177**(2): p. 232-241.
271. Choi, Y., Y.W. Yoon, H.S. Na, S.H. Kim, and J.M. Chung, *Behavioral signs of ongoing pain and cold allodynia in a rat model of neuropathic pain.* Pain, 1994. **59**(3): p. 369-76.
272. Kaether, C., P. Skehel, and C.G. Dotti, *Axonal membrane proteins are transported in distinct carriers: a two-color video microscopy study in cultured hippocampal neurons.* Molecular biology of the cell, 2000. **11**(4): p. 1213-1224.
273. Wang, Q. and S.H. Green, *Functional role of neurotrophin-3 in synapse regeneration by spiral ganglion neurons on inner hair cells after excitotoxic trauma in vitro.* J Neurosci, 2011. **31**(21): p. 7938-49.
274. García-Alías, G., H.A. Petrosyan, L. Schnell, P.J. Horner, W.J. Bowers, L.M. Mendell, J.W. Fawcett, and V.L. Arvanian, *Chondroitinase ABC Combined with Neurotrophin NT-3 Secretion and NR2D Expression Promotes Axonal Plasticity and Functional Recovery in Rats with Lateral Hemisection of the Spinal Cord.* Journal of Neuroscience, 2011. **31**(49): p. 17788-17799.

275. Mosser, D.M., *The many faces of macrophage activation.* J Leukoc Biol, 2003. **73**(2): p. 209-12.
276. Sindrilaru, A., T. Peters, S. Wieschalka, C. Baican, A. Baican, H. Peter, A. Hainzl, S. Schatz, Y. Qi, A. Schlecht, J.M. Weiss, M. Wlaschek, C. Sunderkotter, and K. Scharffetter-Kochanek, *An unrestrained proinflammatory M1 macrophage population induced by iron impairs wound healing in humans and mice.* J Clin Invest, 2011. **121**(3): p. 985-97.
277. Goyvaerts, C., T. Liechtenstein, C. Bricogne, D. Escors, and K. Breckpot, *Targeted Lentiviral Vectors: Current Applications and Future Potential*, in *Gene Therapy - Tools and Potential Applications*. 2013, InTech: Rijeka. p. Ch. 0.
278. Schambach, A., D. Zychlinski, B. Ehrnstroem, and C. Baum, *Biosafety features of lentiviral vectors.* Human gene therapy, 2013. **24**(2): p. 132-142.
279. Barouch, R., E. Appel, G. Kazimirsky, and C. Brodie, *Macrophages express neurotrophins and neurotrophin receptors: Regulation of nitric oxide production by NT-3.* Journal of Neuroimmunology, 2001. **112**(1): p. 72-77.
280. Zhang, J., C. Geula, C. Lu, H. Koziel, L.M. Hatcher, and F.J. Roisen, *Neurotrophins regulate proliferation and survival of two microglial cell lines in vitro.* Exp Neurol, 2003. **183**(2): p. 469-81.
281. Sousa-Victor, P., H. Jasper, and J. Neves, *Trophic Factors in Inflammation and Regeneration: The Role of MANF and CDNF.* Frontiers in physiology, 2018. **9**: p. 1629-1629.
282. Barouch, R., E. Appel, G. Kazimirsky, and C. Brodie, *Macrophages express neurotrophins and neurotrophin receptors. Regulation of nitric oxide production by NT-3.* J Neuroimmunol, 2001. **112**(1-2): p. 72-7.
283. Williams, K.S., D.A. Killebrew, G.P. Clary, J.A. Seawell, and R.B. Meeker, *Differential regulation of macrophage phenotype by mature and pro-nerve growth factor.* J Neuroimmunol, 2015. **285**: p. 76-93.
284. Samah, B., F. Porcheray, and G. Gras, *Neurotrophins modulate monocyte chemotaxis without affecting macrophage function.* Clin Exp Immunol, 2008. **151**(3): p. 476-86.
285. Dumont, C.M., J. Park, and L.D. Shea, *Controlled release strategies for modulating immune responses to promote tissue regeneration.* J Control Release, 2015.
286. Dumont, C.M., D.J. Margul, and L.D. Shea, *Tissue Engineering Approaches to Modulate the Inflammatory Milieu following Spinal Cord Injury.* Cells Tissues Organs, 2016. **202**(1-2): p. 52-66.
287. Boehler, R.M., R. Kuo, S. Shin, A.G. Goodman, M.A. Pilecki, J.N. Leonard, and L.D. Shea, *Lentivirus delivery of IL-10 to promote and sustain macrophage polarization towards an anti-inflammatory phenotype.* Biotechnology and Bioengineering, 2014. **111**(6): p. 1210-1221.
288. Walter, M.R., *The Molecular Basis of IL-10 Function: From Receptor Structure to the Onset of Signaling.* Current topics in microbiology and immunology, 2014. **380**: p. 191-212.
289. Verma, R., L. Balakrishnan, K. Sharma, A.A. Khan, J. Advani, H. Gowda, S.P. Tripathy, M. Suar, A. Pandey, S. Gandotra, T.S.K. Prasad, and S. Shankar, *A network map of Interleukin-10 signaling pathway.* Journal of Cell Communication and Signaling, 2016. **10**(1): p. 61-67.
290. Siebert, J.R., F.A. Middleton, and D.J. Stelzner, *Long descending cervical propriospinal neurons differ from thoracic propriospinal neurons in response to low thoracic spinal injury.* BMC Neurosci, 2010. **11**: p. 148.
291. Stelzner, D.J., *Short-circuit recovery from spinal injury.* Nat Med, 2008. **14**(1): p. 19-20.

292. Siebert, J.R., F.A. Middelton, and D.J. Stelzner, *Intrinsic response of thoracic propriospinal neurons to axotomy.* BMC Neurosci, 2010. **11**: p. 69.
293. Conta, A.C. and D.J. Stelzner, *Differential vulnerability of propriospinal tract neurons to spinal cord contusion injury.* J Comp Neurol, 2004. **479**(4): p. 347-59.
294. Loers, G., F. Aboul-Enein, U. Bartsch, H. Lassmann, and M. Schachner, *Comparison of myelin, axon, lipid, and immunopathology in the central nervous system of differentially myelin-compromised mutant mice: a morphological and biochemical study.* Mol Cell Neurosci, 2004. **27**(2): p. 175-89.
295. Coelho, R.P., L.M. Yuelling, B. Fuss, and C. Sato-Bigbee, *Neurotrophin-3 targets the translational initiation machinery in oligodendrocytes.* Glia, 2009. **57**(16): p. 1754-64.
296. Yan, H. and P.M. Wood, *NT-3 weakly stimulates proliferation of adult rat O1(-)O4(+) oligodendrocyte-lineage cells and increases oligodendrocyte myelination in vitro.* J Neurosci Res, 2000. **62**(3): p. 329-35.
297. Pöyhönen, S., S. Er, A. Domanskyi, and M. Airavaara, *Effects of Neurotrophic Factors in Glial Cells in the Central Nervous System: Expression and Properties in Neurodegeneration and Injury.* Frontiers in physiology, 2019. **10**: p. 486-486.
298. Silva-Vargas, V. and F. Doetsch, *A New Twist for Neurotrophins: Endothelial-Derived NT-3 Mediates Adult Neural Stem Cell Quiescence.* Neuron, 2014. **83**(3): p. 507-509.
299. Assinck, P., G.J. Duncan, J.R. Plemel, M.J. Lee, J.A. Stratton, S.B. Manesh, J. Liu, L.M. Ramer, S.H. Kang, D.E. Bergles, J. Biernaskie, and W. Tetzlaff, *Myelinogenic Plasticity of Oligodendrocyte Precursor Cells following Spinal Cord Contusion Injury.* The Journal of Neuroscience, 2017. **37**(36): p. 8635.
300. Dyck, S., H. Kataria, A. Alizadeh, K.T. Santhosh, B. Lang, J. Silver, and S. Karimi-Abdolrezaee, *Perturbing chondroitin sulfate proteoglycan signaling through LAR and PTPsigma receptors promotes a beneficial inflammatory response following spinal cord injury.* J Neuroinflammation, 2018. **15**(1): p. 90.
301. Li, X., Y. Zhang, Y. Yan, B. Ciric, C.-G. Ma, B. Gran, M. Curtis, A. Rostami, and G.-X. Zhang, *Neural Stem Cells Engineered to Express Three Therapeutic Factors Mediate Recovery from Chronic Stage CNS Autoimmunity.* Molecular therapy : the journal of the American Society of Gene Therapy, 2016. **24**(8): p. 1456-1469.
302. Duncan, G.J., S.B. Manesh, B.J. Hilton, P. Assinck, J. Liu, A. Moulson, J.R. Plemel, and W. Tetzlaff, *Locomotor recovery following contusive spinal cord injury does not require oligodendrocyte remyelination.* Nature communications, 2018. **9**(1): p. 3066-3066.
303. Khan, N. and M.T. Smith, *Neurotrophins and Neuropathic Pain: Role in Pathobiology.* Molecules (Basel, Switzerland), 2015. **20**(6): p. 10657-10688.
304. Bradbury, E.J., S. Khemani, R. Von, King, J.V. Priestley, and S.B. McMahon, *NT-3 promotes growth of lesioned adult rat sensory axons ascending in the dorsal columns of the spinal cord.* Eur J Neurosci, 1999. **11**(11): p. 3873-83.
305. Obata, K., H. Yamanaka, Y. Dai, T. Mizushima, T. Fukuoka, A. Tokunaga, H. Yoshikawa, and K. Noguchi, *Contribution of degeneration of motor and sensory fibers to pain behavior and the changes in neurotrophic factors in rat dorsal root ganglion.* Exp Neurol, 2004. **188**(1): p. 149-60.
306. Siniscalco, D., C. Giordano, F. Rossi, S. Maione, and V. de Novellis, *Role of neurotrophins in neuropathic pain.* Current neuropharmacology, 2011. **9**(4): p. 523-529.

307. Foundation, R. *One degree of separation: paralysis and spinal cord injury in the United States*. 2009; Available from: www.christopherreeve.org/atf/cf/%7B3d83418f-b967-4c18-8ada-adc2e5355071%7D/8112reptfinal.pdf
308. Dalamagkas, K., M. Tsintou, A. Seifalian, and A.M. Seifalian, *Translational Regenerative Therapies for Chronic Spinal Cord Injury.* 2018. **19**(6).
309. Wang, X., P. Duffy, A.W. McGee, O. Hasan, G. Gould, N. Tu, N.Y. Harel, Y. Huang, R.E. Carson, D. Weinzimmer, J. Ropchan, L.I. Benowitz, W.B.J. Cafferty, and S.M. Strittmatter, *Recovery from Chronic Spinal Cord Contusion after Nogo Receptor Intervention.* Annals of neurology, 2011. **70**(5): p. 805-821.
310. Rasouli, A., N. Bhatia, P. Dinh, K. Cahill, S. Suryadevara, and R. Gupta, *Resection of glial scar following spinal cord injury.* J Orthop Res, 2009. **27**(7): p. 931-6.
311. Busch, S.A. and J. Silver, *The role of extracellular matrix in CNS regeneration.* Current Opinion in Neurobiology, 2007. **17**(1): p. 120-127.
312. Rong Hu, Jianjun Zhou, Chunxia Luo, Jiangkai Lin, Xianrong Wang, Xiaoguang Li, Xiuwu Bian, Yunqing Li, Qi Wan, Yanbing Yu, and Hua Feng, *Glial scar and neuroregeneration: histological, functional, and magnetic resonance imaging analysis in chronic spinal cord injury.* Journal of Neurosurgery: Spine, 2010. **13**(2): p. 169-180.
313. Zhu, Y., C. Soderblom, M. Trojanowsky, D.-H. Lee, and J.K. Lee, *Fibronectin Matrix Assembly after Spinal Cord Injury.* Journal of Neurotrauma, 2015. **32**(15): p. 1158-1167.
314. Ampofo, E., B.M. Schmitt, M.D. Menger, and M.W. Laschke, *The regulatory mechanisms of NG2/CSPG4 expression.* Cellular & molecular biology letters, 2017. **22**: p. 4-4.
315. Andrews, E.M., R.J. Richards, F.Q. Yin, M.S. Viapiano, and L.B. Jakeman, *Alterations in chondroitin sulfate proteoglycan expression occur both at and far from the site of spinal contusion injury.* Experimental neurology, 2012. **235**(1): p. 174-187.
316. Seif, G.I., H. Nomura, and C.H. Tator, *Retrograde axonal degeneration "dieback" in the corticospinal tract after transection injury of the rat spinal cord: a confocal microscopy study.* J Neurotrauma, 2007. **24**(9): p. 1513-28.
317. Yokota, K., K. Kubota, K. Kobayakawa, T. Saito, M. Hara, K. Kijima, T. Maeda, H. Katoh, Y. Ohkawa, Y. Nakashima, and S. Okada, *Pathological changes of distal motor neurons after complete spinal cord injury.* Molecular Brain, 2019. **12**(1): p. 4.
318. Tashiro, S., M. Nakamura, and H. Okano, *The prospects of regenerative medicine combined with rehabilitative approaches for chronic spinal cord injury animal models.* 2017. **12**(1): p. 43-46.
319. Beck, K.D., H.X. Nguyen, M.D. Galvan, D.L. Salazar, T.M. Woodruff, and A.J. Anderson, *Quantitative analysis of cellular inflammation after traumatic spinal cord injury: evidence for a multiphasic inflammatory response in the acute to chronic environment.* Brain, 2010.
320. Bollaerts, I., J. Van Houcke, L. Andries, L. De Groef, and L. Moons, *Neuroinflammation as Fuel for Axonal Regeneration in the Injured Vertebrate Central Nervous System.* Mediators of inflammation, 2017. **2017**: p. 9478542-9478542.
321. Foote, A.K. and W.F. Blakemore, *Inflammation stimulates remyelination in areas of chronic demyelination.* Brain, 2005. **128**(Pt 3): p. 528-39.
322. Wang, H.-F., X.-K. Liu, R. Li, P. Zhang, Z. Chu, C.-L. Wang, H.-R. Liu, J. Qi, G.-Y. Lv, G.-Y. Wang, B. Liu, Y. Li, and Y.-Y. Wang, *Effect of glial cells on remyelination after spinal cord injury.* Neural regeneration research, 2017. **12**(10): p. 1724-1732.

323. Hesp, Z.C., E.A. Goldstein, C.J. Miranda, B.K. Kaspar, and D.M. McTigue, *Chronic Oligodendrogenesis and Remyelination after Spinal Cord Injury in Mice and Rats.* The Journal of Neuroscience, 2015. **35**(3): p. 1274-1290.
324. Tanabe, N., T. Kuboyama, and C. Tohda, *Matrine promotes neural circuit remodeling to regulate motor function in a mouse model of chronic spinal cord injury.* Neural Regen Res, 2019. **14**(11): p. 1961-1967.
325. Arnold, S.A. and T. Hagg, *Anti-inflammatory treatments during the chronic phase of spinal cord injury improve locomotor function in adult mice.* J Neurotrauma, 2011. **28**(9): p. 1995-2002.
326. Anderson, M.A., T.M. O'Shea, J.E. Burda, Y. Ao, S.L. Barlatey, A.M. Bernstein, J.H. Kim, N.D. James, A. Rogers, B. Kato, A.L. Wollenberg, R. Kawaguchi, G. Coppola, C. Wang, T.J. Deming, Z. He, G. Courtine, and M.V. Sofroniew, *Required growth facilitators propel axon regeneration across complete spinal cord injury.* Nature, 2018.
327. Haberman, R.P., T.J. McCown, and R.J. Samulski, *Inducible long-term gene expression in brain with adeno-associated virus gene transfer.* Gene Ther, 1998. **5**(12): p. 1604-11.
328. Naidoo, J. and D. Young, *Gene regulation systems for gene therapy applications in the central nervous system.* Neurol Res Int, 2012. **2012**: p. 595410.
329. Hou, S., L. Nicholson, E. van Niekerk, M. Motsch, and A. Blesch, *Dependence of regenerated sensory axons on continuous neurotrophin-3 delivery.* J Neurosci, 2012. **32**(38): p. 13206-20.
330. Braun, Simon M.G., Raquel A.C. Machado, and S. Jessberger, *Temporal Control of Retroviral Transgene Expression in Newborn Cells in the Adult Brain.* Stem Cell Reports, 2013. **1**(2): p. 114-122.
331. Satoh, J., Y. Kino, N. Asahina, M. Takitani, J. Miyoshi, T. Ishida, and Y. Saito, *TMEM119 marks a subset of microglia in the human brain.* Neuropathology, 2016. **36**(1): p. 39-49.
332. Pepper, R.E., K.A. Pitman, C.L. Cullen, and K.M. Young, *How Do Cells of the Oligodendrocyte Lineage Affect Neuronal Circuits to Influence Motor Function, Memory and Mood?* Frontiers in Cellular Neuroscience, 2018. **12**(399).
333. Tauchi, R., S. Imagama, T. Natori, T. Ohgomori, A. Muramoto, R. Shinjo, Y. Matsuyama, N. Ishiguro, and K. Kadomatsu, *The endogenous proteoglycan-degrading enzyme ADAMTS-4 promotes functional recovery after spinal cord injury.* Journal of Neuroinflammation, 2012. **9**(1): p. 53.
334. Spejo, A.B. and A.L.R. Oliveira, *Synaptic rearrangement following axonal injury: Old and new players.* Neuropharmacology, 2015. **96, Part A**: p. 113-123.
335. Donovan, J. and S. Kirshblum, *Clinical Trials in Traumatic Spinal Cord Injury.* Neurotherapeutics, 2018. **15**(3): p. 654-668.
336. Skoumal, M., S. Seidlits, S. Shin, and L. Shea, *Localized lentivirus delivery via peptide interactions.* Biotechnol Bioeng, 2016. **113**(9): p. 2033-40.
337. Rank, M.M., J.R. Flynn, M.P. Galea, R. Callister, and R.J. Callister, *Electrophysiological characterization of spontaneous recovery in deep dorsal horn interneurons after incomplete spinal cord injury.* Exp Neurol, 2015. **271**: p. 468-78.
338. Prasad, A. and M. Sahin, *Multi-channel recordings of the motor activity from the spinal cord of behaving rats.* Conf Proc IEEE Eng Med Biol Soc, 2006. **1**: p. 2288-91.
339. Prasad, A. and M. Sahin, *Characterization of Neural Activity Recorded from the Descending Tracts of the Rat Spinal Cord.* Frontiers in Neuroscience, 2010. **4**: p. 21.

340. Prasad, A. and M. Sahin, *Can motor volition be extracted from the spinal cord?* Journal of NeuroEngineering and Rehabilitation, 2012. **9**: p. 41-41.
341. Prasad, A. and M. Sahin, *Chronic recordings from the rat spinal cord descending tracts with microwires.* Conference proceedings : ... Annual International Conference of the IEEE Engineering in Medicine and Biology Society. IEEE Engineering in Medicine and Biology Society. Conference, 2011. **2011**: p. 2993-2996.
342. Benzel, E.C., B.L. Hart, P.A. Ball, N.G. Baldwin, W.W. Orrison, and M.C. Espinosa, *Magnetic resonance imaging for the evaluation of patients with occult cervical spine injury.* J Neurosurg, 1996. **85**(5): p. 824-9.
343. Chen, L.M., A. Mishra, P.F. Yang, F. Wang, and J.C. Gore, *Injury alters intrinsic functional connectivity within the primate spinal cord.* Proc Natl Acad Sci U S A, 2015. **112**(19): p. 5991-6.
344. Hsieh, F.Y., H.H. Lin, and S.H. Hsu, *3D bioprinting of neural stem cell-laden thermoresponsive biodegradable polyurethane hydrogel and potential in central nervous system repair.* Biomaterials, 2015. **71**: p. 48-57.
345. Li, Q., M.C. Ford, E.B. Lavik, and J.A. Madri, *Modeling the neurovascular niche: VEGF- and BDNF-mediated cross-talk between neural stem cells and endothelial cells: an in vitro study.* J Neurosci Res, 2006. **84**(8): p. 1656-68.
346. Nazmi, A., I. Mohamed Arif, K. Dutta, K. Kundu, and A. Basu, *Neural stem/progenitor cells induce conversion of encephalitogenic T cells into CD4+-CD25+- FOXP3+ regulatory T cells.* Viral Immunol, 2014. **27**(2): p. 48-59.
347. Campos, L.S., D.P. Leone, J.B. Relvas, C. Brakebusch, R. Fassler, U. Suter, and C. ffrench-Constant, *Beta1 integrins activate a MAPK signalling pathway in neural stem cells that contributes to their maintenance.* Development, 2004. **131**(14): p. 3433-44.
348. Chaerkady, R., B. Letzen, S. Renuse, N.A. Sahasrabuddhe, P. Kumar, A.H. All, N.V. Thakor, B. Delanghe, J.D. Gearhart, A. Pandey, and C.L. Kerr, *Quantitative temporal proteomic analysis of human embryonic stem cell differentiation into oligodendrocyte progenitor cells.* Proteomics, 2011. **11**(20): p. 4007-20.
349. Gurok, U., C. Steinhoff, B. Lipkowitz, H.H. Ropers, C. Scharff, and U.A. Nuber, *Gene expression changes in the course of neural progenitor cell differentiation.* J Neurosci, 2004. **24**(26): p. 5982-6002.
350. Abaskharoun, M., M. Bellemare, E. Lau, and R.U. Margolis, *Glypican-1, phosphacan/receptor protein-tyrosine phosphatase-zeta/beta and its ligand, tenascin-C, are expressed by neural stem cells and neural cells derived from embryonic stem cells.* ASN Neuro, 2010. **2**(3): p. e00039.
351. Sakaguchi, M., T. Shingo, T. Shimazaki, H.J. Okano, M. Shiwa, S. Ishibashi, H. Oguro, M. Ninomiya, T. Kadoya, H. Horie, A. Shibuya, H. Mizusawa, F. Poirier, H. Nakauchi, K. Sawamoto, and H. Okano, *A carbohydrate-binding protein, Galectin-1, promotes proliferation of adult neural stem cells.* Proc Natl Acad Sci U S A, 2006. **103**(18): p. 7112-7.
352. Chirasani, S.R., A. Sternjak, P. Wend, S. Momma, B. Campos, I.M. Herrmann, D. Graf, T. Mitsiadis, C. Herold-Mende, D. Besser, M. Synowitz, H. Kettenmann, and R. Glass, *Bone morphogenetic protein-7 release from endogenous neural precursor cells suppresses the tumourigenicity of stem-like glioblastoma cells.* Brain, 2010. **133**(Pt 7): p. 1961-72.
353. Llado, J., C. Haenggeli, N.J. Maragakis, E.Y. Snyder, and J.D. Rothstein, *Neural stem cells protect against glutamate-induced excitotoxicity and promote survival of injured motor*

neurons through the secretion of neurotrophic factors. Mol Cell Neurosci, 2004. **27**(3): p. 322-31.
354. Kamei, N., N. Tanaka, Y. Oishi, T. Hamasaki, K. Nakanishi, N. Sakai, and M. Ochi, *BDNF, NT-3, and NGF released from transplanted neural progenitor cells promote corticospinal axon growth in organotypic cocultures.* Spine (Phila Pa 1976), 2007. **32**(12): p. 1272-8.
355. Laterza, C., A. Merlini, D. De Feo, F. Ruffini, R. Menon, M. Onorati, E. Fredrickx, L. Muzio, A. Lombardo, G. Comi, A. Quattrini, C. Taveggia, C. Farina, E. Cattaneo, and G. Martino, *iPSC-derived neural precursors exert a neuroprotective role in immune-mediated demyelination via the secretion of LIF.* Nat Commun, 2013. **4**: p. 2597.
356. Hawryluk, G.W., A. Mothe, J. Wang, S. Wang, C. Tator, and M.G. Fehlings, *An in vivo characterization of trophic factor production following neural precursor cell or bone marrow stromal cell transplantation for spinal cord injury.* Stem Cells Dev, 2012. **21**(12): p. 2222-38.
357. Nishimura, S., A. Yasuda, H. Iwai, M. Takano, Y. Kobayashi, S. Nori, O. Tsuji, K. Fujiyoshi, H. Ebise, Y. Toyama, H. Okano, and M. Nakamura, *Time-dependent changes in the microenvironment of injured spinal cord affects the therapeutic potential of neural stem cell transplantation for spinal cord injury.* Mol Brain, 2013. **6**: p. 3.
358. Parr, A.M., I. Kulbatski, T. Zahir, X. Wang, C. Yue, A. Keating, and C.H. Tator, *Transplanted adult spinal cord-derived neural stem/progenitor cells promote early functional recovery after rat spinal cord injury.* Neuroscience, 2008. **155**(3): p. 760-770.
359. Cusimano, M., D. Biziato, E. Brambilla, M. Donega, C. Alfaro-Cervello, S. Snider, G. Salani, F. Pucci, G. Comi, J.M. Garcia-Verdugo, M. De Palma, G. Martino, and S. Pluchino, *Transplanted neural stem/precursor cells instruct phagocytes and reduce secondary tissue damage in the injured spinal cord.* Brain, 2012. **135**(Pt 2): p. 447-60.
360. Butenschon, J., T. Zimmermann, N. Schmarowski, R. Nitsch, B. Fackelmeier, K. Friedemann, K. Radyushkin, J. Baumgart, B. Lutz, and J. Leschik, *PSA-NCAM positive neural progenitors stably expressing BDNF promote functional recovery in a mouse model of spinal cord injury.* Stem Cell Res Ther, 2016. **7**: p. 11.
361. Bonnamain, V., I. Neveu, and P. Naveilhan, *Neural stem/progenitor cells as a promising candidate for regenerative therapy of the central nervous system.* Front Cell Neurosci, 2012. **6**: p. 17.
362. Cooke, M.J., K. Vulic, and M.S. Shoichet, *Design of biomaterials to enhance stem cell survival when transplanted into the damaged central nervous system.* Soft Matter, 2010. **6**(20): p. 4988-4998.
363. Piltti, K.M., D.L. Salazar, N. Uchida, B.J. Cummings, and A.J. Anderson, *Safety of epicenter versus intact parenchyma as a transplantation site for human neural stem cells for spinal cord injury therapy.* Stem Cells Transl Med, 2013. **2**(3): p. 204-16.
364. Piltti, K.M., S.N. Avakian, G.M. Funes, A. Hu, N. Uchida, A.J. Anderson, and B.J. Cummings, *Transplantation dose alters the dynamics of human neural stem cell engraftment, proliferation and migration after spinal cord injury.* Stem Cell Res, 2015. **15**(2): p. 341-53.
365. Suzuki, Y., M. Yanagisawa, H. Yagi, Y. Nakatani, and R.K. Yu, *Involvement of beta1-integrin up-regulation in basic fibroblast growth factor- and epidermal growth factor-induced proliferation of mouse neuroepithelial cells.* J Biol Chem, 2010. **285**(24): p. 18443-51.